A Stereo-Atlas of Ostracod Shells

edited by J. Athersuch, D. J. Horne, D. J. Siveter,
and J. E. Whittaker

Volume 16, Part 2; 31st December, 1989

Published by the British Micropalaeontological Society, London

ISSN 0952-7451

Instructions to Authors

Contributions illustrated by scanning electron micrographs of Ostracoda in stereo-pairs are invited. Format should follow the style set by the papers in this issue. Descriptive matter apart from illustrations should be cut to a minimum; preferably each plate should be accompanied by one page of text only. Blanks to aid in mounting figures for plates may be obtained from any one of the Editors or Editorial Board. Completed papers should be sent to Dr David J. Siveter.

The front cover shows a female left valve (**OS13377**) of *Bromidella reticulata* Harris from the Simpson Group, middle Ordovician, Oklahoma, USA (see M. Williams & D. J. Siveter, *Stereo-Atlas Ostracod Shells*, **16**, 1–8, 1989).

Printed in the UK by BPCC BLACKPOOL Ltd., Stanley Road, Blackpool FY1 4QN
A Member of BPCC Ltd

A Stereo-Atlas of Ostracod Shells

edited by J. Athersuch, D. J. Horne, D. J. Siveter
and J. E. Whittaker

Volume 16, 1989

Part 1 (pp. 1–77); 31st July, 1989

Part 2 (pp. 78–157); 31st December, 1989

Published by the British Micropalaeontological Society, London

Contents

Stereo-Atlas of Ostracod Shells 16 (19) 78–85 (**1989**)
595.337.23 (113.331) (420 : 161.003.52 + 485 : 161.018.57) : 551.351 + 552.54

ON *PRIMITIVOTHLIPSURELLA V-SCRIPTA* (JONES & HOLL)

by Robert F. Lundin & Lee E. Petersen
(Arizona State University, Tempe, U.S.A. & Anadarko Petroleum Corporation, Houston, USA)

Genus *PRIMITIVOTHLIPSURELLA* gen. nov.
Type-species: *Thlipsura v-scripta* Jones & Holl, 1869

Derivation of name: Latin *primitivus*, early, and *Thlipsurella*, indicating the genus is ancestral to *Thlipsurella* Swartz, 1932.

Diagnosis: Thlipsuridae with one vertical or subvertical preadductorial sulcus and two oblique posterior, straight to slightly curved sulci which form a variable but distinctly acute angle with each other and are bounded posteriorly by a distinct lobe which approximately parallels the posterior border of the carapace. Adductor muscle attachment marked by large subcircular depression at mid-length slightly above mid-height on interior surface of valves. Hinge distinctly inclined to longitudinal axis of valves.

Remarks: The type-species of *Primitivothlipsurella* is considered to be a direct descendant of *P. obtusa* Petersen & Lundin (*Stereo-Atlas Ostracod Shells*, **16**, 86–93, 1989). This relationship clearly suggests that the genus is ancestral to *Thlipsurella* Swartz.

Primitivothlipsurella is distinguished from *Thlipsurella* by the arrangement of the sulci, especially the posterior ones. Nevertheless, the two genera show distinct similarities in the basic shape and sculpture of the valves. Hingement and other interior structures in the type-species of *Thlipsurella*, *T. ellipsoclefta* Swartz, 1932, are not known. However, Lundin's (*Okla. Geol. Surv. Bull.*, **116**, 85–87, pl. 17, fig. 2, 1968) description of *T. putea* Coryell & Cuskley, 1934, which is closely related to the type-species, indicates that the hinge and contact margin structures of the

Explanation of Plate 16, 79

Figs. 1, 2, car. (**ASU X–109**, 921 μm long): fig. 1, ext. rt. lt.; fig. 2, ext. lt. lat. Figs. 3, 4, car. (**ASU X–116**, 865 μm long): fig. 3, ext. vent.; fig. 4, ext. rt. lat. Scale A (200 μm; ×65), figs. 1, 2; scale B (200 μm; ×69), figs. 3, 4.

two genera are similar. However, the place of the adductor muscle attachment in *Thlipsurella* is represented exteriorly by an adductorial sulcus. The new genus presented here has no S2, but rather the typical thlipsurid characteristic of a circular depression on the interior surface at the place of adductor muscle attachment. Swartz's (*J. Paleont.* **6**, pl. 10, fig. 6c, 1932) illustration of a juvenile of the type-species of *Thlipsurella*, as well as variations observed in and comparison of *P. v-scripta* and *P. obtusa*, suggest a phylogeny in which the posterior sulci became separated and more parallel with time.

Primitivothlipsurella is presently known only from *P. v-scripta* (Jones & Holl) and *P. obtusa* Petersen & Lundin, both from the Silurian strata of the Welsh Borderland area of Britain.

Primitivothlipsurella v-scripta (Jones & Holl, 1869)

1869 *Thlipsura v-scripta* sp. nov. T. R. Jones & H. B. Holl, *Ann. Mag. nat. Hist.*, (4), **3**, 214, pl. 15, figs. 3a–c.
1887 *Thlipsura v-scripta* var. *discreta* nov. T. R. Jones. *Notes on some Silurian ostracoda from Gothland*, Stockholm, 6 (*nom. nud.*).
1887 *Thlipsura v-scripta* Jones & Holl; T. R. Jones, *Ann. Mag. nat. Hist.*, (5), **19**, 403.
1887 *Octonaria octoformis* var. *informis* nov. T. R. Jones, *Ann. Mag. nat. Hist.*, (5), **19**, 405, pl. 12, figs. 5a, b.
1888 *Thlipsura v-scripta* Jones & Holl var. *discreta* Jones; T. R. Jones, *Ann. Mag. nat. Hist.*, (6) **1**, 404, pl. 22, figs. 9a–c, 10.
1919 *Thlipsura v-scripta* var. *discreta* Jones; J. E. Hede, *Geol. För. Stock. Förh.*, **41**, 139, 147, pl. 6, fig. 1.
1932 *Thlipsurella v-scripta* (Jones & Holl); F. M. Swartz, *J. Paleont.*, **6**, 44, pl. 10, fig. 7.
1956 *Thlipsurella discreta* (Jones); A. Martinsson, *Publ. Palaeontol. Inst. Univ. Uppsala*, **14**, 33, pl. 5, figs. 43–49.
1965 *Thlipsurella discreta* (Jones); V. Pokorný, *Principles Zool. Micropalaeontol.*, 229, fig. 852, Pergamon Press, Oxford.
1966 *Thlipsurella discreta* (Jones); F. J. Adamczak, *Geol. För. Stock. Förh.*, **88**, 466, fig. 5.
1968 *Thlipsurella v-scripta* (Jones & Holl); V. S. Krandijevsky, *Paleont. & Stratigr. of the Lower Palaeozoic of Volyn-Podolia*, Acad. Nauk Ukr. SSR, 70, pl. 11, fig. 11.
1968 *Octonaria informis* Jones; V. S. Krandijevsky, *Paleontol. & Stratigr. of the Lower Palaeozoic of Volyn-Podolia*, Acad. Nauk Ukr. SSR, 74.
1978 "*Thlipsura*" *v-scripta* Jones & Holl; D. J. Siveter, *in*: R. H. Bate & E. Robinson (eds.), *A Stratigraphical Index of British Ostracoda, Geol. J. Spec. Issue*, **8**, 74, pl. 3, figs. 1, 2, tab. 3.

Explanation of Plate 16, 81

Figs. 1, 2, juv. car. (**ASU X–117**, 771 μm long): fig. 1, ext. rt. lat.; fig. 2, ext. lt. lat. Fig. 3, juv. car., ext. rt. lat. (**ASU X–118**, 808 μm long). Scale A (200 μm; ×78), figs. 1, 2; scale B (200 μm; ×74), fig. 3.

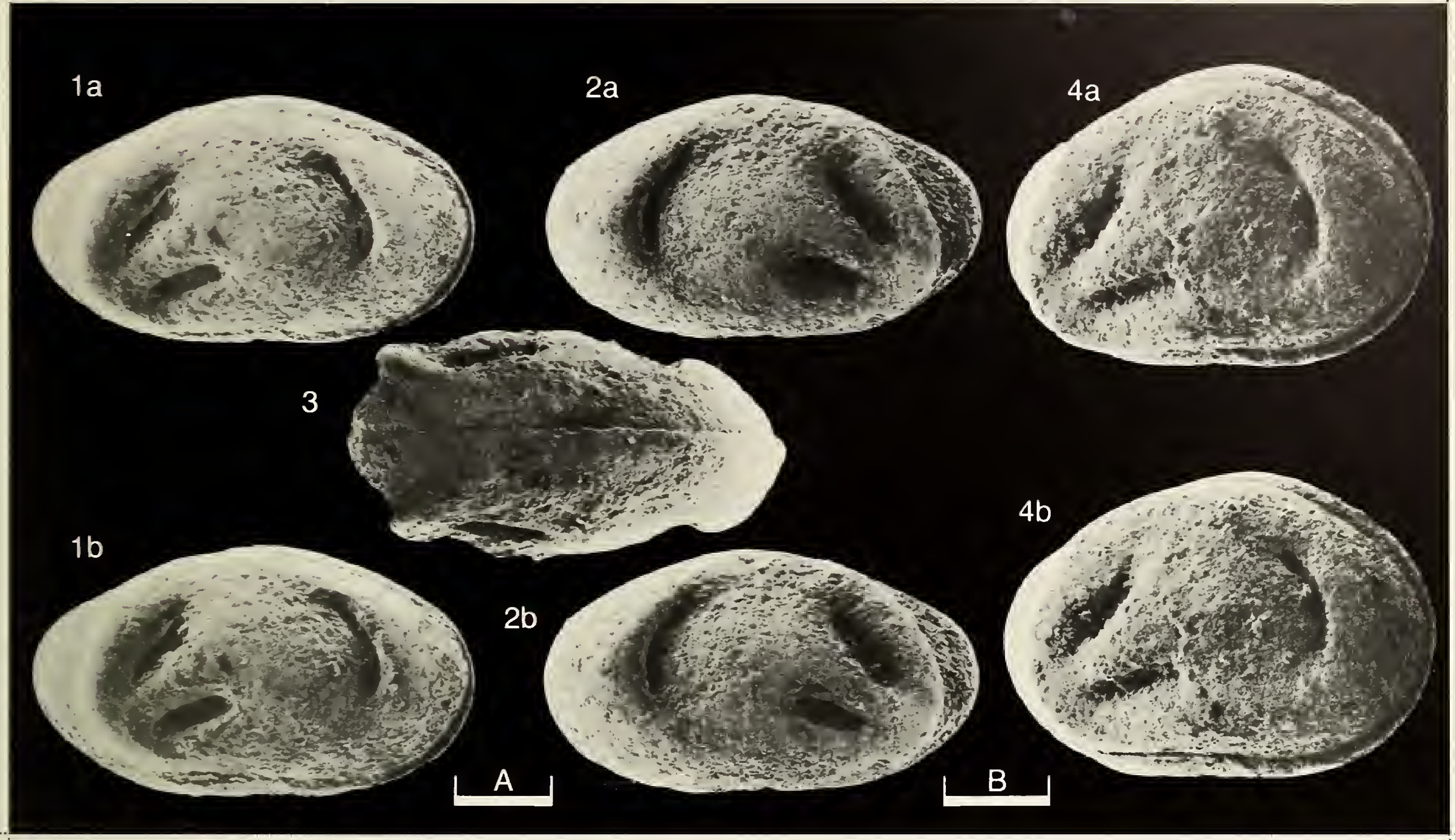
1a
2a
4a
3
4b
1b
2b
A
B

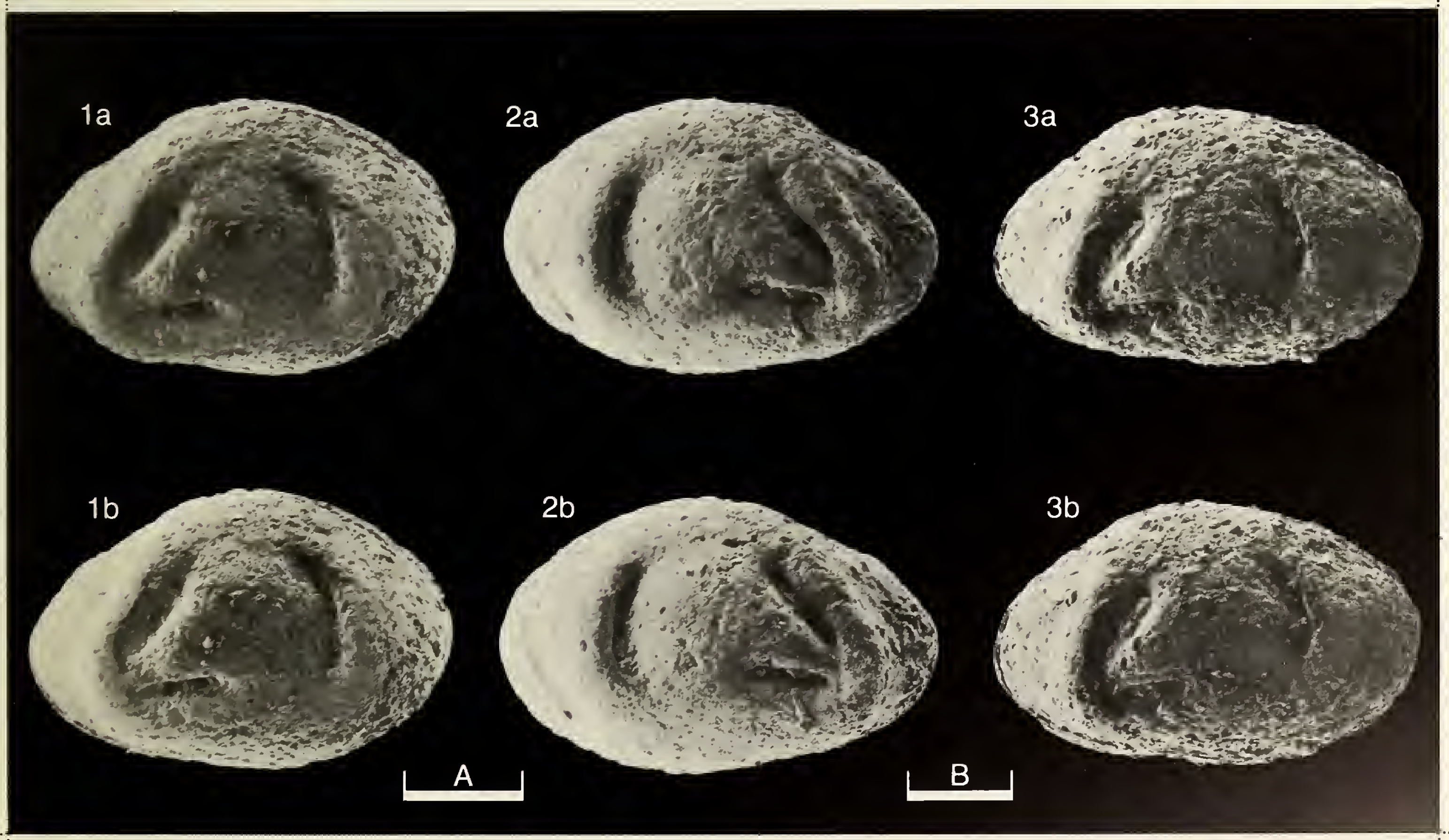
1a
2a
3a
1b
2b
3b
A
B

1981 "*Thlipsura*" *v-scripta* Jones & Holl; R. J. Aldridge, K. J. Dorning & D. J. Siveter, *in*: J. W. Neale & M. Brasier (Eds.), *Microfossils from Recent & Fossil Shelf Seas*, 22, 28, pl. 2.3, fig. 17, Ellis Horwood, Chichester.

1984 "*Thlipsura*" *v-scripta* Jones & Holl; D. J. Siveter, *Spec. Pap. Palaeontol.*, 32, 81, text-fig. 3:8.

1987 "*Thlipsurella*" *v-scripta* (Jones & Holl); L. E. Petersen & R. F. Lundin, *J. Micropalaeontol.*, **6**, 80, pl. 1. fig. 1 (authorship given on pl. 1, fig. 1 is in error).

Lectotype: Designated herein. British Museum (Nat. Hist.) no. **I 2078**; juvenile left valve. Specimen illustrated by Jones & Holl 1869, pl. 15, figs. 3a–c.

Type locality: "Croft's Quarry", 0.5 km W of Malvern, Hereford & Worcester, England; approximately Nat. Grid Ref. SO 757464, lat. 52° 08′ N, long. 2° 18′ W. Much Wenlock Limestone Formation, Wenlock Series, Silurian.

Figured specimens: Department of Geology, Arizona State University, (**ASU**), nos. **X–109** (car.: Pl. **16**, 79, figs. 1, 2), **X–116** (car. Pl. **16**, 79, figs. 3, 4), **X–117** (juv. car.: Pl. **16**, 81, figs. 1, 2), **X–118** (juv. car.: Pl. **16**, 81, fig. 3), **X–111** (car.: Pl. **16**, 83, fig. 1; Pl. **16**, 85, fig. 6), **X–112** (RV: Pl. **16**, 83, fig. 2), **X–113** (LV: Pl. **16**, 83, fig. 3), **X–114** (car.: Pl. **16**, 85, figs. 1, 2), **X–115** (car.: Pl. **16**, 85, fig. 3), **X–110** (LV: Pl. **16**, 85, fig. 5). British Museum (Nat. Hist.), No. **I 2078** (lectotype, juv. LV: Pl. **16**, 85, fig. 4).

The lectotype and **ASU X–110** are from the type locality. **ASU X–109** and **ASU X–116** are from the Farley Member, Coalbrookdale Formation at Ironbridge, Shropshire, England; lat. 52° 38′ N, long. 2° 30′ W. **ASU X–117** and **ASU X–118** are from Farley Member, Coalbrookdale Formation at Harley Hill near Much Wenlock, Shropshire; lat. 52° 36′ N, long. 2° 34′ W. **ASU X–111 – ASU X–115** are from the Mulde Beds at Mulde, Gotland, Sweden; approximately lat. 52° 32′ N, long. 18° 28′ E. All specimens are from the Homerian, Wenlock Series, Silurian.

Diagnosis: *Primitivothlipsurella* in which the posterior border of the carapace extends distinctly beyond the lobe behind the posterior sulci. Posterior sulci normally separated posteriorly; posteroventral sulcus subparallel to longitudinal axis of valve.

Remarks: Jones (*Ann. Mag. nat. Hist.*, (7), **1**, 6, 1887) erected a new variety, *Thlipsura v-scripta* var.

Explanation of Plate 16, 83

Fig. 1, car. ext. lt. lat. (**ASU X–111**, 996 μm long): fig. 2, RV, int. lat. (**ASU X–112**, 996 μm long); fig. 3, LV, int. lat. (**ASU X–113**, 940 μm long). Scale A (200 μm; ×62), fig. 1; scale B (200 μm; ×60), fig. 2; scale C (200 μm; ×65), fig. 3.

Remarks (contd.): *discreta*, on the basis that this material from Gotland differed from the British specimens in that the posterior sulci on the former were separated and thus did not form a "*V*". In fact the same is true for most of the British specimens and we see no reason to recognise two species as has been done by Martinsson (*Publ. Palaeontol. Inst. Univ. Uppsala*, **14**, 33, 1956) and Adamczak (*Geol. För. Stock. Förh.*, **88**, 466, 1967). Typically, in both the British and Gotland specimens, the posterior sulci are not confluent posteroventrally. However, the two posterior sulci are confluent, at least on the right valve of a few specimens (Pl. **16**, 81, fig. 3). *P. v-scripta* is readily distinguished from *P. obtusa* Petersen & Lundin, from which it was derived, by differences in orientation of the posterior sulci, by its greater size and by the fact that in *P. v-scripta* the posterior border of the carapace is distinctly more posterior than the lobe behind the posterior sulci. In *P. obtusa* this lobe forms the posterior border of the carapace or is very near it.

Martinsson (1956, *op. cit.*) questioned whether *P. v-scripta* was dimorphic. His data on size (length and height) do not clearly demonstrate any shell dimorphism, although it could be argued that two vaguely differentiated groups of adults exist. We illustrate herein two specimens (Pl. **16**, 85, figs. 2, 3) which show differences in posterior morphology and length-width ratio. One of us (R.F.L.) is presently studying a population to determine if the species exhibits dimorphic characters of the shell.

Distribution: Known only from many samples and localities in the Welsh Borderland area and Gotland. In the Welsh Borderland the species ranges throughout the Homerian Stage (late Wenlock Series) and into at least the early Gorstian Stage (early Ludlow Series), Silurian. In Gotland the range is not fully established, but it is well represented in the Mulde Beds, Homerian, Wenlock, Silurian.

Acknowledgements: R.F.L. acknowledges support of the College of Liberal Arts and Sciences, Arizona State University, the National Science Foundation (Grant No. EAR–8200816) and NATO. He also thanks David J. Siveter for help with fieldwork.

Explanation of Plate 16, 85

Figs. 1, 2, car. (**ASU X–114**, 1034 μm long): fig. 1, ext. dors.; fig. 2, ext. vent. Fig. 3, car., ext. vent. (**ASU X–115**, 1015 μm long). Fig. 4, juv. LV, ext. lat. (lectotype **BMNH I 2078**, 763 μm long). Fig. 5, LV, ext. lat. (**ASU X–110**, 1128 μm long). Fig. 6, car., ext. rt. lat. (**ASU X–111**, 996 μm long).

Scale A (200 μm; ×59), figs. 1, 2; scale B (200 μm; ×60), fig. 3; scale C (200 μm; ×72), fig. 4; scale D (200 μm; ×54), fig. 5; scale E (200 μm; ×62), fig. 6.

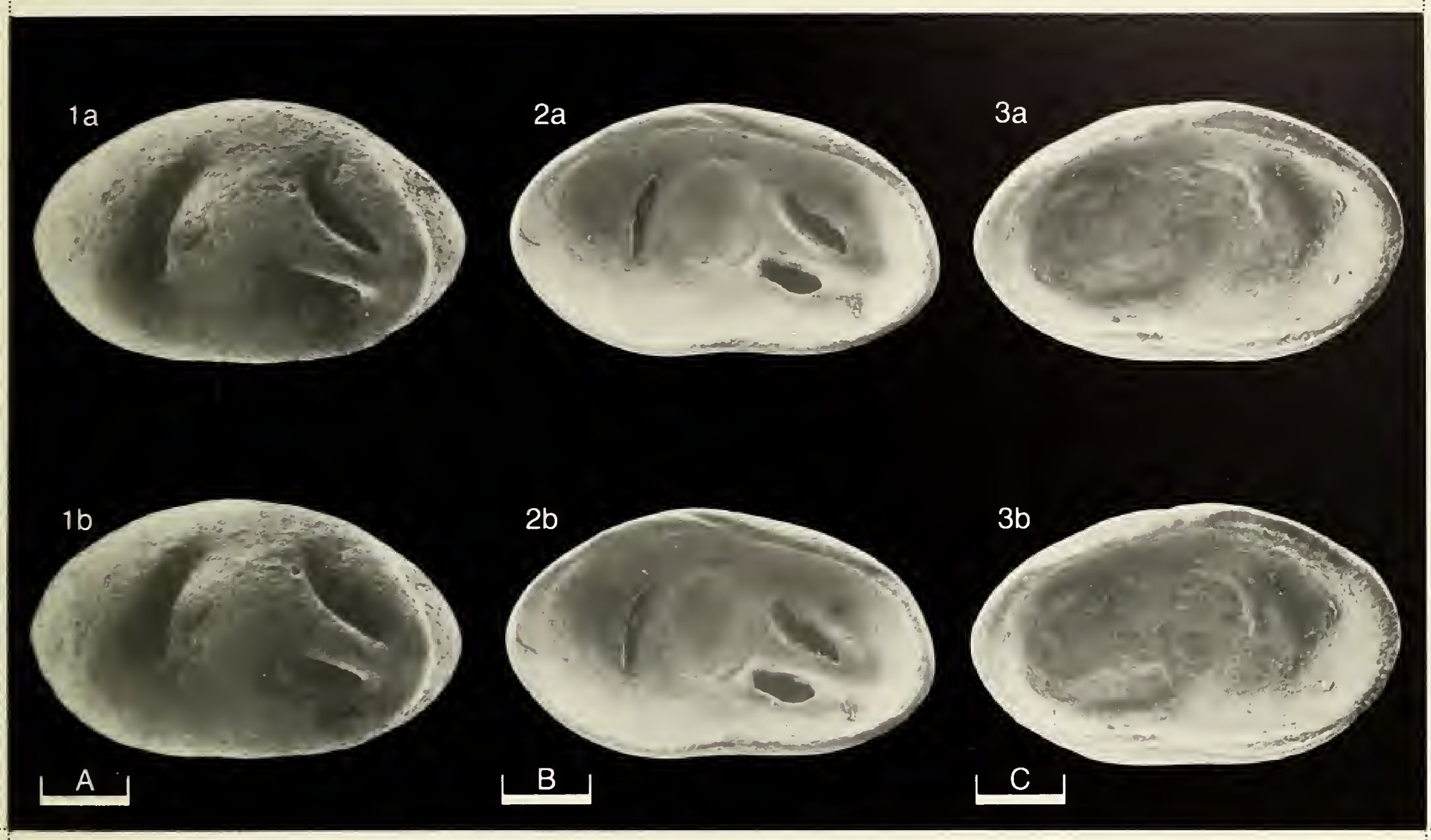
1a
2a
3a
1b
2b
3b
A
B
C

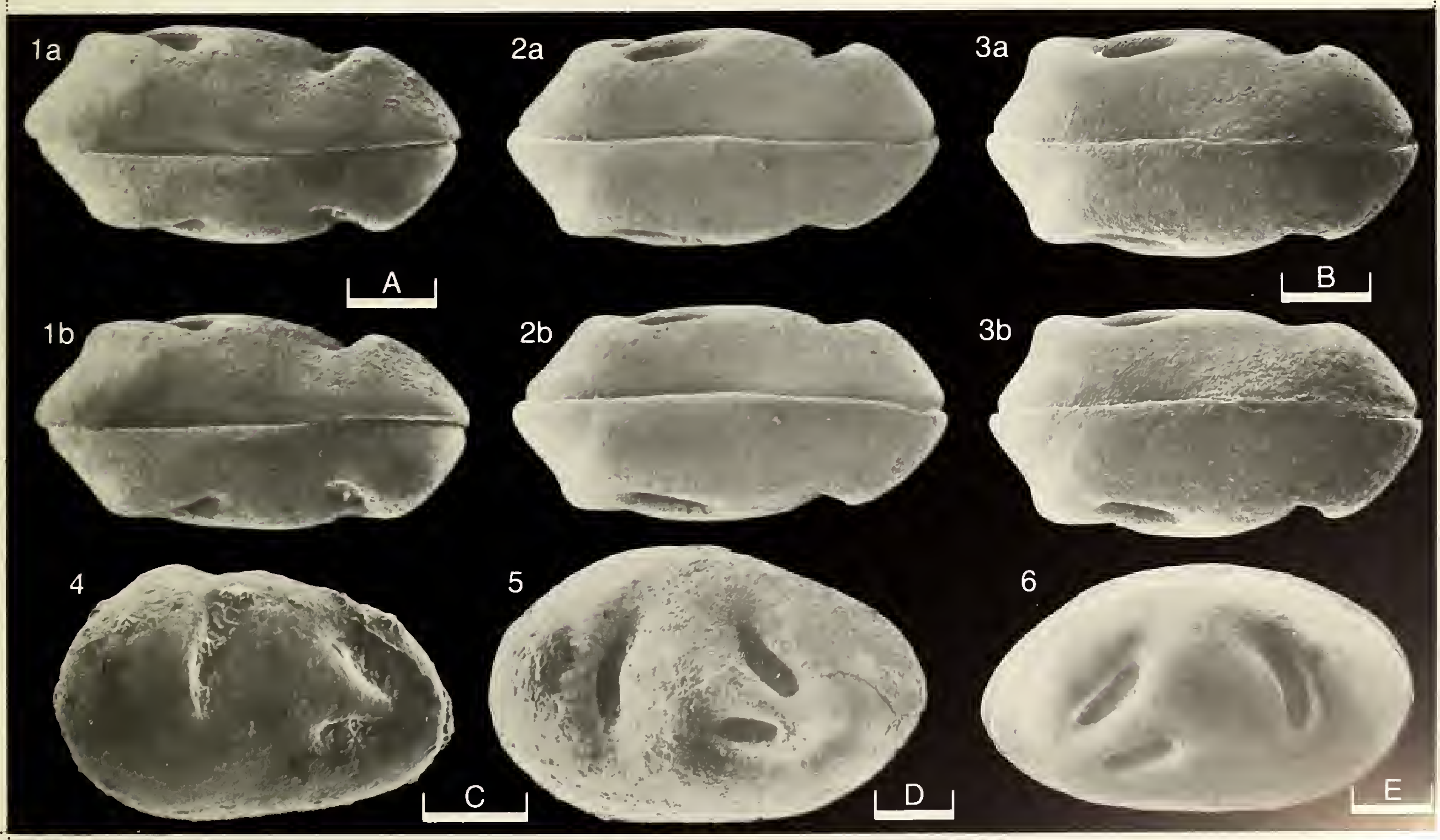
1a
2a
3a
A
B
1b
2b
3b
4
5
6
C
D
E

Stereo-Atlas of Ostracod Shells 16 (20) 86–93 (**1989**)
595.337.23 (113.331) (420 : 162.003.52) : 551.351 + 552.52

ON *PRIMITIVOTHLIPSURELLA OBTUSA* PETERSEN & LUNDIN sp. nov.

by Lee E. Petersen & Robert F. Lundin
(Anadarko Petroleum Corp., Houston & Arizona State University, Tempe, USA)

Primitivothlipsurella obtusa sp. nov.

Holotype: Department of Geology, Arizona State University (**ASU**), USA, no. **ASU X–119**; carapace.

Type locality: The north bank of the River Severn opposite Buildwas Abbey, Buildwas, Shropshire, England (National Grid Reference, SJ 6435 0450); approximately lat. 52° 39′ N, long. 2° 33′ W. The sample is from the upper (but not the uppermost) part of the Buildwas Formation, late early Sheinwoodian Stage, Wenlock Series, Silurian.

Derivation of name: Latin *obtusa*; referring to the orientation of the posteroventral sulcus relative to the longitudinal axis of the valve.

Explanation of Plate 16, 87

Figs. 1–4, car. (holotype **ASU X–119**, 789 μm long): fig. 1, ext. rt. lat.; fig. 2, ext. dors.; fig. 3, ext. vent.; fig. 4, ext. lt. lat. Scale (200 μm; ×77), figs. 1–4.

Figured specimens: Department of Geology, Arizona State University (**ASU**) nos. **X–119** (holotype, car.: Pl. **16**, 87, figs. 1–4), **X–120** (paratype, car.: Pl. **16**, 89, figs. 1–4), **X–122** (paratype, car.: Pl. **16**, 91, figs. 1–3), **X–123** (paratype, car.: Pl. **16**, 93, fig. 1), **X–121** (paratype, juvenile car.: Pl. **16**, 93, figs. 2, 3).

X–121 is from the Buildwas Formation, sample approximately 1 m higher in the section than the sample yielding the holotype. All of the other figured specimens are from the same sample as the holotype.

Diagnosis: *Primitivothlipsurella* species in which the posterior lobe of each valve forms or is very close to the posterior border of the valve. Posteroventral sulci oriented at distinct angle to the ventral border of the carapace.

Explanation of Plate 16, 89

Figs. 1–4, car. (**ASU X–120**, 865 μm long): fig. 1, ext. rt. lat.; fig. 2, ext. dors.; fig. 3, ext. vent.; fig. 4, ext. lt. lat. Scale (200 μm; ×71), figs. 1–4.

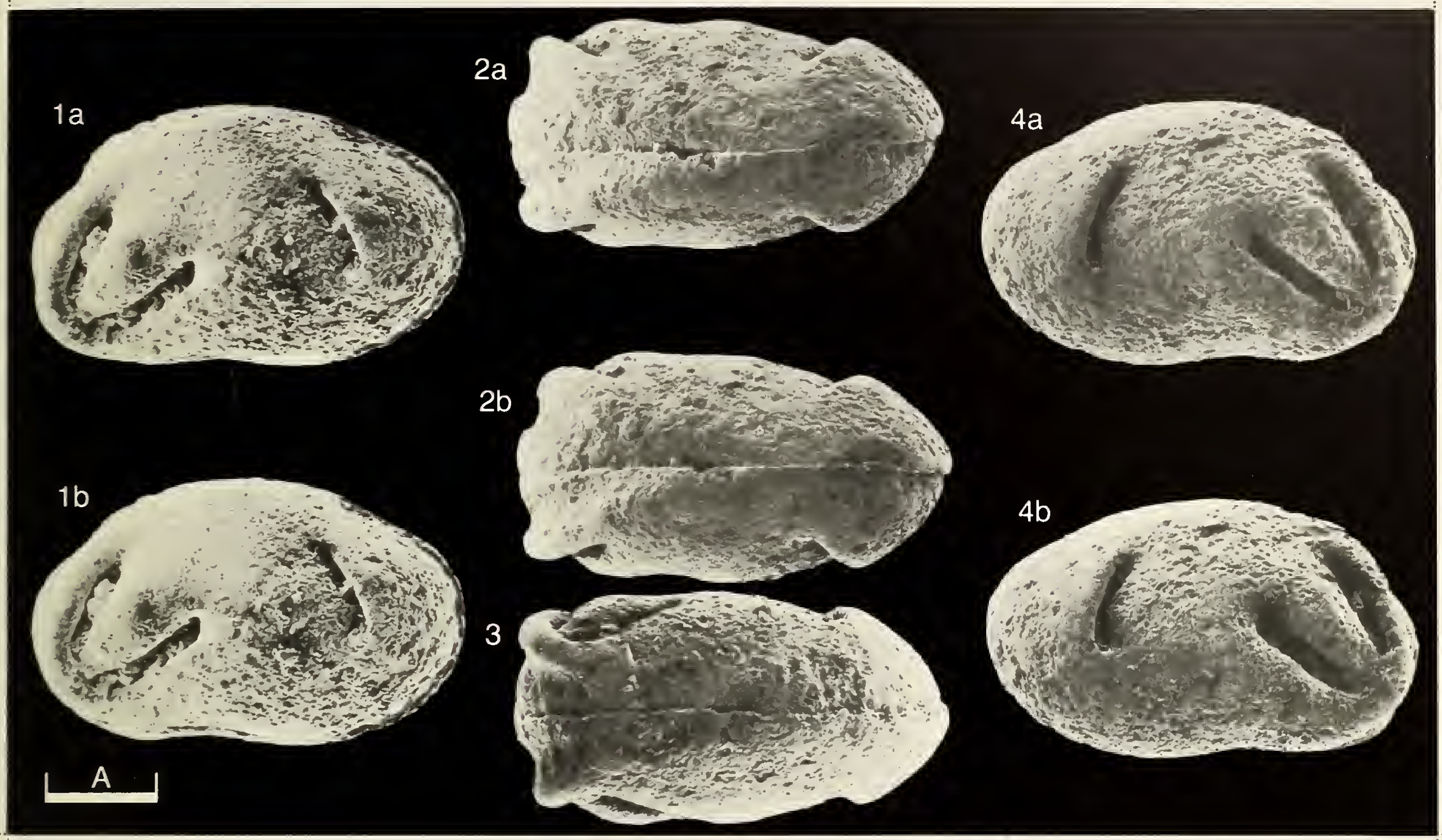
1a
2a
4a
2b
1b
4b
3
A

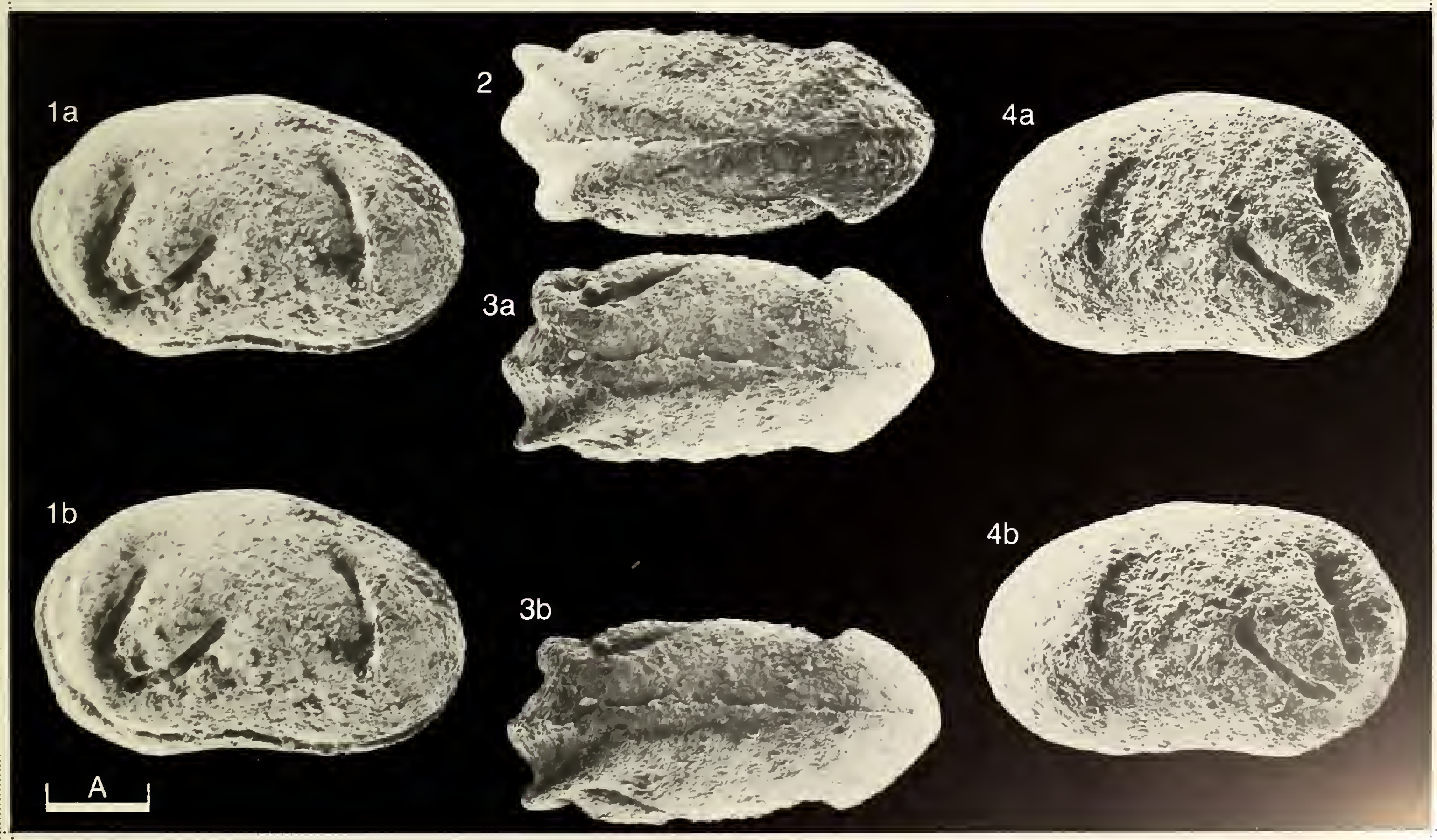
1a
2
4a
3a
1b
4b
3b
A

Remarks: *Primitivothlipsurella obtusa* is ancestral to the type species *Primitivothlipsurella v-scripta* (Jones & Holl, 1869) (see Lundin & Petersen, *Stereo-Atlas Ostracod Shells*, **16**, 78–85, 1989) and is distinguished from the latter species by: its smaller size; the fact that the posterior lobes form or are nearly coincident with the posterior border of the carapace; and the fact that normally the posteroventral sulcus is orientated at a more distinct angle to the ventral border of the carapace than it is in *P. v-scripta*. The posterior sulci are fused to form a continuous v-shaped sulcus on some valves (especially right valves) and this fusion seems to be more common in *P. obtusa* than in *P. v-scripta*. This suggests a trend toward separation and more parallel alignment of the posterior sulci through time. If this is true, we can speculate that *P. obtusa* was derived from a species such as *Thlipsuroides walensis* (Krandijevsky, 1963).

P. obtusa is a diagnostic species for recognition of lower Sheinwoodian strata in the type Wenlock Series in the Welsh Borderland.

Distribution: Known from the Buildwas and Coalbrookdale formations in the type Wenlock area, Shropshire, in the Welsh borderland; in strata ranging from the upper *Cyrtograptus centrifugus* Biozone through the lower *Monograptus riccartonensis* Biozone; lower Sheinwoodian Stage, Wenlock Series, Silurian.

Acknowledgements: R. F. L. acknowledges support of the College of Liberal Arts and Sciences, Arizona State University, the National Science Foundation (Grant No. EAR–8200816) and NATO. D. J. Siveter is thanked for help with fieldwork.

Explanation of Plate 16, 91

Figs. 1–3, car. (**ASU X–122**, 789 μm long): fig. 1, ext. dors.; fig. 2, ext. rt. lat.; fig. 3, ext. lt. lat.
Scale (200 μm; ×77), figs. 1–3.

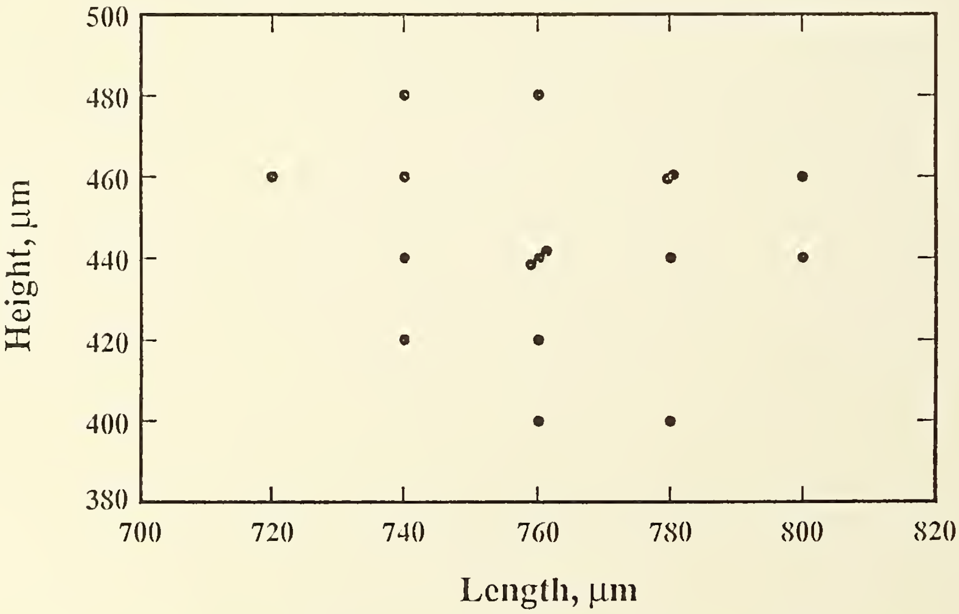

Text-fig. 1: Size dispersion diagram for 17 right valves of *P. obtusa* from the type locality.

Explanation of Plate 16, 93

Fig. 1, car. ext. rt. lat. (**ASU X–123**, 714 μm long): figs. 2, 3, juvenile car. (**ASU X–121**, 620 μm long): fig. 2, ext. rt. lat.; fig. 3, ext. lt. lat.
Scale A (200 μm; ×84), fig. 1; scale B (200 μm; ×97), figs. 2, 3.

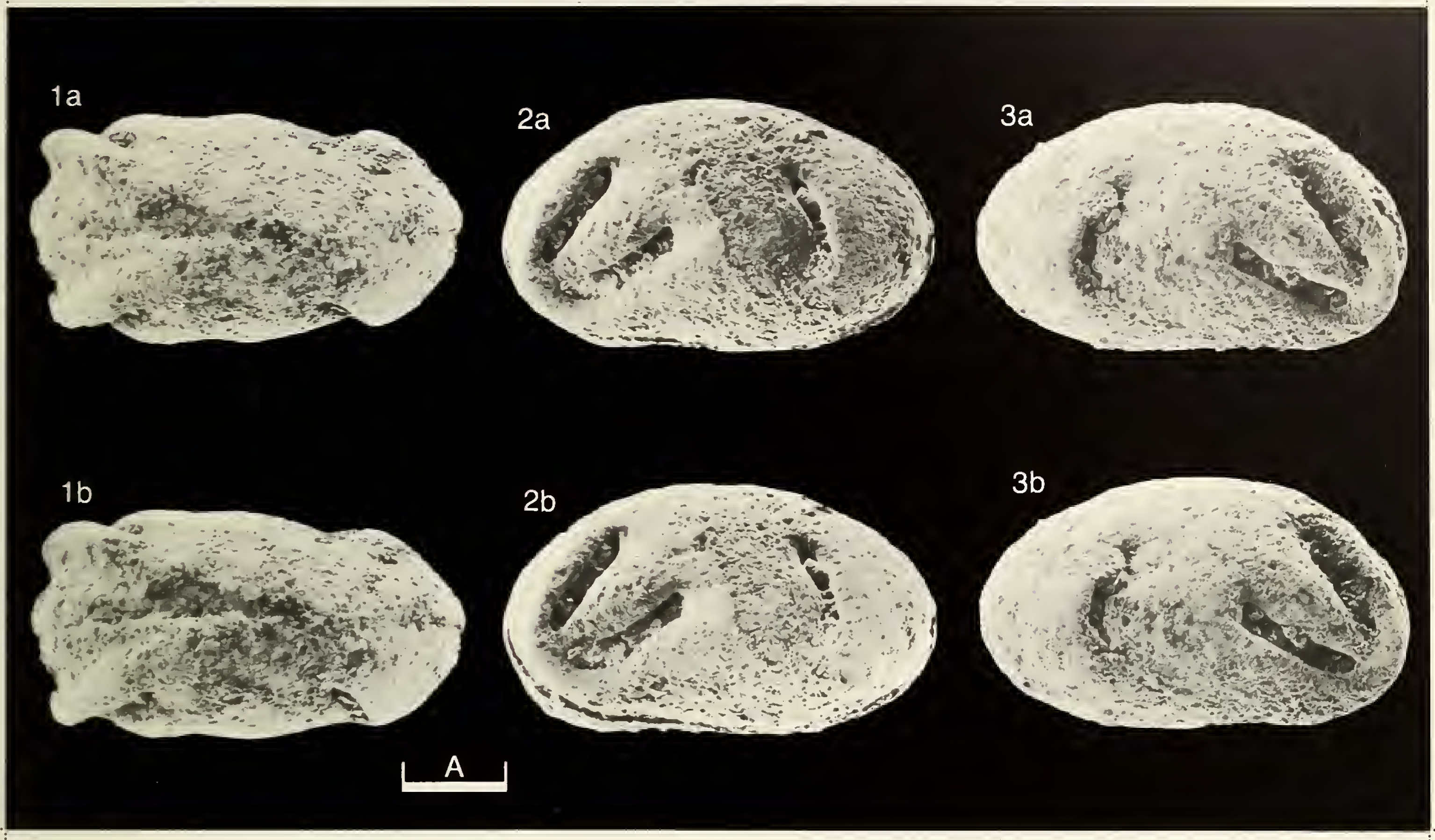
1a
2a
3a
1b
2b
3b
A

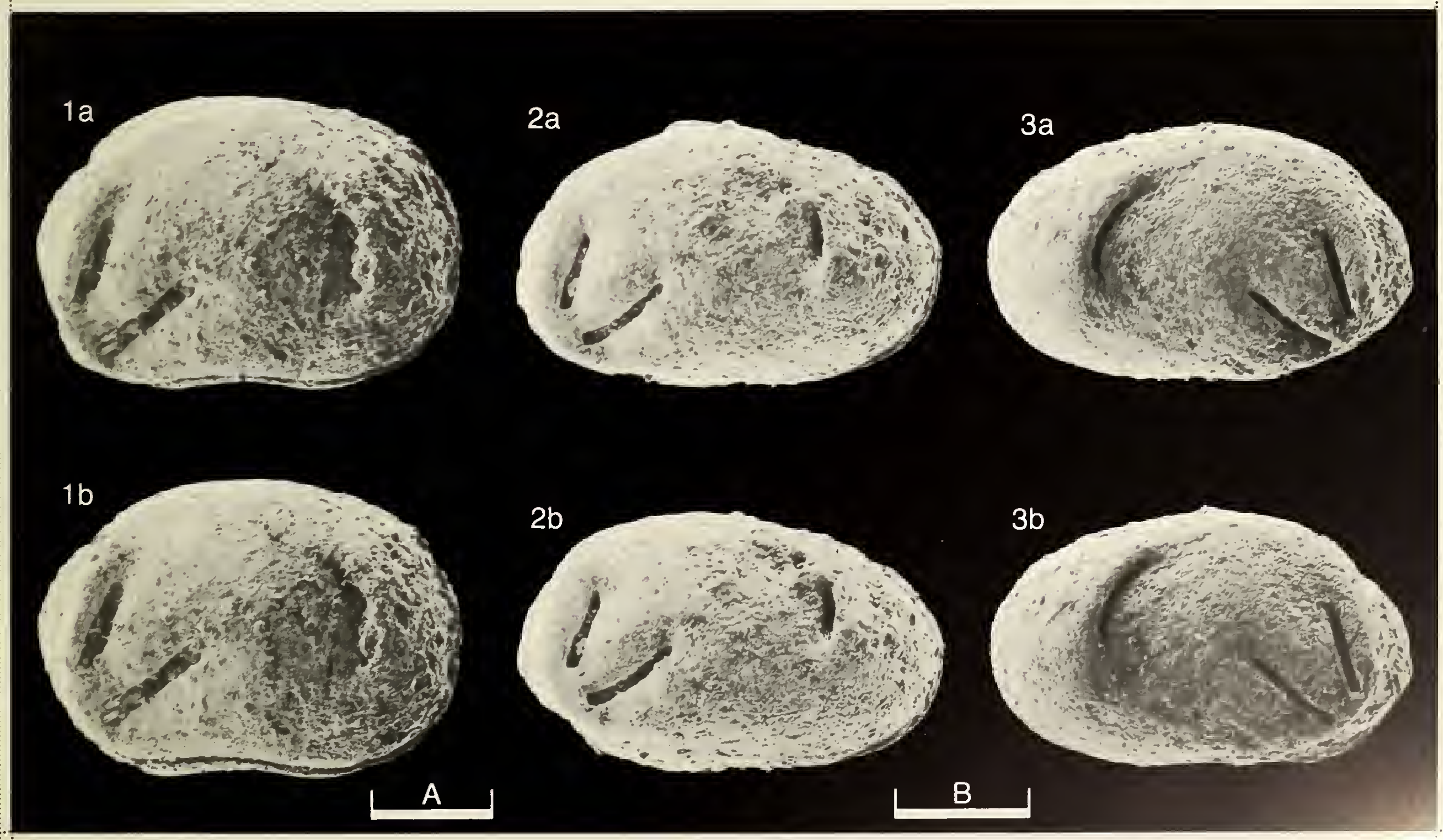
1a
2a
3a
1b
2b
3b
A
B

ON *BALTICELLA DECKERI* (HARRIS)

by Mark Williams & David J. Siveter
(University of Leicester, England)

Balticella deckeri (Harris, 1931)

1931 *Leperditella ? deckeri* n. sp., R. W. Harris, *in* C. E. Decker, *Okla. Geol. Surv. Bull.*, **55**, 89, pl. 14, figs. 5a–c.
1934 *Leperditella ? deckeri* Harris; R. S. Bassler & B. Kellet, *Geol. Soc. Am. Spec. Pap.*, **1**, 373.
1957a *Balticella deckeri* (Harris); R. W. Harris, *Okla. Geol. Surv. Bull.*, **75**, 242, pl. 8, figs. 7a–c.
1957b *Balticella deckeri* subsp. *elongata* n. subsp., R. W. Harris, *Okla. Geol. Surv. Bull.*, **75**, 242, pl. 8, fig. 8.
1962 *Balticella deckeri* (Harris); J. C. Kraft, *Geol. Soc. Am. Mem.*, **86**, 57–58, pl. 13, figs. 16, 17, pl. 14, figs. 1–10, text-figs. 10f–h.
1968 *Balticella deckeri elongata* Harris; R. E. L. Schallreuter, *Wissensch. Zeitskr. Der Ernst Moritz-Arndt-Univ. Greifswald*, **17**, Mathemat.-Naturwissensch. Reihe, 1/2, 135.

Holotype: The holotype is in the collections of the Museum of Comparative Zoology, Harvard University, USA, but without a reference number. The slide containing the holotype refers to the original figures of Harris (1931, pl. 14, figs. 5a–c). This specimen was refigured by Harris (1957a, pl. 8, figs. 7a–c). In neither publication did Harris refer his type specimen to published figures, or mention its museum reference number.

Type locality: From the top of Decker's zone 24 (see Harris, 1957), Bromide Formation; approximately 18 m below the top of the Simpson Group, Ordovician. US Highway 99 (Sec. 11, T. 1s, R3E), 3 km S of

Explanation of Plate 16, 95

Fig. 1, car. RV, ext. lat. (**MCZ unnumbered** holotype, 1.47 mm long); fig. 2, car. RV, ext. lat. (**MCZ4636**, 1.40 mm long); fig. 3, juv. LV, ext. lat. (**OS13427**, 1.27 mm long); fig. 4, juv. LV, ext. lat. (**OS13438**, 0.94 mm long); fig. 5, juv. LV, ext. lat. (**OS13439**, 0.72 mm long).

Scale A (250 μm; ×37), fig. 1; scale B (250 μm; ×44), fig. 2; scale C (250 μm; ×40), fig. 3; scale D (200 μm; ×45), fig. 4; scale E (200 μm; ×57), fig. 5.

Fittstown, Arbuckle Mountains, Oklahoma, USA; approximately latitude 34° 35′ N, longitude 96° 41′ W.

Figured specimens: Museum of Comparative Zoology (MCZ), Harvard University, USA, unnumbered specimen (holotype car.: Pl. **16**, 95, fig. 1), **MCZ4636** (car.: Pl. **16**, 95, fig. 2). British Museum (Nat. Hist.) nos. **OS13427** (juv. LV: Pl. **16**, 95, fig. 3), **OS13438** (juv. LV: Pl. **16**, 95, fig. 4), **OS13439** (juv. LV: Pl. **16**, 95, fig. 5), **OS13428** (LV: Pl. **16**, 97, fig. 1), **OS13425** (LV: Pl. **16**, 97, fig. 2, 3), **OS13426** (car.: Pl. **16**, 97, fig. 4), **OS13430** (car.: Pl. **16**, 97, fig. 5), **OS13429** (RV: Pl. **16**, 97, fig. 6).

MCZ4636 is from Decker's Zone 36, Mountain Lake Member, Bromide Formation, H99 Section, Arbuckle Mountains, Oklahoma. **OS13430** is from the Mountain Lake Member, Bromide Formation, at Rock Crossing, Criner Hills, Oklahoma. All other figured specimens are from the Edinburg Limestone, middle Ordovician, Virginia.

Diagnosis: Bisulcate balticellid; adductorial sulcus deep, preadductorial sulcus well developed. Preadductorial node pronounced, sometimes with a posterodorsally directed spine. Anterior lobe moderately well developed. Valve surface smooth. No acroidal spines.

Remarks: Harris (1957b, 242) considered his new taxon *Balticella deckeri elongata* to be a seperate subspecies of *Balticella deckeri* primarily because of its more elongate carapace and its apparently straighter and longer ventral overlap. Harris (1957b) also considered *B. deckeri elongata* to be restricted to the Tulip Greek Formation of the Simpson Group, and to be ancestral to *B. deckeri* which he considered exclusive to the Bromide Formation. Harris' referal of the distribution of *B. deckeri elongata* to the Tulip Creek Formation is incorrect, as this was based on the Highway 99 Simpson Group section. Reappraisal of the stratigraphy of this section by Fay & Grafham (*Univ. Kansas Paleontol. Contrib. Monograph* 1, 14, 1982) and by us shows that the sequence from which Harris collected his balticellids at Highway 99 in fact represents the lower member of the Bromide Formation. Balticellid ostracodes are thus restricted in Oklahoma to the Bromide Formation, Simpson Group, and do not occur in the Tulip Creek Formation.

Explanation of Plate 16, 97

Fig. 1, LV, ext. lat. (**OS13428**, 1.83 mm long); figs 2, 3, LV (**OS13425**, 1.6 mm long); fig. 2, detail of stop pegs; fig. 3, int. lat.; fig. 4, car. vent. (**OS13425**, 1.61 mm long); fig. 5, car. dors. (**OS13430**, 1.81 mm long; fig. 6, RV, int. lat. (**OS13429**, 1.40 mm long).
Scale A (250 μm; ×33), fig. 1; scale B (100 μm ×60), fig. 2; scale C (250 μm ×32), figs. 3, 4; scale D (250 μm ×32), figs. 5, 6.

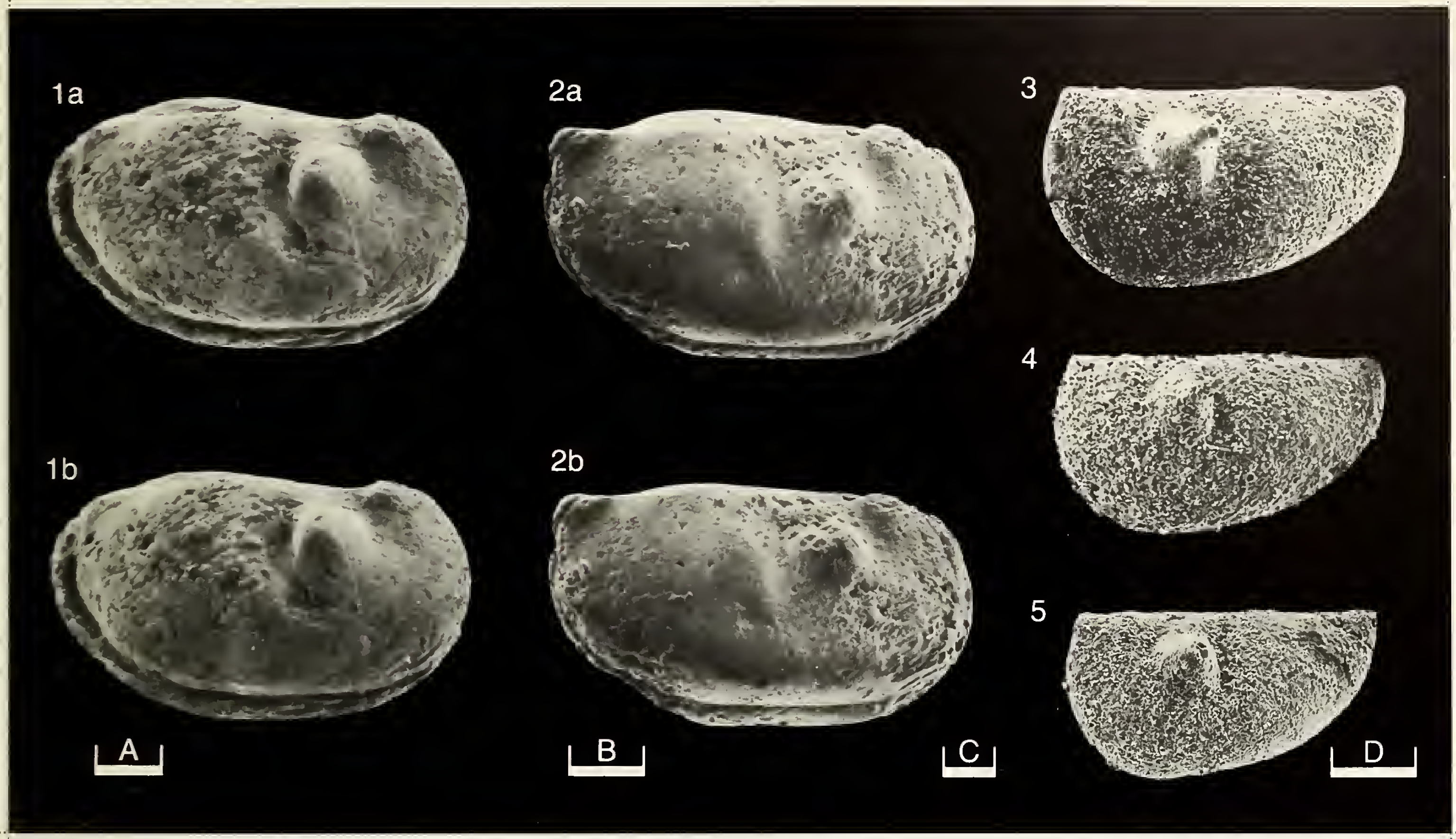
1a
2a
3
4
1b
2b
5
A
B
C
D

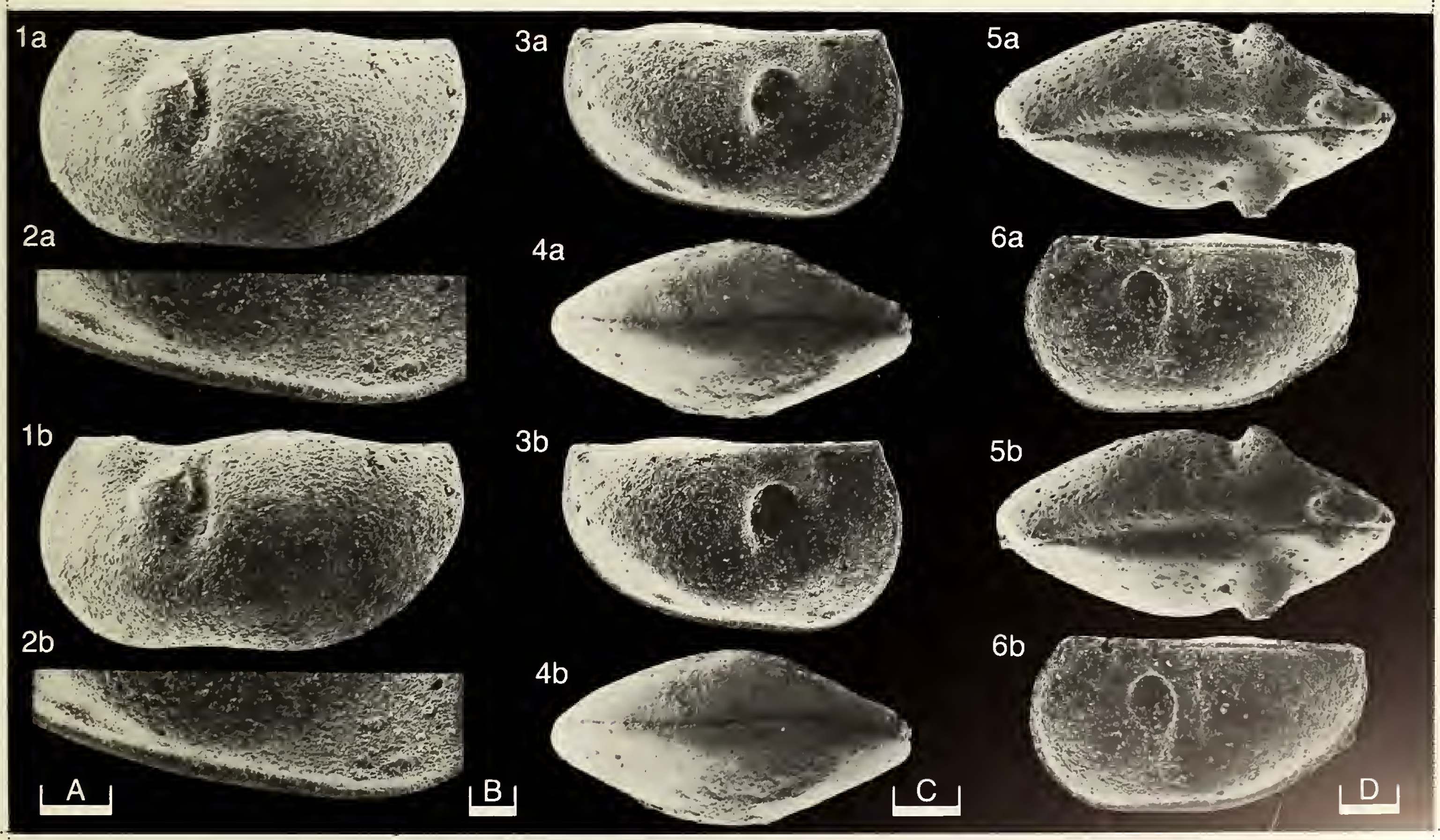
1a
3a
5a
2a
4a
6a
1b
3b
5b
2b
4b
6b
A
B
C
D

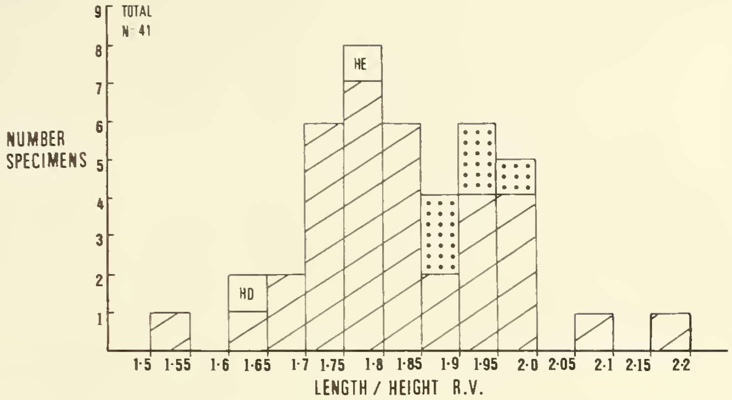

Text-fig. 1. Length–height ratios for right valves of all specimens of *B. deckeri* recovered from the Bromide Formation and some conspecific material from the Edinburg Limestone of Virginia (dotted). Holotypes: *B. deckeri elongata* of Harris (HE) and *B. deckeri* Harris (HD).

Remarks (contd.) Studies of length – height ratios for assemblages of balticellids which we have recovered from Oklahoma also convince us that *B. deckeri* and *B. deckeri elongata* should be treated as a single taxon (Text-figs. 1, 2). Both holotypes plot close together and well within the range of variation encountered in the assemblages studied. A single histogram based on all specimens of *B. deckeri* recovered from the Bromide Formation, together with additional specimens from the Edinburg Limestone of Virginia (Text-fig. 1), clearly shows that no major difference in the degree of valve elongation exists between *B. deckeri* and *B. deckeri elongata*. There is also no difference in the overlap conditions of the valves in the *Balticella* specimens that we have studied from Oklahoma.

B. deckeri is very similar to the Swedish type-species *Balticella oblonga* (Thorslund, *Sver. Geol. Unders. Ser.* C., **436**, 179, pl. 1, figs. 18–20, 1940), differing only in the more pronounced anterior lobe, the spine on the preadductorial node, and the lack of fine tuberculate ornament.

The ontogeny of *B. deckeri* is figured for the first time herein (Pl. **16**, 95). At least four moult stages are recognised. The spine on the preadductorial node appears to occur in all juvenile stages,

while the anterior lobe and the dorsal inflation of the posterior lobal area become more pronounced during ontogeny. Dimorphism is recognised in other species of *Balticella* (Schallreuter, 1968 *op. cit.*) but has not been recognised in our specimens of *B. deckeri*.

Distribution: *B. deckeri* occurs in the upper part of the Mountain Lake and Pooleville members of the Bromide formation (Whiterockian-early Mohawkian), Simpson Group, middle Ordovician, Oklahoma, USA. Also known from the Edinburg Limestone, middle Ordovician, Virginia, USA (Kraft, 1962, *op. cit.*).

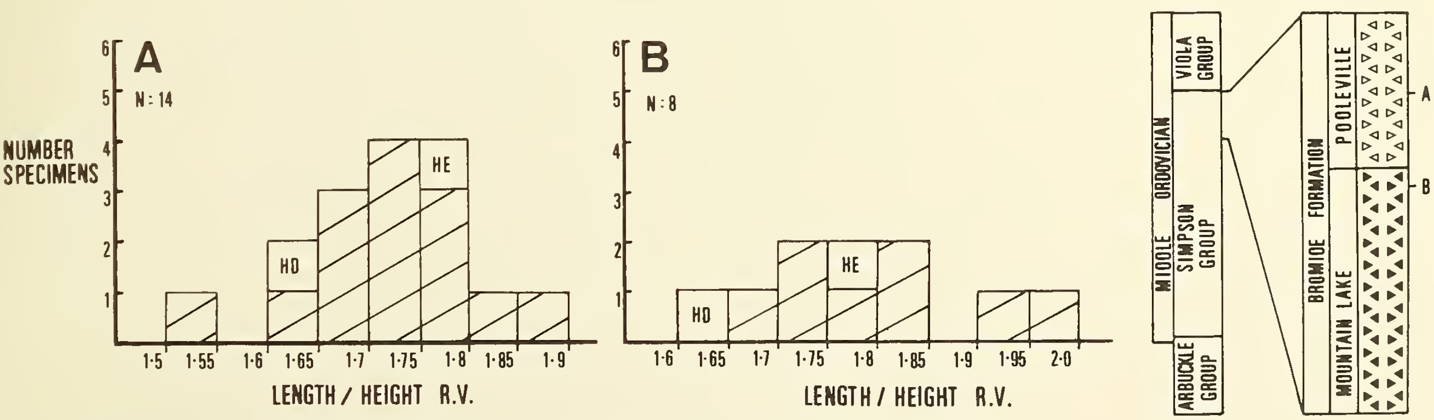

Text-fig. 2. Length–height ratio for right valves of *B. deckeri* recovered from two assemblages from the Bromide Formation. A, from the Pooleville Member; B, from the Mountain Lake Member. Holotypes: *B. deckeri elongata* of Harris (HE) and *B. deckeri* of Harris (HD).

595.336.11 (113.333) (430.2 : 161.013.53 + 013.54 + 438 : 161.017.51) : 551.351 + 552.54

ON *MACRYPSILON SALTERIANUM* (JONES)

by David J. Siveter & Wolfgang Hansch
(University of Leicester, England & University of Greifswald, GDR)

Genus *MACRYPSILON* Martinsson, 1962

Type-species (by original designation): *Beyrichia salteriana* Jones, 1855

Diagnosis: Amphitoxotidinae with very broad lobes. In tecnomorphs the more or less distinctly developed, narrow prenodal and adductorial sulci are united below the preadductorial lobe into a sulcus. Velum forms a narrow, tubulous flange extending between the anterior and the posterior cardinal cormers. Crumina large, subrounded or more elongated posteroventrally with subcruminal velar edge passing over the crumina but separated from the postcruminal part of the velum. Lobes reticulate to smooth.

Macrypsilon salterianum (Jones, 1855)

1855 *Beyrichia salteriana* nov. sp. T. R. Jones, *Ann. Mag. nat. Hist.*, ser. 2, **16**, 89, pl. 5, figs 15, 16.
1862 *Beyrichia salteriana* Jones; E. Boll, *Arch. Ver. Freunde Nat. Mecklenburg*, **16** (7), 135, pl. 1, fig. 12.
?1877 *Beyrichia salteriana* Jones; A. Krause, *Z. Dt. Geol. Ges.*, **29** (1), 35, pl. 1, fig. 17.
?1885 *Beyrichia salteriana* Jones; F. Roemer, *Pal. Abh.*, **2** (5), 109, fig. 356.
?1885 *Beyrichia salteriana* Jones; G. Reuter, *Z. Dt. Geol. Ges.*, **37** (4), 645, pl. 26, figs. 19a, b (collection is lost).
?1887 *Beyrichia salteriana* Jones; M. Verworn, *Ibid.*, **39** (1), 31, pl. 3, figs. 8, 10 (collection is lost).
?1897 *Beyrichia salteriana* Jones; K. A. Grönwall, *Sver. Geol. Unders.*, ser. C, no. 170, **19** (4), 18.
1909 *Beyrichia salteriana* Jones; J. Ch. Moberg & K. A. Grönwall, *Lunds Univ. Årsskr.*, N.F. **5** (1), 7–9, 62.

Explanation of Plate 16, 101

Figs. 1–3, 5: ♂ RV (**I 7099**, 1410 μm long): fig. 1, ext. lat.; fig. 2, ext. vent.; fig. 3, ext. post.; fig. 5, detail of syllobium. Fig. 4, tecnomorphic RV, ext. lat. (lectotype, **I 7100**, approx. 910 μm long). Fig. 6, tecnomorphic LV, ext. lat. (**I 7118**, 890 μm long). Figs. 7, 8, ♂ RV (**SGWG 83/3**, 1450 μm long): fig. 7, ext. lat.; fig. 8, ext. vent.
Scale A (200 μm; ×37), figs. 1, 2; scale B (200 μm; ×50), fig. 3; scale C (200 μm; ×52), fig. 4; scale D (150 μm; ×70), fig. 5; scale E (200 μm; ×50), fig. 6; scale F (300 μm; ×35), figs. 7, 8.

1957 *Neobeyrichia salteriana* (Jones); R. V. Kesling & K. J. Rogers, *J. Paleont.*, **31** (5), 1003, tab. 1, pl. 128, figs. 14–18.
1962 *Macrypsilon salterianum* (Jones); A. Martinsson, *Bull. Geol. Inst. Univ. Uppsala*, **41**, 17, 257, 357, fig. 2D.
1964 *Macrypsilon salterianum* (Jones); A. Martinsson, *Geol. För. Stockh. Förh.*, **86** (2), 126, 128, 133, 156, 159, fig. 15.
1964 *Macrypsilon salterianum* (Jones); M. J. Copeland, *Bull. Geol. Surv. Can.*, **117**, 5, pl. 1, figs. 4, 5.
1965 *Macrypsilon salterianum* (Jones); L. Gailite, *Izv. Akad. Nauk Latv. SSR*, **2** (211), 68.
1966 *Macrypsilon salterianum* (Jones); D. Kaljo & L. Sarv, *Izv. Akad. Nauk Est. SSR*, ser. F.- techn. nauk, **2**, 279, tab. 1.
1967 *Macrypsilon salterianum* (Jones); E. Witwicka, *Kwart. Geol.*, **2** (1), 48, pl. 2, figs. 9a–c.
1967 *Macrypsilon salterianum* (Jones); L. Gailite, *in*: L. Gailite, M. Rybnikowa & R. Ulste, *Stratigrafija, fauna i uslovija obrazovania silurijskich srednej Pribaltiki*, 128, pl. 9, figs. 5a, b, Riga (Zinatne).
1967 *Macrypsilon salterianum* A. Martinsson, *Geol. För. Stockh. Förh.*, **89** (4), 377.
1968 *M. salterianum* (Jones); L. Sarv, *Ostr. Crasp. Beyr. i Primit. silura Estoni*, 28, 98, pl. 9, fig. 1, tabs. 2, 3, Tallinn.
1969 *Macrypsilon salterianum* (Jones); R. W. L. Shaw, *Geol. För. Stockh. Förh.*, **91** (1), 68, fig. 8.
1970 *Macrypsilon salterianum* (Jones); A. Pranskevicius, *Dokl. Akad. Nauk SSSR*, **192** (6), 85.
1970 *Macrypsilon salterianum* (Jones); L. Sarv, *in*: D. Kaljo (ed.), *Silur Estonii*, 158, 169, 299, Tallinn (Valgus).
1971 *Macrypsilon salterianum* (Jones); L. Sarv, *Izv. Akad. Nauk Est. SSR*, ser. Chimija-Geol., **20** (4), 353, 355, tabs. 2, 3.
1971 *Macrypsilon salterianum* (Jones); R. W. L. Shaw, *Palaeontology*, **14** (4), 599, pl. 109, figs. 7, 8.
1972 *Macrypsilon salterianum* (Jones); L. Gailite, *Izv. Akad. Nauk Est. SSR*, ser. Chimija-Geol., **21** (4), 352.
1972 *Macrypsilon salterianum* (Jones); A. Pranskevicius, *Geol. För. Stockh. Förh.*, **94** (4), 439, 441.
1972 *Macrypsilon salterianum* (Jones); A. Pranskėvicius, *Trudy LitNIGRI*, **15**, 35, 80, 187, tabs. 4, 5, 7, 11, pl. 10, fig. 2.
1973 *Macripsilon* [*sic*] *salterianum* (Jones); B. Zbikowska, *Acta Geol. Pol.*, **23** (4), 609, 611, 613–614, 625, tab. 2, pl. 4, figs. 9, 10.
1974 *Macrypsilon salterianum* (Jones); E. Tomczykowa & E. Witwicka, *Bull. Inst. Geol.*, **276**, 59, 61, 69, figs. 2, 3.
1974 *Macrypsilon salterianum* (Jones); B. Zbikowska, *Bull. Akad. Pol. Sci.*, ser. Sci. de la Terre, **22** (1), 47.
1975 *M. salterianum*; A. Pranskevicius, *Geol. För. Stockh. Förh.*, **97** (1), 53–54.
1976 *Macrypsilon salterianum* (Jones); D. Kaljo & L. Sarv, *Izv. Akad. Nauk Est. SSR*, ser. Chimija-Geol., **25** (4), 326, 328–329.
1977 *M. salterianum*; L. Sarv, *in*: D. Kaljo (ed.), *Fazii i fauna Silura Pribaltiki*, 161, 164, 169, 173, tab. 1–3, 5, 7, Tallinn.

Explanation of Plate 16, 103

Figs. 1–3, ♀ car. (**SGWG 83/4**, 1700 μm long): fig. 1, ext. lat.; fig. 2, detail of syllobium of RV; fig. 3, ext. vent. Fig. 4, ♀ LV, detail of ventral part of crumina (**SGWG 83/5**, approx. 1540 μm long). Figs. 5–7: ♀ LV (**SGWG 83/6**, 1340 μm long): fig. 5, ext. post.; fig. 6, ext. lat.; fig. 7, ext. vent. Scale A (200 μm; ×30), figs. 1, 3; scale B (75 μm; ×120), fig. 2; scale C (20 μm; ×540), fig. 4; scale D (200 μm; ×45), fig. 5; scale E (200 μm; ×40), figs. 6, 7.

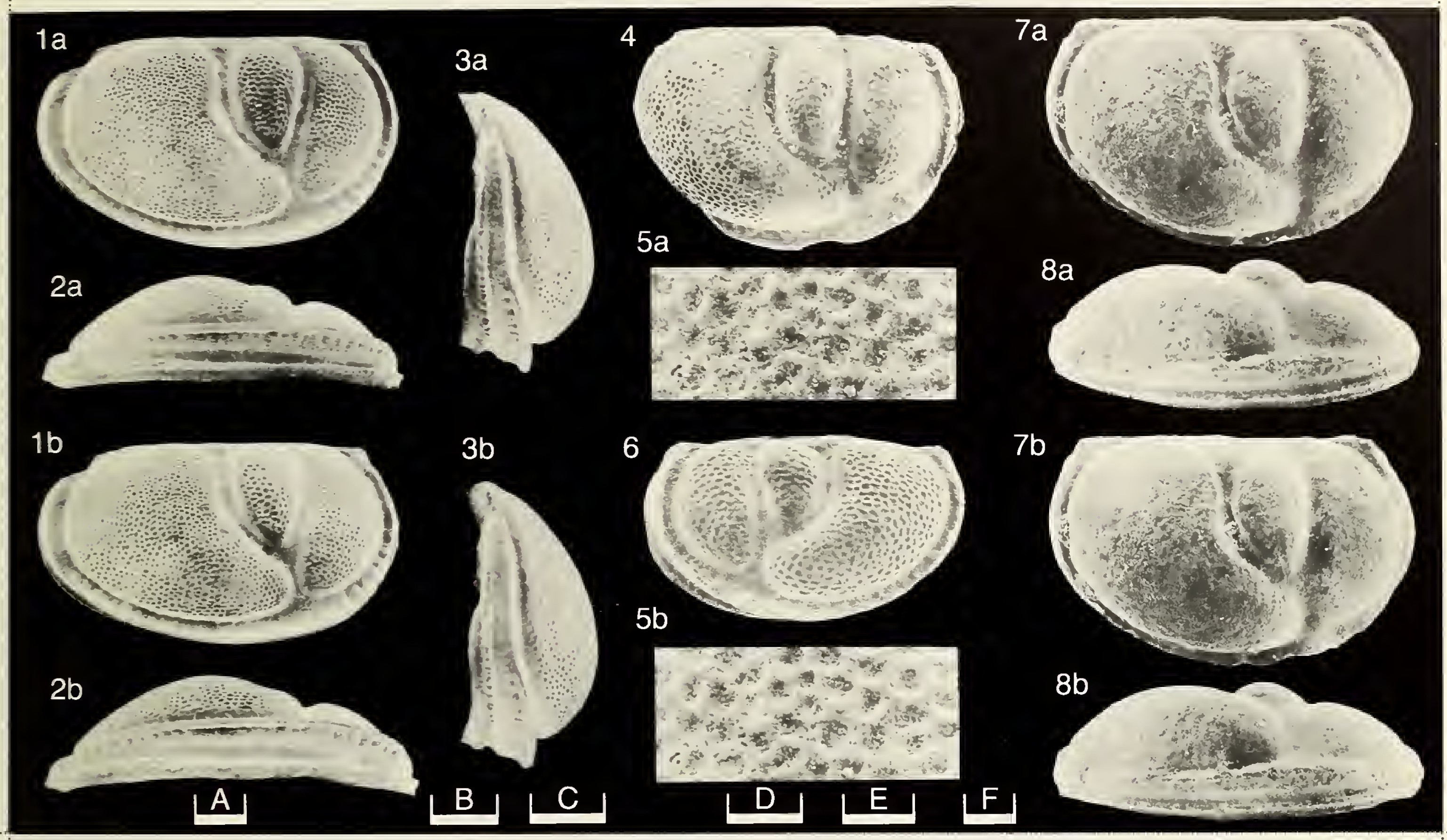
1a
3a
4
7a
5a
2a
8a
1b
3b
6
7b
5b
2b
8b
A
B
C
D
E
F

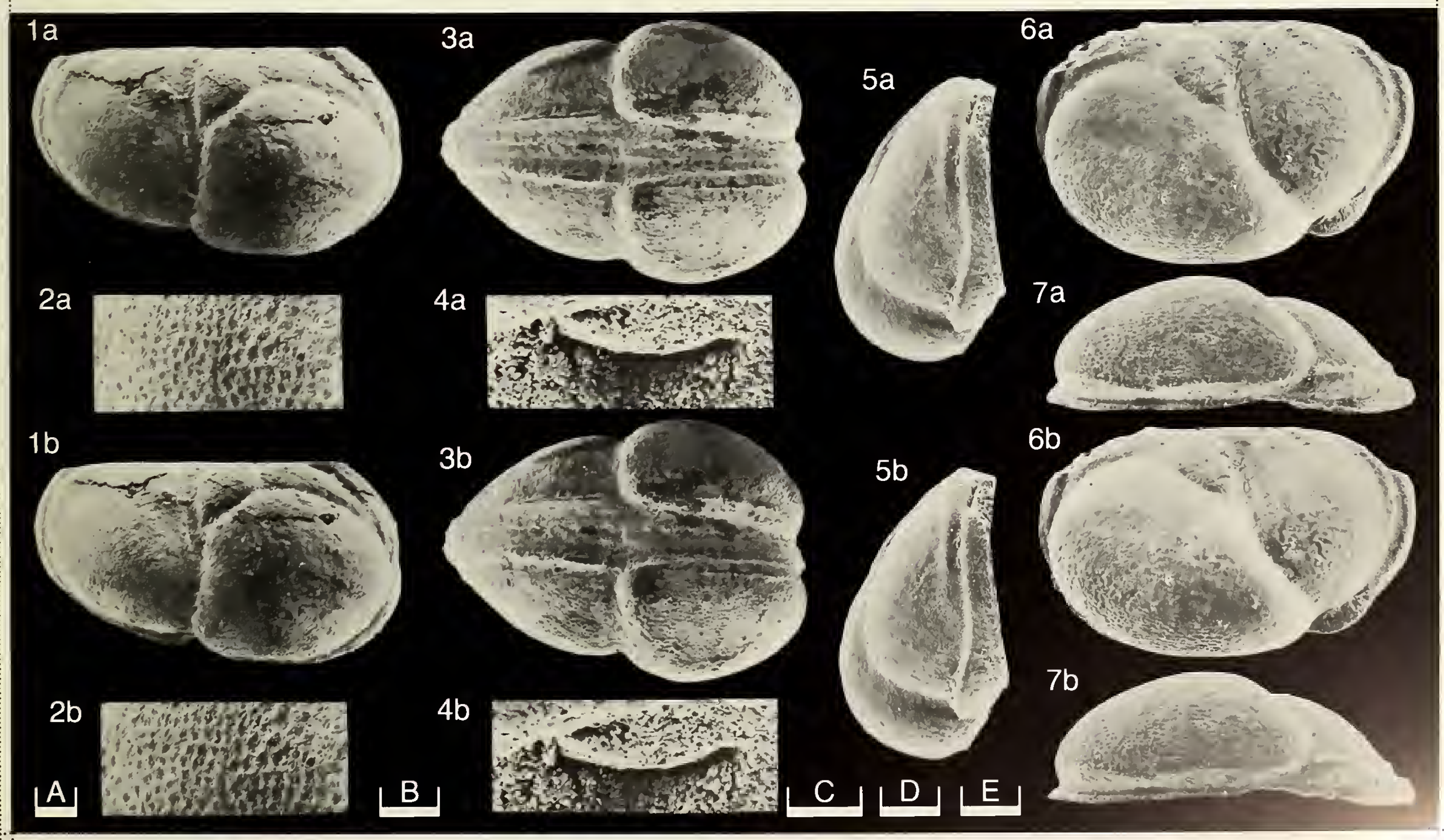
1a
3a
6a
5a
2a
4a
7a
1b
3b
6b
5b
7b
2b
4b
A
B
C
D
E

1977 *Macrypsilon salterianum* (Jones); M. J. Copeland & J. M. Berdan, *Geol. Surv. Canada, Paper* **77–1B**, pl. 2, 3, figs. 17, 18.
?1977 *Macrypsilon* sp.; M. J. Copeland & J. M. Berdan, *Ibid.*, pl. 2, 3, fig. 27.
1977 *Macrypsilon salterianum*; A. Martinsson. *The Silurian-Devonian Boundary, IUGS* ser. A, no. 5, 48, 329.
1978 *Macrypsilon salterianum*; D. J. Siveter. *in*: R. H. Bate & E. Robinson (eds.), *Geol. J. Sp. Iss.*, **8**, 68, 8, pl. 8, figs. 1, 2.
1978 *Macrypsilon salterianum* (Jones); L. Gailite, *in*: *Stratigrafija fanerozoja Pribaltiki*, 13, 16, 18–19, 21, Riga (Zinatne).
1980 *Macrypsilon salterianum* (Jones); D. J. Siveter, *Palaeontogr. Soc. (Monogr.)*, **133** (556), 54, pl. 10, figs. 8, 13.
1982 *Macrypsilon salterianum*; L. Sarv, *in*: *Ecostratigraphy of the East Baltic Silurian*, 75, Tallinn (Valgus).
1985 *Macrypsilon salterianum* (Jones); W. Hansch, *Lethaia*, **18** (4), 375, tab. 1.
1986 *M. salterianum* (Jones); N. Sidaraviciene, *in*: D. Kaljo & E. Klaamann (eds.), *Teorija opyt ekostratigrafija*, 120, 124, Tallinn.
1986 *Macrypsilon salterianum* (Jones); L. Gailite, *Ibid.*, 114.
1989 *M. salterianum* (Jones); D. Siveter, *in*: C. Holland & M. Bassett (eds.), *Global standard for the Silurian*, fig. 1681, Nat. Mus. Wales **9**, Cardiff.

Lectotype: British Museum (Nat. Hist.), no. **I7100**; tecnomorphic RV. Martinsson, 1962, fig. 2D.
[Paratypes: British Museum (Nat. Hist.) **I7118**, tecnomorphic LV; Jones, 1855, pl. 5, fig. 16, **I7099**, ♂ RV; Jones, 1855, pl. 5, fig. 15a, b.]

Type locality: Erratic boulder no. 5 of Jones, 1855, near Breslau (Wrowław), Poland; approx. lat. 51°5′ N, long. 17°E. Upper Silurian.

Figured specimens: British Museum (Nat. Hist.) nos. **I7100** (lectotype, tecnomorphic RV: Pl. **16**, 101, fig. 4), **I7099** (paratype, ♂ RV: Pl. **16**, 101, figs. 1–3, 5), **I7118** (paratype, tecnomorphic LV: Pl. **16**, 101, fig. 6). All from erratic boulder no. 5 of Jones, 1855, near Breslau (Wrocław), Poland. Sektion Geologische Wissenschaften der E.-M.-Arndt-Universitat Greifswald, German Democratic Republic (GDR), nos. **SGWG 83/3** (♂ RV: Pl. **16**, 101, figs. 7, 8), from erratic boulder no. Bey. A20, Zarrenthin b. Jarmen, GDR, approx. lat. 53°56′ N, long. 13°21′ E; **SGWG 83/4** (♀ car.: Pl. **16**, 103, figs. 1–3), from erratic boulder no. Bey. E50, Gager, Isle of Ruegen, GDR, approx. lat. 54°17′ N, long. 13°35′ E; **SGWG 83/5** (♀ LV: Pl. **16**, 103, fig. 4), from erratic boulder no. Bey. A32, Zarrenthin b. Jarmen, GDR; **SGWG 83/6** (♀ LV: Pl. **16**, 103, figs. 5–7) from erratic boulder no. Bey. E12, Gager, Isle of Ruegen, GDR. All specimens Upper Silurian.

Diagnosis: Species of *Macrypsilon* in which the tecnomorphs have narrow, distinct sulci.

Remarks: *M. salterianum* differs from *M. parvisulcatum* (Sarv 1968) in its more distinctly developed sulci. The wide stratigraphic range of *M. salterianum* may be due to confusion between closely related species (Martinsson 1977, Siveter 1989). *M. salterianum* shows wide variation between populations in surface ornament, cruminal shape, the development of the supersulcal tubercle-like feature, the extent of the depression in the posterodorsal part of the syllobium and the development of the postcruminal wing-like part of the velum. It is not obvious that the variations are restricted to a stratigraphic level or geographic province. The occurrence of *M. salterianum* in Scania (L. Jeppsson & S. Laufeld 1987, *Sver. Geol. Unders.*, ser. Ca, no. 58, fig. 3) is probable because the species occurs in the coeval "Red Beyrichienkalk boulders" (Hansch 1985).

Distribution: Upper Ludlow Přidoli series, Silurian, Canada: Stonehouse Formation, Nova Scotia (Copeland 1964, Copeland & Berdan 1977). Pembroke Formation, Maine, USA? (Siveter 1980).

Great Britain: Kirkby Moor Flags and Scout Hill Flags, Lake District; Upper Whitcliffe and Downton Castle Sandstone formations, Long Mountain region (Shaw 1969, 1971; Siveter 1980).

Peribaltic area of Poland: Chlapowo borehole; post-Ludlow (Witwicka 1967). Łeba 1 borehole, Beyrichienkalk pebbles in the Zechsteinkonglomerat (Martinsson 1964). Leba 2 & 8, Debki 2 and Piasnica 2 boreholes; post-Ludlow, *Neobeyrichia incerta* to *Nodibeyrichia tuberculata* zones (Zbikowska 1973). Miloszewo, Wejherowo, Karwia, Opalino, Salino, Białogard and Łeba-IG 1 boreholes; post-Ludlow, *Frostiella pliculata* to *Nodibeyrichia gedanensis* zones (Tomczykowa & Witwicka 1974). Chojnice borehole; post-Ludlow (Zbikowska 1974).

East Baltic area, USSR: Ohesaare 1 & 2 boreholes, Isle of Saaremaa, Estonia; Kaugatuma and Ohesaare formations (Sarv 1971). Piltene 1, 31 & 32, Stoniskjaj, Kolka 4 & 54 and Pavilosta 51 boreholes, Latvia; Minija and Jura formations (Gailite 1967, 1978). Taurage and Kunkojaj boreholes, Minija Formation (Pranskevicius 1972); boreholes 87, 94, 96, 98, 108, 110, 112 (Minija Formation), boreholes 89, 94, 96, 98, 108, 110, 112 (Jura Formation), Arjogalskij profile, Lithuania (Sidaraviciene 1986). Gusev 5 borehole, Minija Formation (Pranskevicius 1972) and Dubovskoje borehole, Kaugatuma Formation, Kaliningrad district (Kaljo & Sarv 1976).

Sweden: Klinta Formation and Öved Sandstone *sensu* Jeppsson & Laufeld (1987), Scania; see also Grönwall (1897), Moberg & Grönwall (1909), and Martinsson (1967, 375).

Erratic boulders: Beyrichienkalk *sensu* Martinsson (1963, 1967, 1977); Beyrichienkalk type B, C, D and "Red Beyrichienkalk" *sensu* Hansch (1985).

595.336.11 (113.333) (430.2 : 161.013.52 + 013.54) : 551.351 + 552.54

ON *BEROLINELLA STEUSLOFFI* (KRAUSE)

by Wolfgang Hansch & David J. Siveter
(University of Greifswald, German Democratic Republic & University of Leicester, England)

Genus *BEROLINELLA* Martinsson, 1962
Type-species (by original designation): *Beyrichia steusloffi* Krause, 1891

Diagnosis: Amphitoxotidinae having a basal crest along a wide tubulous velum in both sexes. The tubulous, uninterrupted velar edge and the torus, which forms a sharp basal ridge, both continue across the crumina (slightly modified after Martinsson 1962, *op. cit.*).

Remarks: The beyrichiacean Amphitoxotidinae *Berolinella, Dibolbina* Ulrich & Bassler, 1923, *Huntonella* Lundin, 1968, and *Tropidotoxotis* Siveter, 1980 all have a reasonably complete velar edge cross the crumina, and are distinguished largely on details of subcruminal, velar and basal crest morphology (see Siveter, *Palaeontogr. Soc. (Monogr.)*, **133** (556), 69, 1980). Besides *B. steusloffi* the genus currently includes only *B. praevia* Sarv, 1968, and an undescribed species from Baltic erratic boulders (Martinsson, 1962).

Explanation of Plate 16, 107

Figs. 1, 2, ♀ LV (**SGWG 83/1**, approx. 1040 μm long): fig. 1, ext. lat.; fig. 2, ext. vent. Figs. 3, 4, ♂ RV (**SGWG 83/2**, approx. 1200 μm long): fig. 3, ext. vent.; fig. 4, ext. lat.
Scale A (200 μm; ×55), figs. 1, 2; scale B (200 μm; ×65), fig. 3; scale C (200 μm; ×45), fig. 4.

Berolinella steusloffi (Krause, 1891)

1891 *Beyrichia steusloffi* sp. nov. A. Krause, *Z. Dt. Geol. Ges.*, **43** (2), 505, pl. 32, figs. 6, 8, 9; ?7a, b.
?1894 *B. steusloffi* Kr.; A. Steusloff, *Ibid.*, **46** (4), 786.
?1895 *Beyrichia steusloffi* Krause; J. Ch. Moberg, *Sver. Geol. Unders.*, ser. C, no. 156, 7, 14.
?1897 *Beyrichia steusloffi* Krause; K. A. Grönwall, *Ibid.*, no. 170, 204, 218, 224, 227, 238.
?1908 *Beyrichia steusloffi* Krause; E. O. Ulrich & R. S. Bassler, *Proc. U.S. Nat. Mus.*, **35** (1646), 286.
non 1909 *Beyrichia steusloffi* A. Krause; J. Ch. Moberg & K. A. Grönwall, *Lunds Univ. Årsskr.*, N.F. **5** (1), 7, 9, 12, 25, 63, 81, 86, pl. 4, figs. 14, 15.
?1916 *B. steusloffi* Krause; J. Botke, *Verh. Geol.-Mijnbouwk. Genootschap v. Nederland en Kolonien*, 3, 26.
non 1919 *Beyrichia steusloffi* Krause; J. Hede, *Geol. För. Stockh. Förh.*, **41**, 135, pl. 5.
?1934 *Beyrichia steusloffi* Krause; R. S. Bassler & B. Kellett, *Geol. Soc. America*, Spec. Pap. **1**, 206.
?1954 *Beyrichia steusloffi*; G. Henningsmoen, *Norsk. Geol. Tidsskr.*, **34**, 29.
1956 *Dibolbina steusloffi* (Krause); R. V. Kesling, *Contr. Mus. Paleont. Univ. Michigan*, **13** (2), 56, pl. 4, figs. 1–10, pl. 5, figs. 1–6 (incorrect reconstruction).
1957 *Dibolbina steusloffi* (Krause); R. V. Kesling & K. J. Rogers, *J. Paleont.*, **31** (4), 1000, pl. 127, figs. 15–21.
1962 *Berolinella steusloffi* (Krause); A. Martinsson, *Bull. Geol. Inst. Univ. Uppsala*, **41**, 107, 253, figs. 39:9, 129A.
1963 *Berolinella steusloffi*; A. Martinsson, *Geol. För. Stockh. Förh.*, **85** (3), 293, 295.
1964 *Berolinella steusloffi* (Krause); A. Martinsson, *Ibid.*, **86** (2), 128. 135, 156, 159, fig. 15 (log).
1966 *Berolinella steusloffi* (Krause); D. Kaljo & L. Sarv, *Izv. Akad. Nauk Est. SSR*, ser. Fisiko-Matem. i techn. nauk, **2**, 279, tab. 1.
1967 *Berolinella steusloffi*; A. Martinsson, *Geol. För. Stockh Förh.*, **89** (4), 377.

Explanation of Plate 16, 109

Fig. 1, ♀ RV, ext. lat. (**I 6007a**, 1210 μm long); fig. 2, ♀ LV, ext. ant. (**SGWG 83/1**). Figs. 3, 4, tecnomorphic RV (**I 6007b**, 1010 μm long): fig. 3, ext. lat.; fig. 4, ext. vent. Figs. 5, 6, ♂ RV (**SGWG 83/2**): fig. 5, detail of post. margin; fig. 6, detail of velum.
Scale A (200 μm; ×45), fig. 1; scale B (200 μm; ×60), fig. 2; scale C (200 μm; ×55), figs. 3, 4; scale D (50 μm; ×190), fig. 5; scale E (50 μm; ×280), fig. 6.

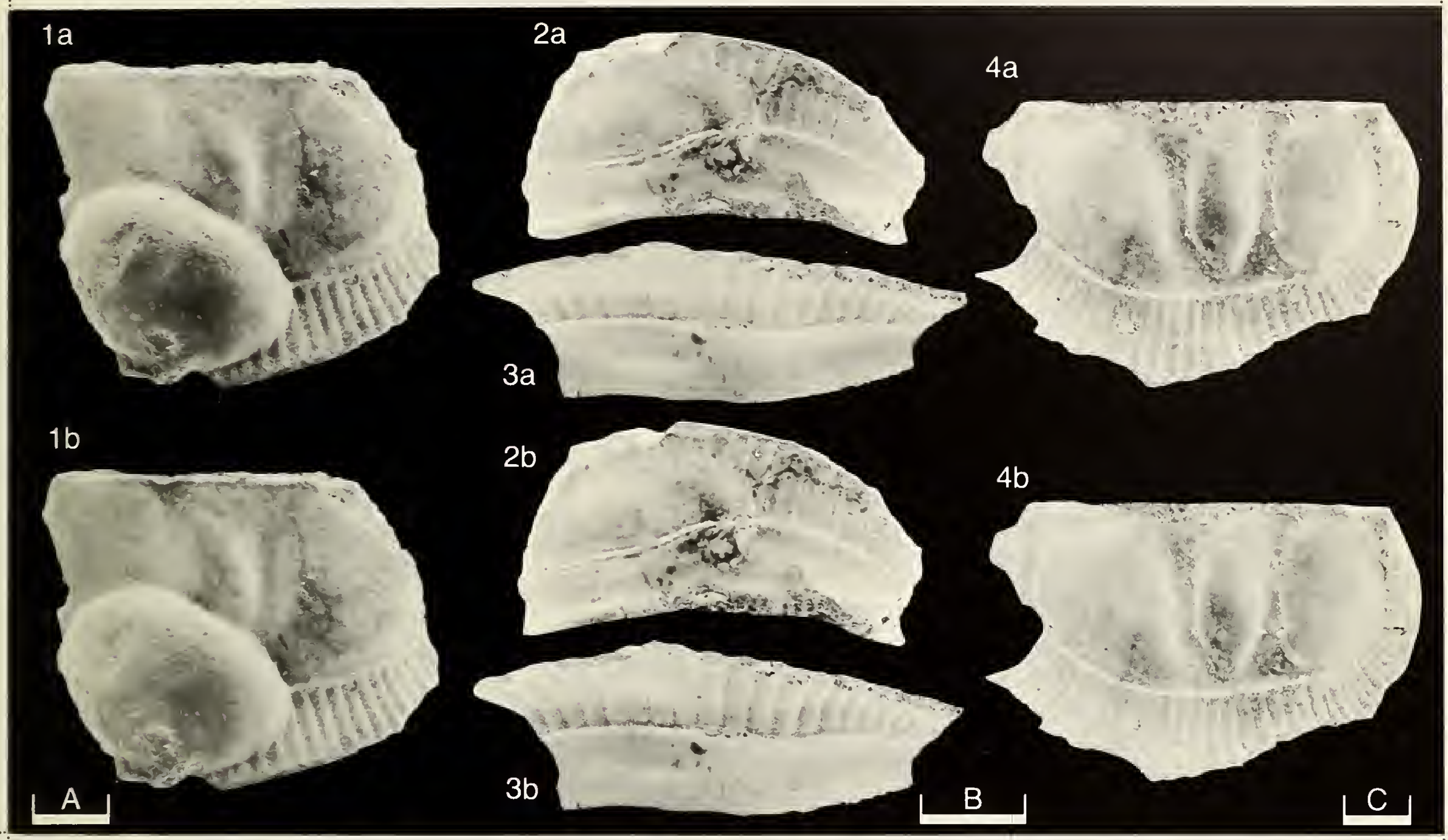
1a
2a
4a
3a
1b
2b
4b
3b
A
B
C

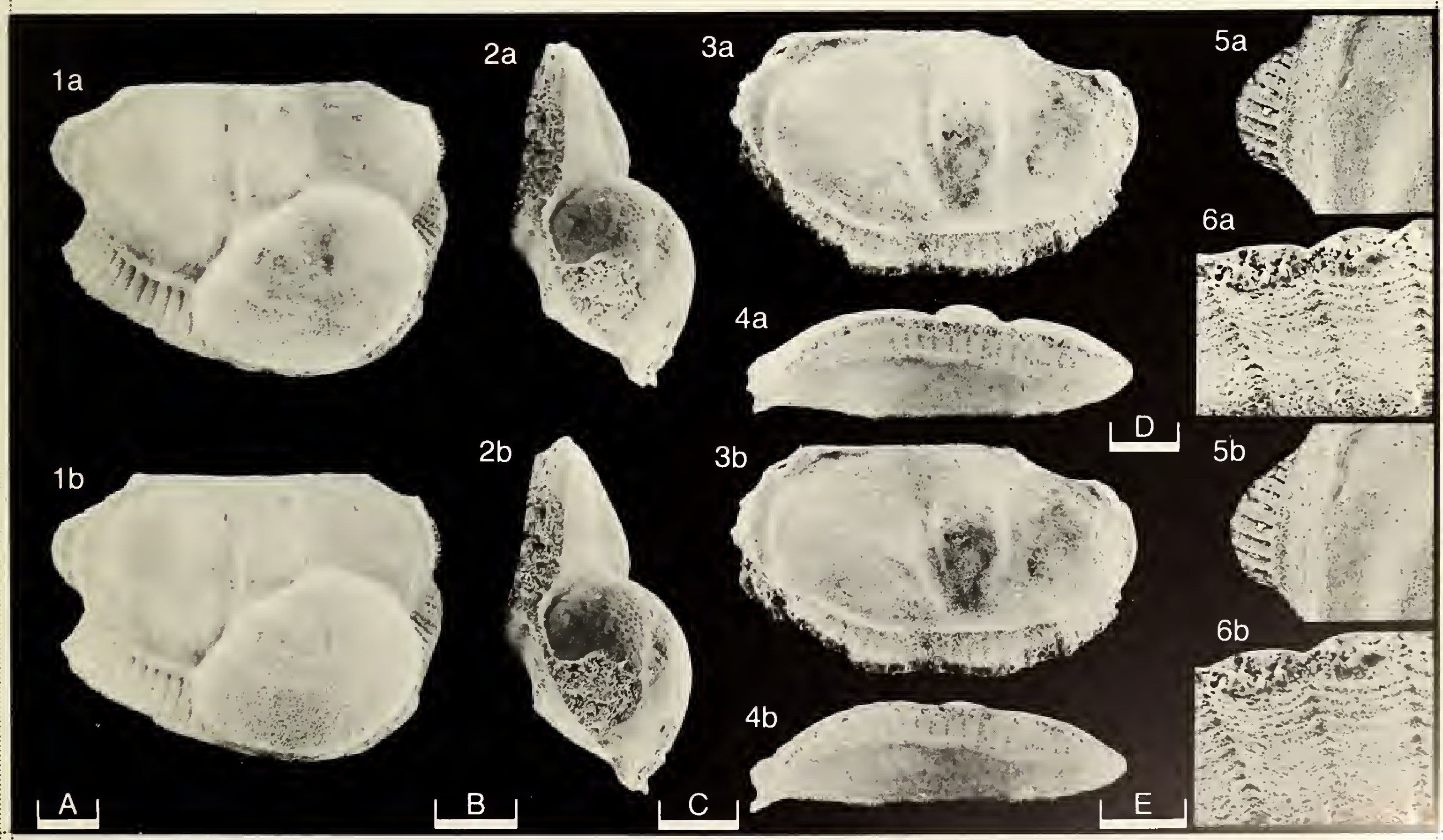
1a
2a
3a
5a
6a
4a
D
1b
2b
3b
5b
6b
4b
A
B
C
E

1968 *Berolinella steusloffi* (Krause); L. Sarv, *Ostrakody Craspedobolbinidae, Beyrichiidae i Primitiopsidae Silur Estonii*, 27, 95, tabs. 2, 3, pl. 7, figs. 9, 10, Tallinn (Valgus).
1970 *Berolinella steusloffi* (Krause); L. Sarv, *in*: D. Kaljo (ed.), *Silur Estonii*, 158, 169, 299, Tallinn (Valgus).
1971 *Berolinella steusloffi*; L. Sarv, *Izv. Akad. Nauk Est. SSR*, ser. Chimija-Geol., **20** (4), 353, tab. 3.
1973 *Berolinella steusloffi* (Krause); B. Zbikowska, *Acta Geol. Pol.*, **23** (4), 613, 625, pl. 4, fig. 8, tab. 2.
?1975 *Berolinella steusloffi*; A. Pranskevicius, *Geol. För. Stockh. Förh.*, **97** (1), 53.
1977 *Berolinella steusloffi*; L. Sarv, *in*: D. Kaljo (ed.), *Fazii i fauna Silura Pribaltiki*, 165, 173, tab. 3, Tallinn (Valgus).
1977 *Berolinella steusloffi*; A. Martinsson, *The Silurian-Devonian Boundary, IUGS* ser. A, no. 5, 48.
1978 *Berolinella steusloffi* (Krause); D. J. Siveter, *in*: R. H. Bate & E. Robinson (eds.), *A Stratigraphical Index of British Ostracoda, Geol. J. Spec. Issue*, **8**, 69.
1985 *Berolinella steusloffi* (Krause); W. Hansch, *Lethaia*, 18 (4), 274, tab. 1.
1989 *Berolinella steusloffi* (Krause); D. J. Siveter, *in*: C. H. Holland & M. G. Bassett (eds.), *A global standard for the Silurian*, 263, fig. 168D, Nat. Mus. Wales Geol. ser. no. 9, Cardiff.

Lectotype: Museum für Naturkunde Berlin, German Democratic Republic (GDR), no. **MBO 117**; ♀ RV. Krause, 1891, pl. 32, fig. 9. Designated by Sarv, 1968.
[Paratype: **MBO 118**, tecnomorphic RV.]

Type locality: Erratic boulder, Beyrichienkalk no. 470 of Krause, 1891. From Müggelheim, Berlin, GDR; approx. lat. 52°32′N, long. 13°25′E. Přidoli Series, Silurian.

Figured specimens: Sektion Geologische Wissenschaften der E.-M.-Arndt-Universitat Greifswald, GDR, nos. **SGWG 83/1** (♀ LV: Pl. **16**, 107, figs. 1, 2; Pl. **16**, 109, fig. 2); **SGWG 83/2** (♂ RV: Pl. **16**, 107, figs. 3, 4; Pl. **16**, 109, figs. 5, 6). Both from erratic boulder no. Bey. E7, Gager, Isle of Ruegen, GDR, approx. lat. 54°17′N, long. 13°45′E. British Museum (Nat. Hist.), nos. **I 6007a** (♀ RV: Pl. **16**, 109, fig. 1), **I 6007b** (tecnomorphic RV: Pl. **16**, 109, figs. 3, 4). Both from erratic boulder no. 600 of Krause, Müggelheim, Berlin, GDR. All specimens are of Přidoli Series age, Silurian.

Diagnosis: Species of *Berolinella* with similar, well developed prenodal and adductorial sulci, in tecnomorphs extending from the dorsal margin to the narrow depression above the basal crest of the wide tubulous velum. Torus and velar edge cross the crumina but not parallel to each other. Velum also occurs in front of the crumina and is restricted posteroventrally in both dimorphs.

Remarks: Kesling's (1956) reconstruction of *B. steusloffi*, showing an entire velum, is incorrect (cf. diagnosis above). *B. praevia* differs by having less distinct sulci, parallel torus and velar edge across the crumina and a more acuminate crumina. The type material of Krause, 1891, figs. 6, 7 is probably lost; according to his figures, it differs somewhat from the typical *B. steusloffi*. *Berolinella* sp. n. of Martinsson (1962, 253, fig. 129B) may be conspecific with *B. praevia*. The "*B. steusloffi*" specimens of Moberg & Grönwall (1909) do not belong to *B. steusloffi*; possibly they represent a new species, but it is impossible to prepare the material in their slabs to confirm this judgement.

Distribution: *B. steusloffi* is the youngest *Berolinella* species and is restricted to the Přidoli Series, Upper Silurian.

Peribaltic area of Poland: Łeba 1 borehole, Beyrichienkalk pebbles in the Zechsteinkonglomerat (Martinsson 1964). Debki 3 borehole, post-Ludlow, *Nodibeyrichia tuberculata* Zone (Zbikowska 1973).

East Baltic area, USSR: Ohesaare 2 borehole, Ohesaare-Kliff, Isle of Saaremaa; Ohesaare Formation (Sarv 1968, 1971). Piltene 32 borehole Latvia; Ohesaare Formation (Sarv 1977).

Erratic boulders: Beyrichienkalk *sensu stricto* (of Martinsson 1963, 1967, 1977 and Beyrichienkalk type C *sensu* Hansch (1985).

595.336.14 (113.6) (775 : 162.102.30) : 551.351 + 552.54

ON *AURIKIRKBYA WORDENSIS* (HAMILTON)

by Gerhard Becker & Franciszek Adamczak
(University of Frankfurt, Federal Republic of Germany & University of Stockholm, Sweden)

Genus *AURIKIRKBYA* Sohn, 1950
Type-species (by original designation): *Kirkbya wordensis* Hamilton, 1942

Diagnosis: Kirkbyid genus with two distinct lateral lobes joined by a connecting lobe.

Remarks: The adventral structure ('velum') is a well developed ridge. The outer list of the contact groove is terminated dorsally by both an anterior and posterior tooth. The right hinge is provided with a list and the left hinge with a groove. The right valve is the larger valve and overlaps the smaller left valve along the free margin. The kirkbyan pit is distinct and situated below the connecting lobe.

Distribution: N America; lower Pennsylvanian to Permian. W Europe; late Upper Devonian (upper Famennian) and Upper Carboniferous (Westphalian).

Aurikirkbya wordensis (Hamilton, 1942)

1942 *Kirkbya wordensis* sp. nov. I. B. Hamilton, *J. Paleont.*, **16**, 713, 714, pl. 110, fig. 13.
1950 *Aurikirkbya wordensis* (Hamilton); I. G. Sohn, *U.S. Geol. Surv. prof. Pap.*, **221–C**, 36, pl. 7, figs. 1–13.
1954 *Aurikirkbya wordensis* (Hamilton); I. G. Sohn, *U.S. Geol. Surv. prof. Pap.*, **264–A**, 9, pl. 4, figs. 9, 21.
1961 *Aurikirkbya wordensis* (Hamilton); I. G. Sohn, *U.S. Geol. Surv. prof. Pap*, **330–A**, 141.
1961 *Aurikirkbya wordensis* (Hamilton); I. G. Sohn, *in*: R. C. Moore (ed.), *Treatise Invert. Paleontol. Pt.*, **Q** (3), 164, text-fig. 95/3.

Holotype: University of Wisconsin, Madison, Wisconsin, USA, no. **22373**; an adult LV.

Explanation of Plate 16, 113

Figs. 1, 2, adult RV (**USNM 110232a**, 1430 μm long): fig. 1, ext. lat.; fig. 2, ext. vent. obl.
Scale (300 μm; ×60), figs. 1, 2.

Type locality: Scarp N of former Old Word Ranch house NE Marathon, Hess Canyon quadrangle, Glass Mountains, Brewster County, W Texas, USA (US National Museum locality 703[c]); lat. 30° 16′ N, long. 103° 10′ W. Irregular lenses of bituminous limestone in siliceous shales; uppermost Leonard or lowermost Word Formation, Middle Permian.

Figured specimens: United States National Museum (USNM), Washington DC, USA, nos. **USNM 110232a** (adult RV: Pl. **16**, 113, figs. 1, 2; Pl. **16**, 115, fig. 2), **USNM 110232b** (adult LV: Pl. **16**, 115, fig. 3), **USNM 110232c** (juv. RV: Pl. **16**, 115, fig. 1).
All of the figured specimens are topotype material.

Diagnosis: *Aurikirkbya* species with a crenulated contact groove, an indistinct connecting lobe and very indistinct lobal ridges ('flanges') both anteriorly and posteriorly. Posterior (postsulcal) lobe distinct and subtriangular in dorsal view.

Remarks: Sohn (1954, 9; 1961, 140) described in some N American *Aurikirkbya* species "the shell wall of the venter [to be] very thick" and considered this feature to be characteristic for the genus. In *A. wordensis* the shell of the connecting lobe also seems to be very thick; however, it is (like the shell of the venter) not solid but is porous (= economic construction).

The contact groove of the larger, right valve is crenulated. The crenulation is also visible in the figure as illustrated by Sohn (1959, pl. 7, fig. 12b). A crenulated contact groove is also known in *Ogmoconchella* Gruendel, 1964 (Metacopina). In *A. wordensis* the corresponding contact list is most probably smooth. These contact features are interpreted here as associated with water circulation and filter-feeding ("weir-basket").

In some specimens (see Plate **16**, 115, fig. 3) the internal valve margin seems to be thickened. This does not demonstrate a calcified inner lamella; most probably it is an artifact product of silicification.

Distribution: Texas, USA; uppermost Leonard or lowermost Word Formation, Middle Permian.

Explanation of Plate 16, 115

Fig. 1, juv. RV, int. lat. (**USNM 110232c**, 890 μm long); fig. 2, adult RV, int. lat., detail ant. vent. (**USNM 110232a**, 1430 μm long); fig. 3, adult LV, int. lat. (**USNM 110232b**, 1480 μm long).
Scale A (300 μm; ×98), fig.1; scale B (30 μm; ×215), fig. 2; scale C (300 μm; ×53), fig. 3.

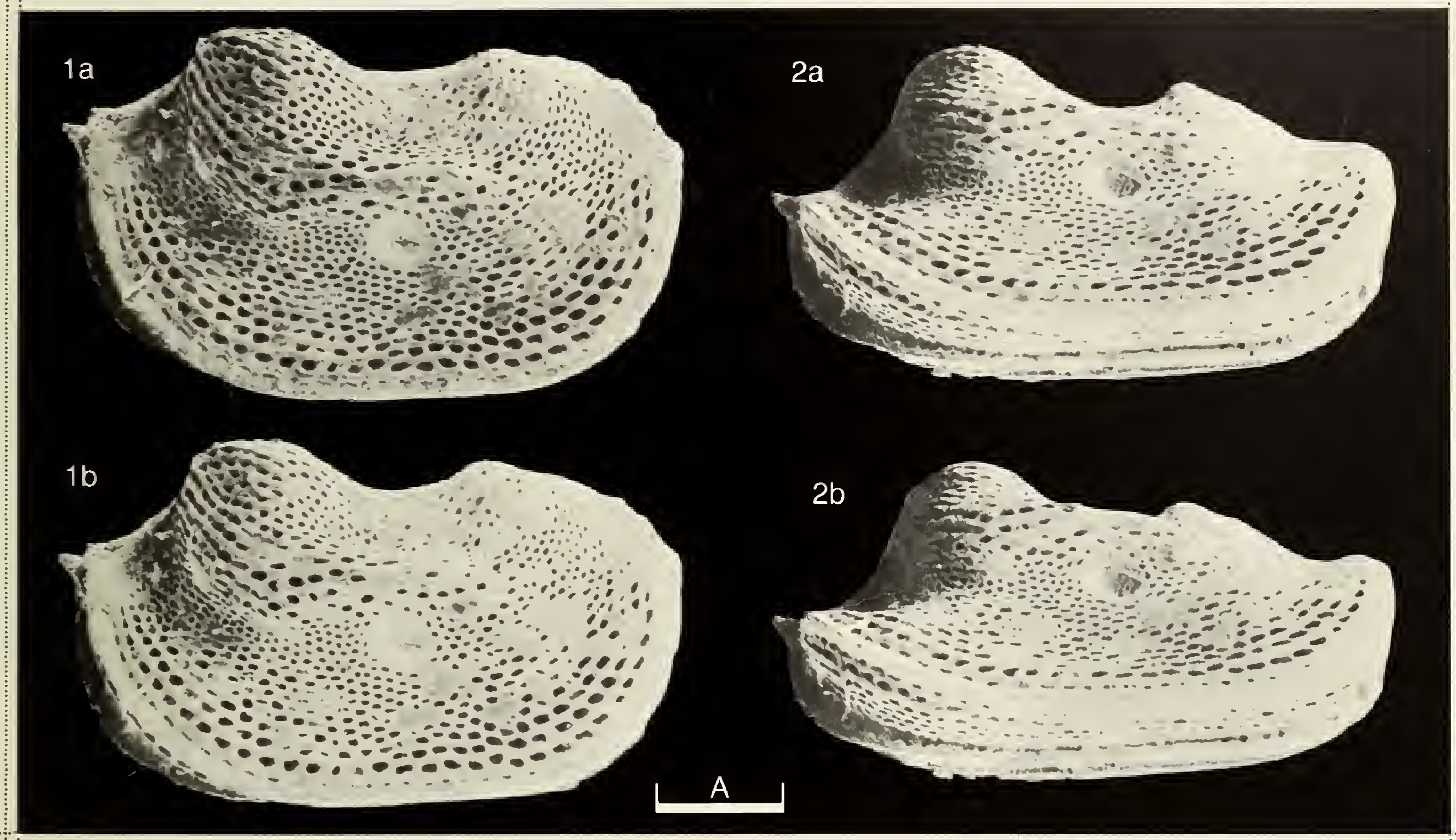
1a
2a
1b
2b
A

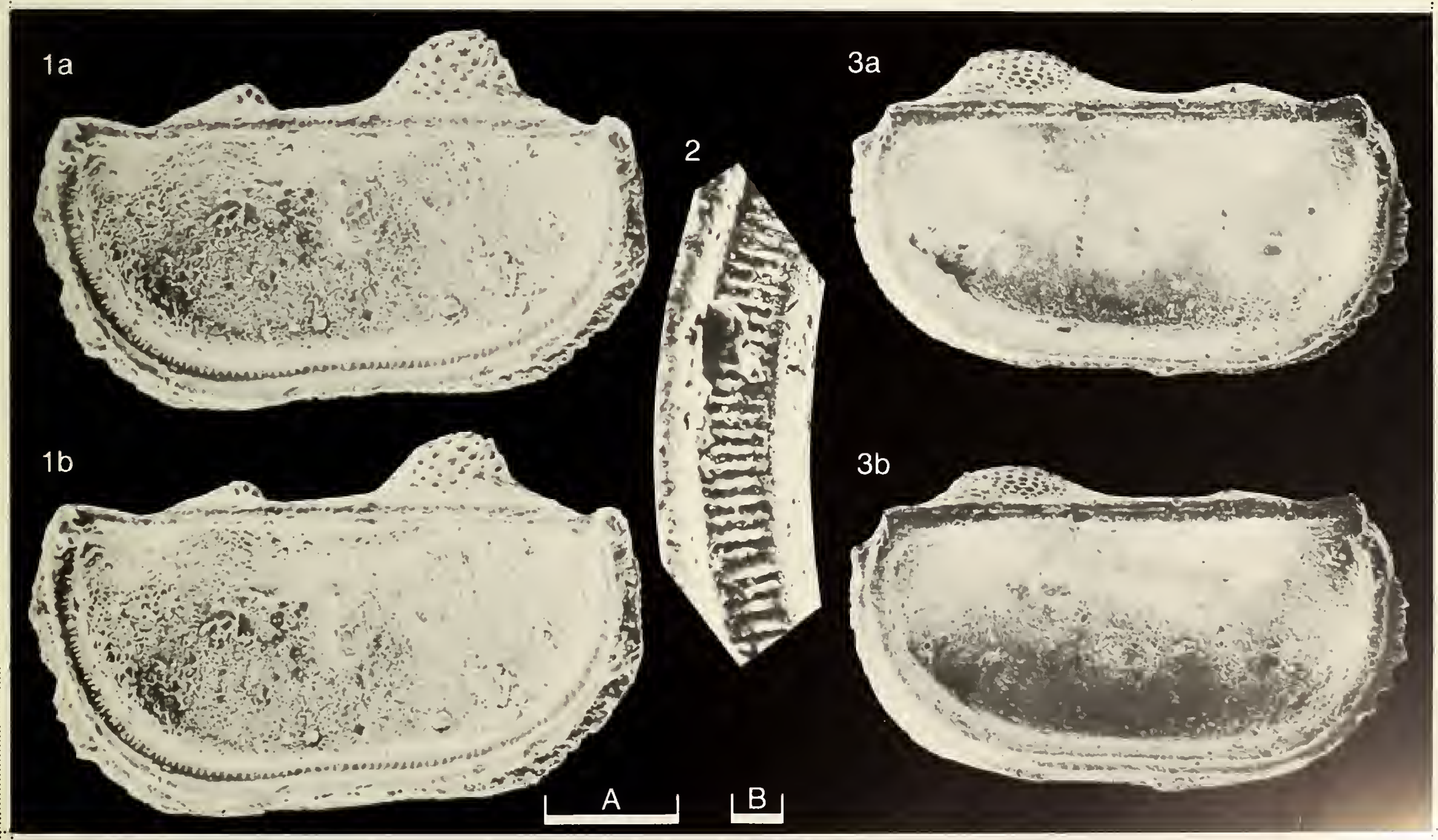
1a
2
3a
1b
3b
A
B

Stereo-Atlas of Ostracod Shells 16 (25) 116–119 (**1989**)
595.336 (113.45) (430.1 : 161.007.50) : 551.351 + 552.54

ON *NODELLA HAMATA* BECKER

by Gerhard Becker
(University of Frankfurt, Federal Republic of Germany

Nodella hamata Becker, 1968

1954 *Drepanellina?* sp. A. K. Krömmelbein, *Senckenberg. leth.*, **34**, 256, pl. 1, fig. 6.
1968a *Nodella hamata* sp. nov. G. Becker, *Natur u. Museum*, **98**, 129, 130, text-figs. 16, 17.
1968b *Nodella hamata* Becker; G. Becker, *Senckenberg. leth.*, **49**, 555–557, text-figs. 1, 2, pl. 1, figs. 1, 2, 6–8.
1985 *Nodella hamata* Becker; M. Coen, *Mém. Inst. Géol. Univ. Louvain*, **32**, 12, tab. 2, pl. 3, fig. 3.

Holotype: Forschungs-Institut Senckenberg, Frankfurt am Main (SMF), Federal Republic of Germany, no. **SMF Xe 5676**; an adult heteromorph LV.

Type locality: Quarry "Steinbreche", about 1 km SW of Refrath village, SW Bergisch-Gladbach, Bergisches Land, Rheinisches Schiefergebirge, Federal Republic of Germany; lat. 50° 59′ N, long. 07° 09′ E. Coral limestones with yellowish marls, Refrath Formation, Frasnian, Upper Devonian.

Figured specimens: Forschungs-Institut Senckenberg (SMF), Frankfurt am Main, Federal Republic of Germany, nos. **SMF Xe 5676** (adult heteromorphic LV, holotype: Pl. **16**, 117, fig. 2, Pl. **16**, 119, fig. 2), **SMF Xe 5677** (adult tecnomorphic car., paratype: Pl. **16**, 117, fig. 1; Pl. **16**, 119, figs. 1, 3, 5), **SMF Xe 5678** (adult heteromorphic LV, paratype: Pl. **16**, 117, fig. 3), **SMF Xe 5679** (adult heteromorphic RV, paratype: Pl. **16**, 119, fig. 4). All topotype material.

Diagnosis: *Nodella* species with a distinct, somewhat elongate presulcal lobe below the dorsal margin and a high, pointed postsulcal lobe. Ventral-anteroventral bend ("carina") and short posteroventral spine. Extradomiciliar dimorphism showing a comparatively strong and long marginal hamus in

Explanation of Plate 16, 117

Fig. 1, adult tecnomorphic car., rt. lat. (paratype, **SMF Xe 5677**, 600 μm long); fig. 2, adult heteromophic LV, ext. lat. (holotype, **SMF Xe 5676**, 550 μm long); fig. 3, adult heteromorphic LV, ext. lat. (paratype, **SMF Xe 5678**, 600 μm long).
Scale (100 μm; $\times$110), figs. 1–3.

tecnomorphs and a long, sickle shaped anterior flange in heteromorphs. Also proportional dimorphism, in which the tecnomorphs are slimmer. Lateral surface of the valves finely reticulate.

Remarks: The extradomiciliar dimorphic structures in *Nodella hamata* are clearly marginal in origin. Both the dimorphic structures, the hamus in tecnomorphs and the flange in heteromorphs, originate anteriorly from the otherwise free marginal positioned marginal ridge. The additional, domiciliar dimorphism is proportional. This combined type of sexual dimorphism was termed "hamal dimorphism" by Becker (1968a, 129).

What we now term hamal structures were first believed to characterise different subspecies (Zaspelova, *Trudy VNIGRI*, **60**, 173, 174, 188, 189, pl. 3, figs. 1–5, pl. 8, figs. 1–3, 1952). Referring to the "modern" taxonomic concepts of Jaanusson (*Bull. Geol. Inst. Univ. Uppsala*, **37**, 197–226, 1957), Becker (1968a, 131) proposed the Suborder Nodellocopina and the Superfamily Nodellacea for palaeocopids with hamal dimorphism. However, Schallreuter (*in*: T. Hanai *et al.* (eds.), *Evolutionary Biology of Ostracoda, Develop. Palaeont. Stratigr.*, Amsterdam, **11**, 1047, 1988) considered that hamal dimorphism was a "special modification" of the antral dimorphism which characterises hollinids. If this were the case, however, then nodellid (marginal) structures would be considered homologous with features which are velar and not marginal – which they clearly, in my opinion, are not. Schallreuter (1988, *op. cit.*) also compared the nodellid marginal structures with the perimarginal structures of primitiopsids; however, the latter are typically primitiopsid features and thus are not homologous or even analogous features. Moreover, (the nodellid) proportional dimorphism is not at all known in hollinids, and the overall morphology of nodellids is rather drepanellid-like. Thus, the Superfamily Nodellacea Becker, 1968 is considered to be a valid taxon, closely related to the Drepanellacea Ulrich & Bassler, 1923.

Distribution: Bergisches Land, Rheinisches Schiefergebirge, Germany; Refrath Formation, Frasnian, Upper Devonian. Dinant Syncline, Ardennes, Belgium; Fromelennes supérieur, supposed late Middle Devonian.

Explanation of Plate 16, 119

Figs. 1, 3, 5, adult tecnomorphic car. (paratype, **SMF Xe 5677**, 600 μm long): fig. 1, vent.; fig. 3, vent. view of atn. end; fig. 5, anterovent. obl. Fig. 2, heteromorphic LV, ext. atn. (holotype, **SMF Xe 5676**, 550 μm long). Fig. 4, heteromorphic RV, ext. vent. (paratype, **SMF Xe 5679**, 560 μm long).
Scale A (100 μm; $\times$110), figs. 1, 4; scale B (100 μm; $\times$205), fig. 2; scale C (30 μm; $\times$300), figs. 3, 5.

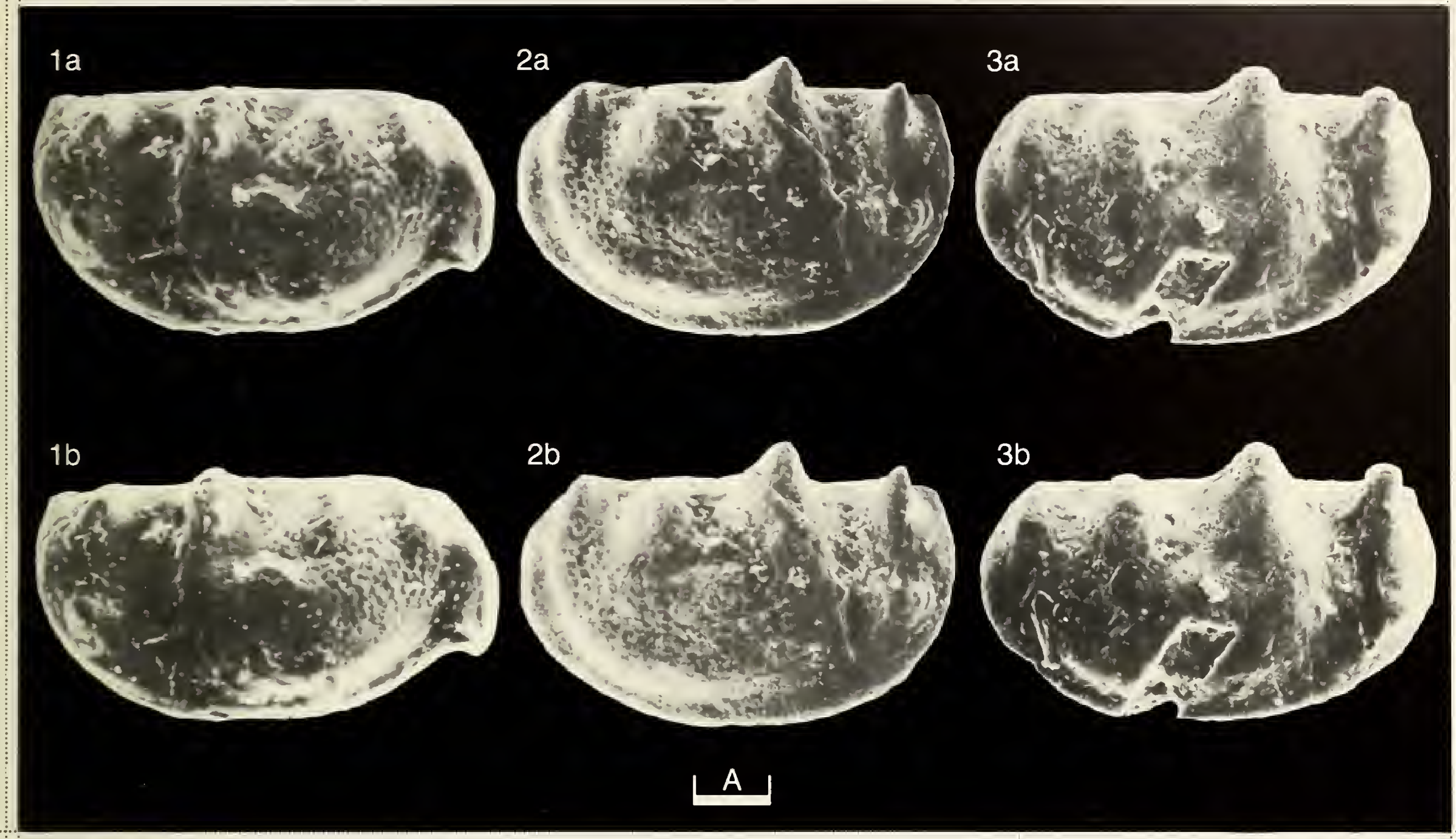
1a
2a
3a
1b
2b
3b
A

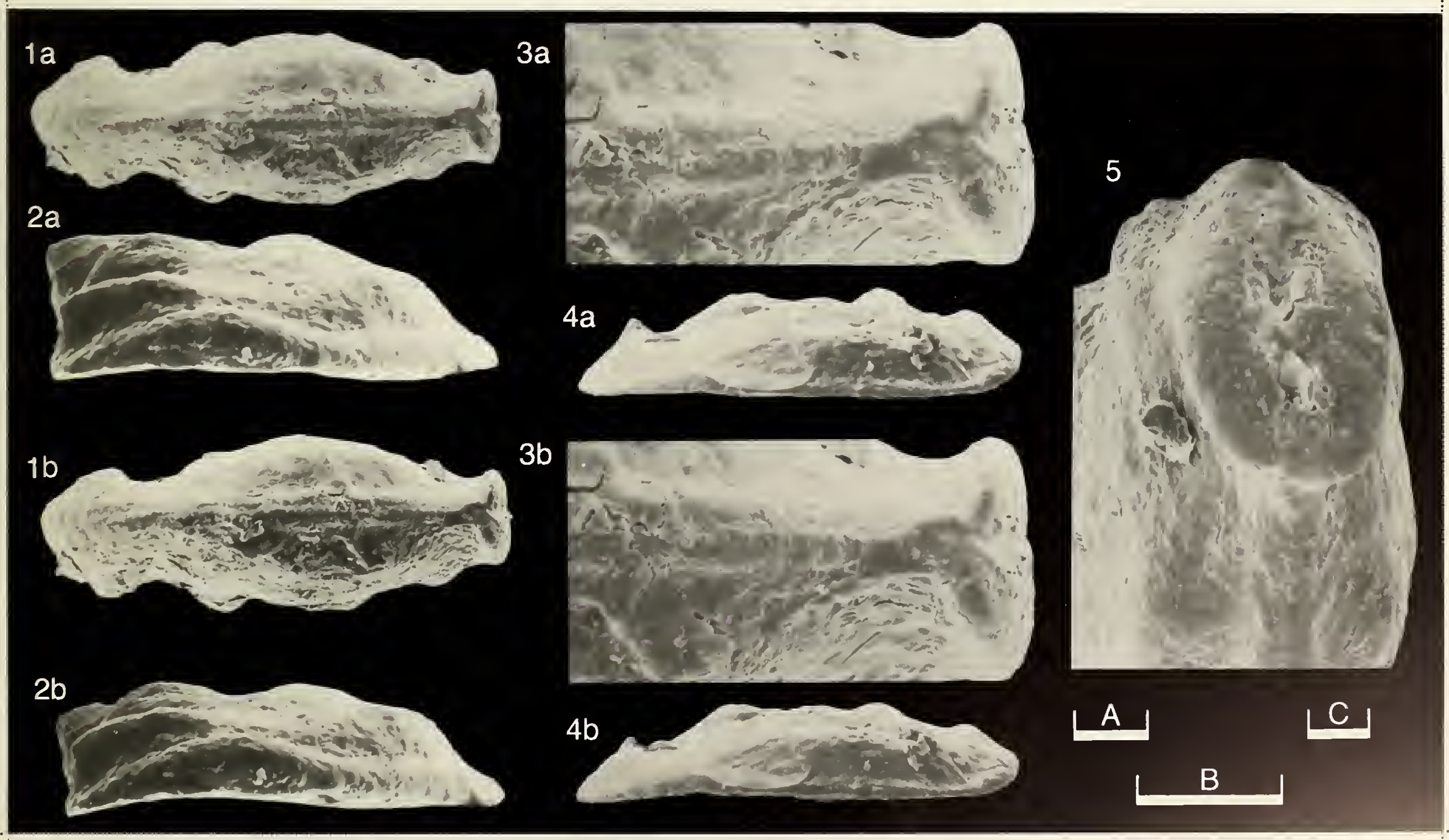
1a
3a
5
2a
4a
1b
3b
2b
4b
A
C
B

Stereo-Atlas of Ostracod Shells 16 (26) 120–127 (**1989**)
595.337.14 (118.15) (430.1 : 161.008.49) : 551.35

ON *CYTHERIDEA SANDBERGERI* KAMMERER sp. nov.

by Thomas Kammerer
(Geologisches Landesamt Rheinland-Pfalz, Mainz, German Federal Republic & University College of Wales, Aberystwyth, UK)

Cytheridea sandbergeri sp. nov.

1905 *Cytheridea muelleri* (v. Münster); E. Lienenklaus, *Ber. senckenb. naturf. Ges.*, **1905**, 38 (pars).
1955 *Cytheridea pernota* sp. nov. H. Oertli & A. J. Key (= Keij), *Bull. Verein. schweiz. Petrol. Geol. Ing.*, **22** (62), 19 (*pars*), pl. 1, figs. 8–13 only (*non* pl. 1, figs. 1–7, text-fig. 2).
1956 *Cytheridea pernota* Oertli & Key; H. J. Oertli, *Schweiz. palaeont. Abh.*, **74**, 36, pl. 2, figs. 33–38.
1960 *Cytheridea pernota* Oertli & Keij; F. Gramann, *Marb. Sitzungsber.*, **82**, 59–88 (*passim*), pl. 1, fig. 4.
1962 *Cytheridea* sp. C 66 [aff. *müllerii* (Münster 1830)] (*sic*); H. Malz, *Ostracoda, in:* F. Doebl & H. Malz, *Tertiär des Rheintal-Grabens. Leitfossilien der Mikropaläontologie*, Gebrüder Borntraeger, Berlin, 394, pl. 58, figs. 1–2.

Holotype: Forschungsinstitut Senckenberg, Frankfurt, no. **SMF Xe 14751**; ♀ left valve.
[Paratypes: nos. **SMF Xe 14752–14764**]

Type locality: Borehole no. 27 (KB 2), sample 6015/5922, depth 83.50–83.75 m, Bodenheim, near Mainz, German Federal Republic (grid ref. R 49 140, H 32 385 – map no. 6015; long. 8° 17′ 31″ E, lat. 49° 55′ 36″ N); restricted marine marl, Schleichsand Formation of Mainz Basin; Rupelian, M. Oligocene.

Explanation of Plate 16, 121

Fig. 1, ♀ LV, ext. lat. (holotype, **Xe 14751**, 865 μm long); fig. 2, ♂ LV, ext. lat. (paratype, **Xe 14752**, 866 μm long); fig. 3, juv. −1 LV, ext. lat. (paratype, **Xe 14753**, 658 μm long).
Scale A (100 μm; ×75), figs. 1–3.

Derivation of name: In honour of C.L.F. Sandberger (1826–1898), in appreciation of his work on the geology of the Mainz Basin.

Figured specimens: Forschungsinstitut Senckenberg nos. **Xe 14751** (holotype, ♀ LV: Pl. **16**, 121, fig. 1); **Xe 14752** (♂ LV: Pl. **16**, 121, fig. 2); **Xe 14753** (juv. LV: Pl. **16**, 121, fig. 3); **Xe 14754** (♀ RV: Pl. **16**, 123, fig. 1); **Xe 14755** (♂ RV: Pl. **16**, 123, fig. 2); **Xe 14756** (♀ car.: Pl. **16**, 123, fig. 3); **Xe 14757** (♀ LV: Pl. **16**, 125, fig. 1); **Xe 14758** (♂ car.: Pl. **16**, 125, fig. 2); **Xe 14759** (♂ LV: Pl. **16**, 125, fig. 3); **Xe 14760** (♀ RV: Pl. **16**, 127, fig. 1); **Xe 14761** (♂ RV: Pl. **16**, 127, fig. 2); **Xe 14762** (♂ RV: Pl. **16**, 127, fig. 3); **Xe 14763** (♀ RV: Text-fig. 1).
All specimens are from the type locality and horizon.

Size:

Sex	N	L (in μm) $\bar{x}$	Min	Max	H (in μm) $\bar{x}$	Min	Max	L/H $\bar{x}$	Min	Max
♀♀ RV	30	788	724	838	425	405	461	1.854	1.749	1.928
♂♂ RV	30	832	783	886	420	394	444	1.989	1.936	2.038
♀♀ LV	30	812	773	875	455	425	497	1.786	1.733	1.855
♂♂ LV	30	847	806	933	434	414	468	1.951	1.892	2.019

Table 1. Measurements on 120 valves (holotype and 119 paratypes); N = no of specimens, $\bar{x}$ = mean, L = length not including marginal denticles, H = height.

Diagnosis: Right valve in lateral view pear-shaped in females, elongate subtrapezoidal in males, ventral margin slightly concave in posterior third; left valve subovate with straight or very slightly concave ventral margin. Anterior margin of both valves high and broadly rounded, forming a nearly symmetrical semicircle; antero-cardinal angle indistinct. Left valve with 5–7 anterior marginal

Explanation of Plate 16, 123

Fig. 1, ♀ RV, ext. lat. (paratype, **Xe 14754**, 796 μm long); fig. 2, ♂ RV, ext. lat. (paratype, **Xe 14755**, 796 μm long); fig. 3, ♀ car., ext. dors. (paratype, **Xe 14756**, 815 μm long).
Scale A (100 μm; ×75), figs. 1–3.

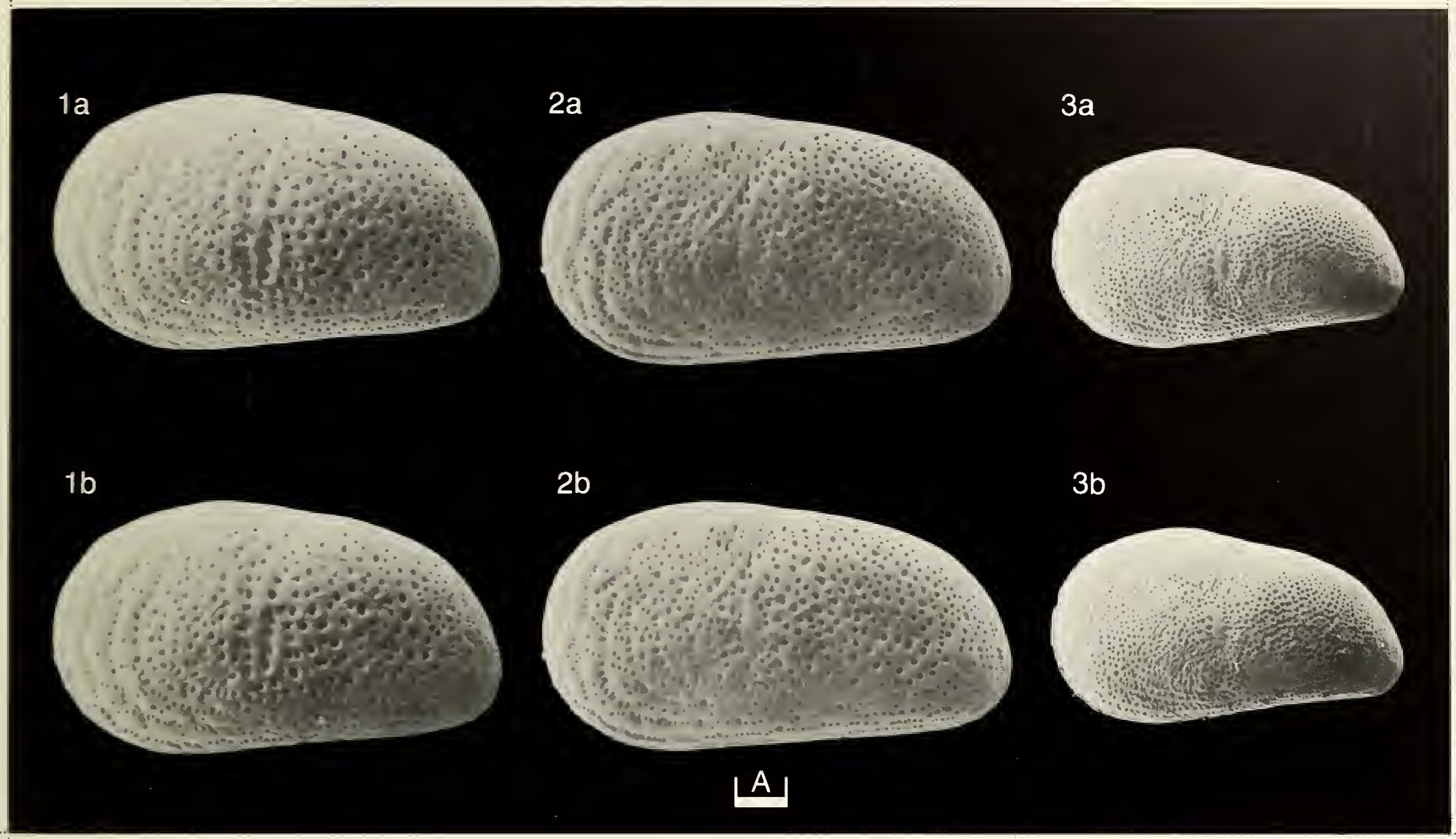
1a
2a
3a
1b
2b
3b
A

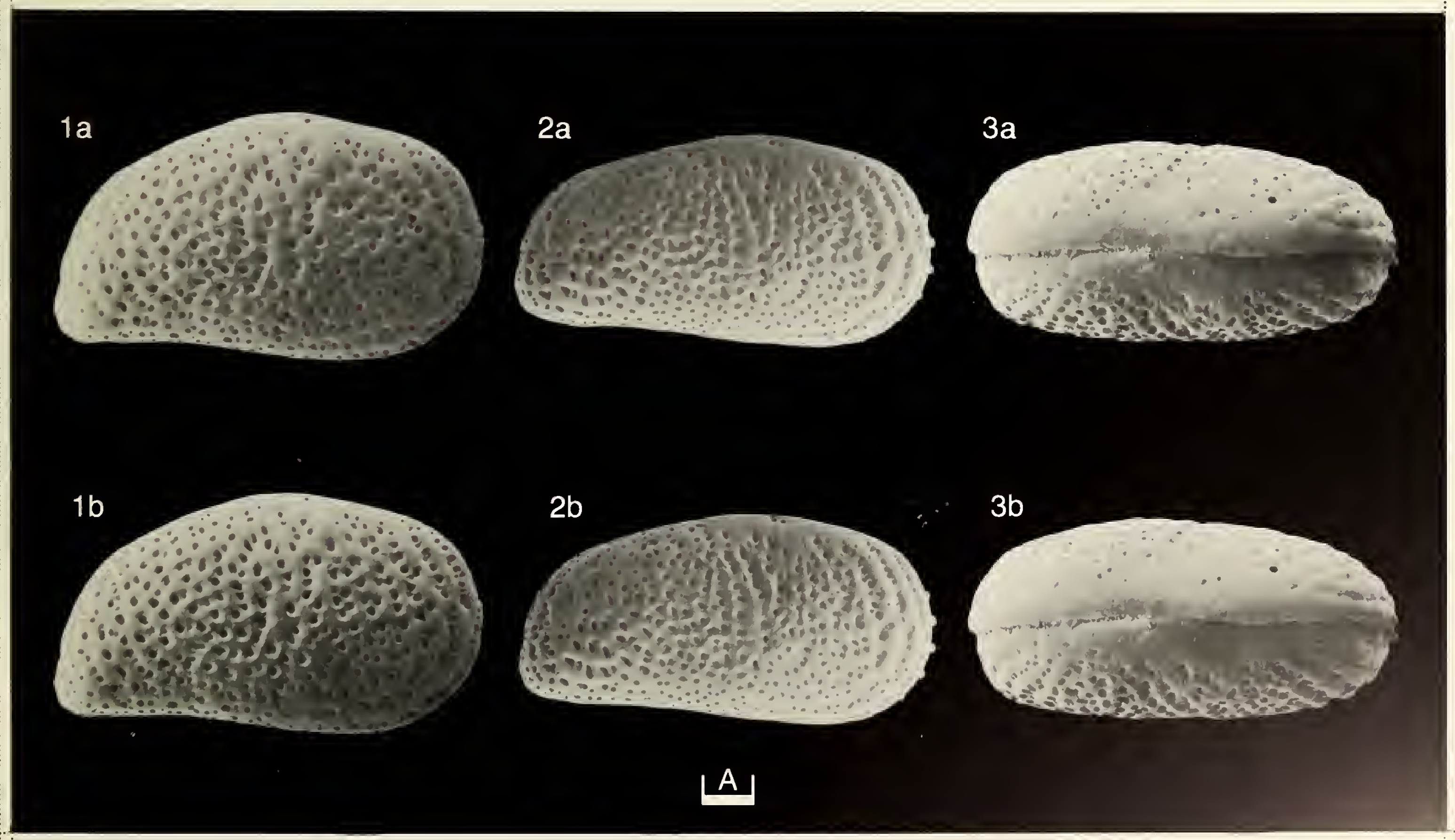
1a
2a
3a
1b
2b
3b
A

denticles, right valve with 7–9 anterior and 4 postero-ventral marginal denticles. Surface punctate, but smooth along the dorsal margin, especially around the antero-cardinal angle.

Remarks: Sexual dimorphism is pronounced, the males being more elongate in lateral view and narrower in dorsal view. The puncta are coarsest centrally, decreasing in diameter towards the periphery; near the free margin they are aligned in several parallel rows. Along the anterior margin these rows form 3 or 4 concentric furrows which in the left valve develop into a mesh-like pattern.

The hinge and internal features are very similar to those of genotype. In *C. muelleri* the adductor and mandibular muscle scars are larger than in *C. sandbergeri* and therefore seem to be positioned closer to each other.

C. sandbergeri was formerly confused with *C. muelleri* or *C. pernota*. The former, from the Chattian of NW Germany, differs in outline and in the number of anterior marginal denticles of its right valve. The latter, from the Oligocene of Belgium, the Isle of Wight and NW Germany, has a distinct antero-cardinal angle and coarser puncta. For a review and re-illustration of *C. muelleri muelleri* (v. Münster), *C. m. toenisbergensis* Weiss and *C. pernota* Oertli & Key, see Weiss (*Stereo-Atlas Ostracod Shells*, **11** (parts 8–10), 1984). *C. sandbergeri* represents a major part of the ostracod fauna within brackish and restricted marine sections of the Schleichsand and Cyrenenmergel formations of the Mainz Basin (Kammerer, in prep.). During the Rupelian and Early Chattian it was widespread in the Upper Rhine Graben and neighbouring areas with several allochronous and allopatric, or parapatric subspecies, or ecotypes, occurring. Similar occurrences are found in the Swiss Molasse (Oertli & Key, and Oertli, *opera cit.*) and in the Hessian Depression (Gramann, *op. cit.*), at the time attributed to *C. pernota*.

Explanation of Plate 16, 125

Fig. 1, ♀ LV, int. lat. (paratype, **Xe 14757**, 830 μm long); fig. 2, ♂ car., ext. dors. (paratype, **Xe 14758**, 882 μm long); fig. 3, ♂ LV, int. lat. (paratype, **Xe 14759**, 818 μm long).
Scale A (100 μm; ×75), figs. 1–3.

Distribution: Oligocene, Rupelian and Early Chattian. Mainz Basin: Schleichsand and Cyrenenmergel, numerous localities; Rhine Graben: Meletta-Schichten and Cyrenenmergel (Malz, *op. cit.*); Hessian Depression: Schleichsand, various localities (Gramann, *op. cit.*); Swiss Molasse: Meeressand, Blaue Tone and Cyrenensand, various localities (Oertli, *op. cit.*).

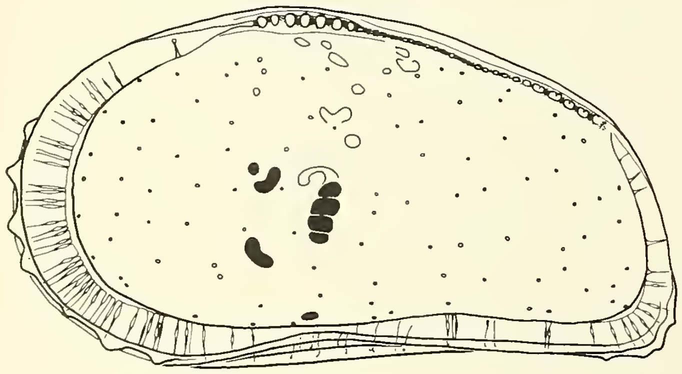

Text-fig. 1. Internal view of *C. sandbergeri* from camera lucida drawing and SEM-micrograph of ♀ RV (paratype, **Xe 14763**, 820 μm long).

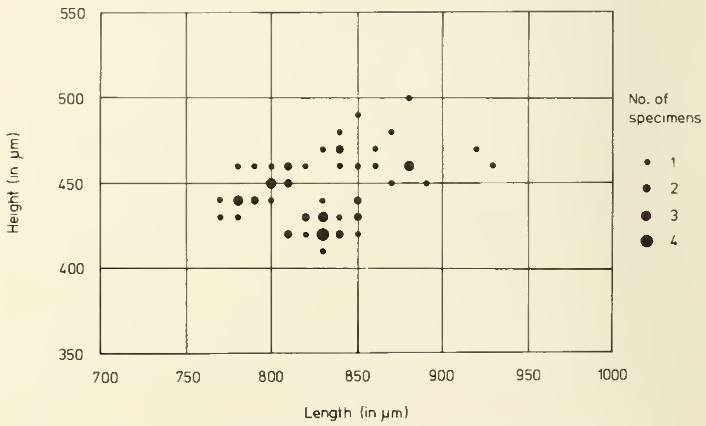

Text-fig. 2. Length/height plot of 60 left valves of *C. sandbergeri* (holotype and paratypes).

Explanation of Plate 16, 127

Fig. 1, ♀ RV, int. lat. (paratype, **Xe 14760**, 818 μm long); fig. 2, ♂ RV (paratype, **Xe 14761**), int. musc. sc.; fig. 3, ♂ RV, int. lat. (paratype, **Xe 14762**, 800 μm long).
Scale A (100 μm; ×75), figs. 1, 3; scale B (100 μm; ×110), fig. 2.

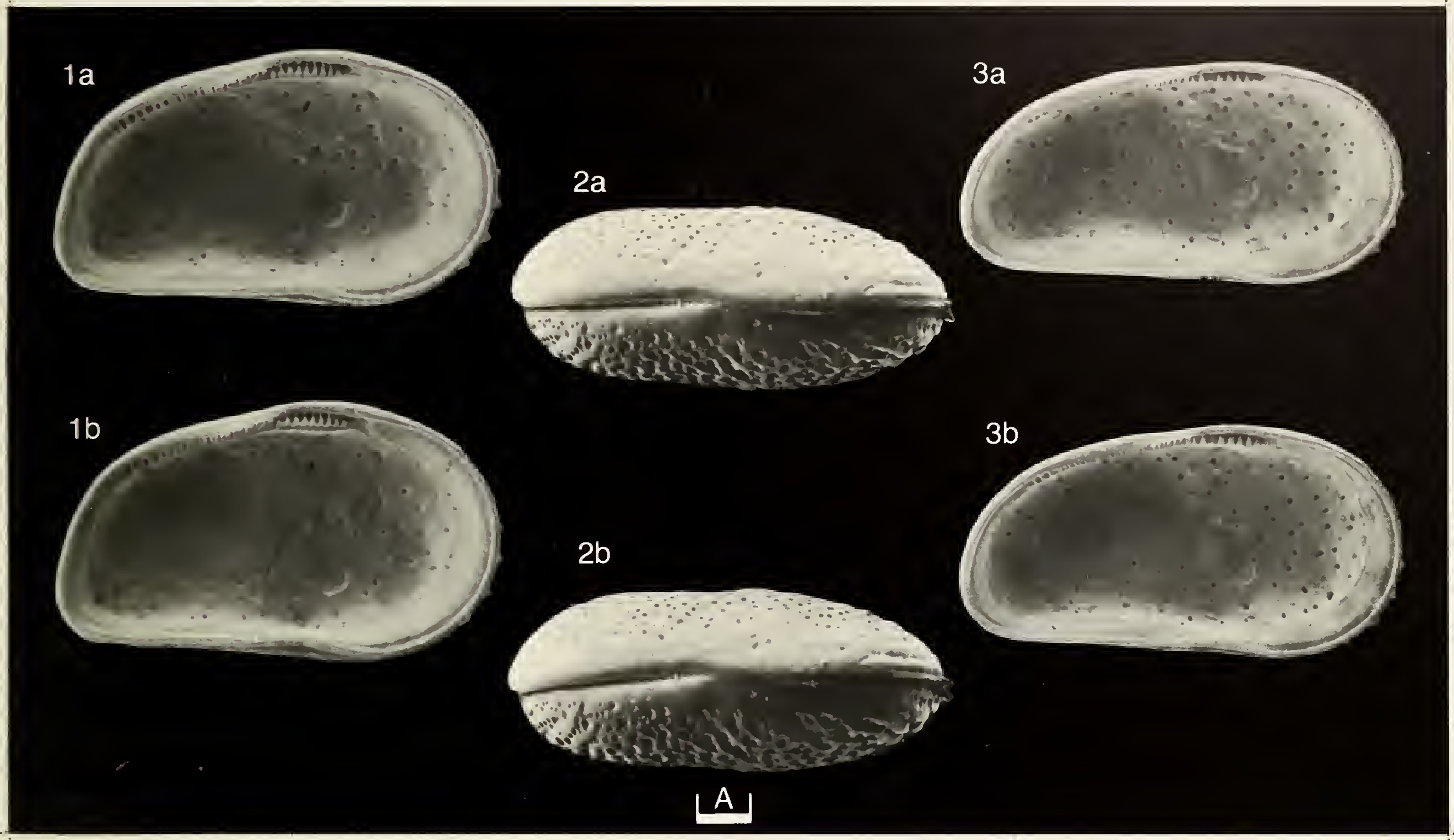
1a
3a
2a
1b
3b
2b
A

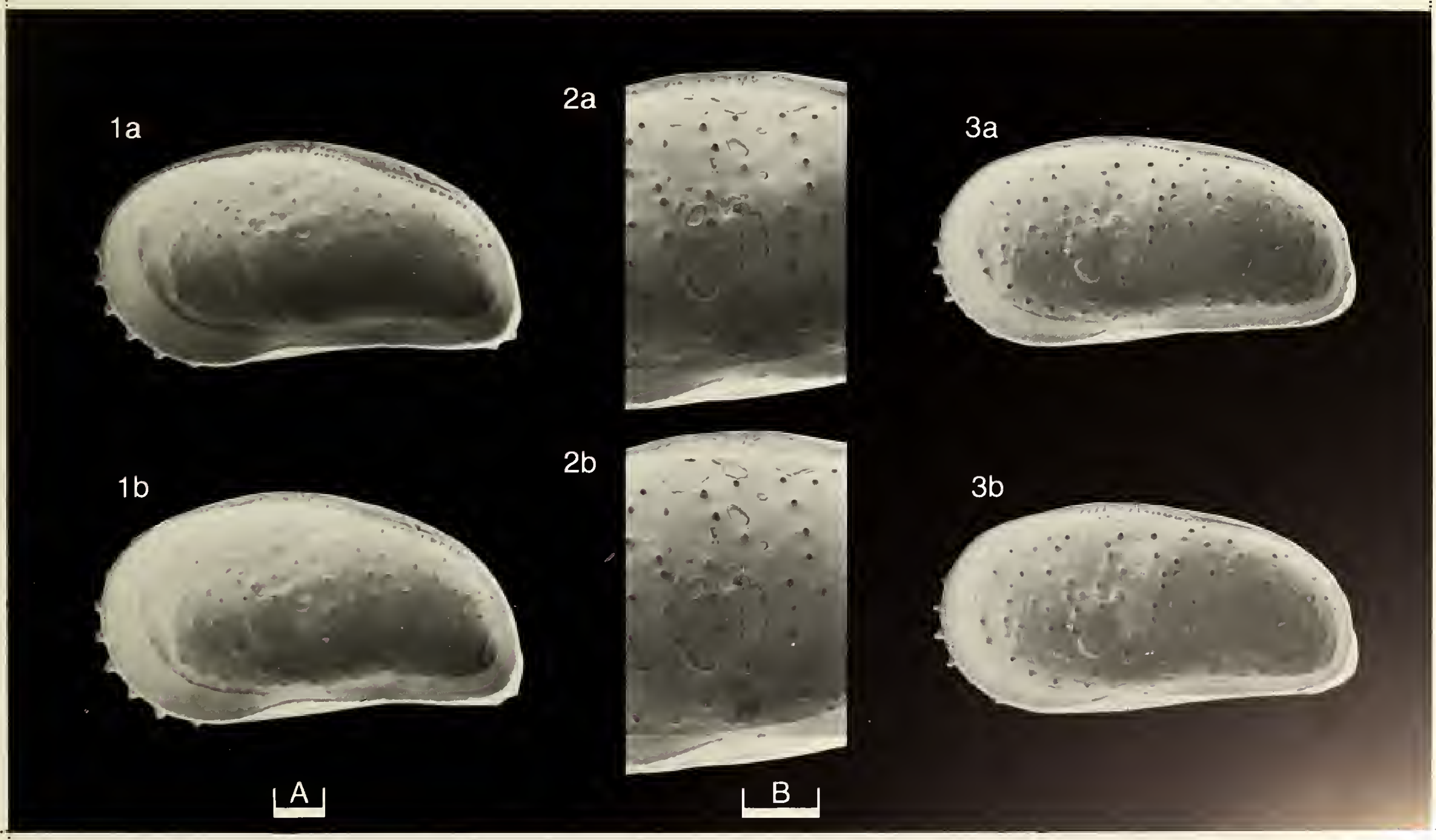
1a
2a
3a
1b
2b
3b
A
B

Stereo-Atlas of Ostracod Shells 16 (27) 128–135 (**1989**)
595.337.12 (119.4 + 119.9) (596 : 161.104.12 + 540 : 161.081.25) : 551.312

ON *STRANDESIA WEBERI* (MONIEZ)

by Dietmar Keyser & S. B. Bhatia
(University of Hamburg, German Federal Republic & Panjab University, Chandigarh, India)

Strandesia weberi (Moniez, 1892)

1892 *Cypris weberi* sp. nov. R. Moniez, *in:* M. Weber, *Zoologische Ergebnisse einer Reise in Niederländisch Ost-Indien*, E. J. Brill, Leiden, **2**, 129–135, pl. 10, figs. 6–11.
1912 *Cypris weberi* Moniez; G. W. Müller, *Tierreich*, **31**, 233.
1923 *Cypris magnifica* sp. nov. V. Brehm, *Treubia*, **3**, 222, figs. 1–3.
1932 *Eucypris weberi* (Moniez); W. Klie, *Arch. Hydrobiol.*, suppl. **11**, 459.
1964 *Strandesia spinifera* sp. nov. G. Hartmann, *Int. Revue ges. Hydrobiol.*, Syst. Beih., **3**, 141–144, figs. 63a–c, 64a–c.
1979 *Strandesia weberi* (Moniez); R. Victor & C. H. Fernando, *Can. J. Zool*, **57**, 7, fig. 4.
1980 *Strandesia weberi* (Moniez); R. Victor *et al.*, *Can. J. Zool.*, **58**, 730.
1983 *Strandesia spinifera* Hartmann; S. B. Bhatia, *in:* R. Maddocks, *Applications of Ostracoda*, University of Houston Geoscience, 442–458, pl. 1, figs. 1–6.
1983 *Strandesia weberi* (Moniez); N. W. Broodbakker, *Bijdr. Dierk.*, **53**, 347, fig. 9H.

Explanation of Plate 16, 129

Fig. 1, LV ext. lat. (**ZIM K-34 332**, 1095 μm long, 1278 μm long with spines); fig. 2, RV ext. lat. (**ZIM K-34 332**, 1145 μm long, 1541 μm long with spines).
Scale A (300 μm; ×73), figs. 1, 2.

Lectotype: Zoologisch Museum, Amsterdam, no. **ZMA, Ostr. 150.710A**; designated by Victor & Fernando (1979).
[Paralectotypes: **ZMA, Ostr. 150.710B**]

Type locality: Celebes, Lumu (approx. lat. 2°30′ S, long. 119°00′ E). Recent, freshwater.

Figured specimens: Zoologisches Museum, Hamburg (**ZIM**) no. **K-27 470** (appendages; Text-figs. 1, 2). From a small lake near Krakor, Pursat Province, Cambodia (Kampuchea) (approx. lat. 12°30′ N, long. 104°00′ E); coll. Lindberg.
ZIM no. K-34 332 (♀ RV and LV: Pl. **16**, 129, figs. 1, 2; Pl. **16**, 131, figs. 1, 2; Pl. **16**, 133, figs. 1, 2; Pl. **16**, 135, figs. 1, 2). From Holocene marls, Indo-Ganges Plain, at Misa Tal, near Lucknow, India (approx. lat. 25° N, long. 81° E); coll. Bhatia.

Diagnosis: A distinctive *Strandesia* with a long, hollow posterior spine, about half the length of the shell, in the RV and with two short, curved anterior spines, one-sixth to one-seventh the length, in the LV. Surface of valves finely pitted with minute granules on intervening ridges. Shell, in life, is brownish with blue spots.

Remarks: For extensive discussion of this and related species, see Victor & Fernando (1979, *op. cit.*). It could be confused with *S. trispinosa* Pinto & Purpur (*Publcões Esp. Esc. Geol. Porto Alegre*, **7**, 1–53, 1965) from South America and the Caribbean, as noted by Broodbakker (1983, *op. cit.*), but there is some difference in dorsal gibbosity between the two, as well as slight differences in the spines on some of the legs.
So far, only females have been found.

Distribution: Recent, freshwater: Celebes (Moniez, 1892); Java, Philippines, Malaya, India (Victor & Fernando, 1979); Cambodia (Hartmann, 1964 and herein). Fossil: Holocene marls from the Indo-Ganges Plain, near Lucknow (Bhatia, 1983 and herein).

Explanation of Plate 16, 131

Fig. 1, RV int. lat. (**ZIM K-34 332**); fig. 2, LV int. lat. (**ZIM K-34 332**).
Scale A (300 μm; ×73), figs. 1, 2.

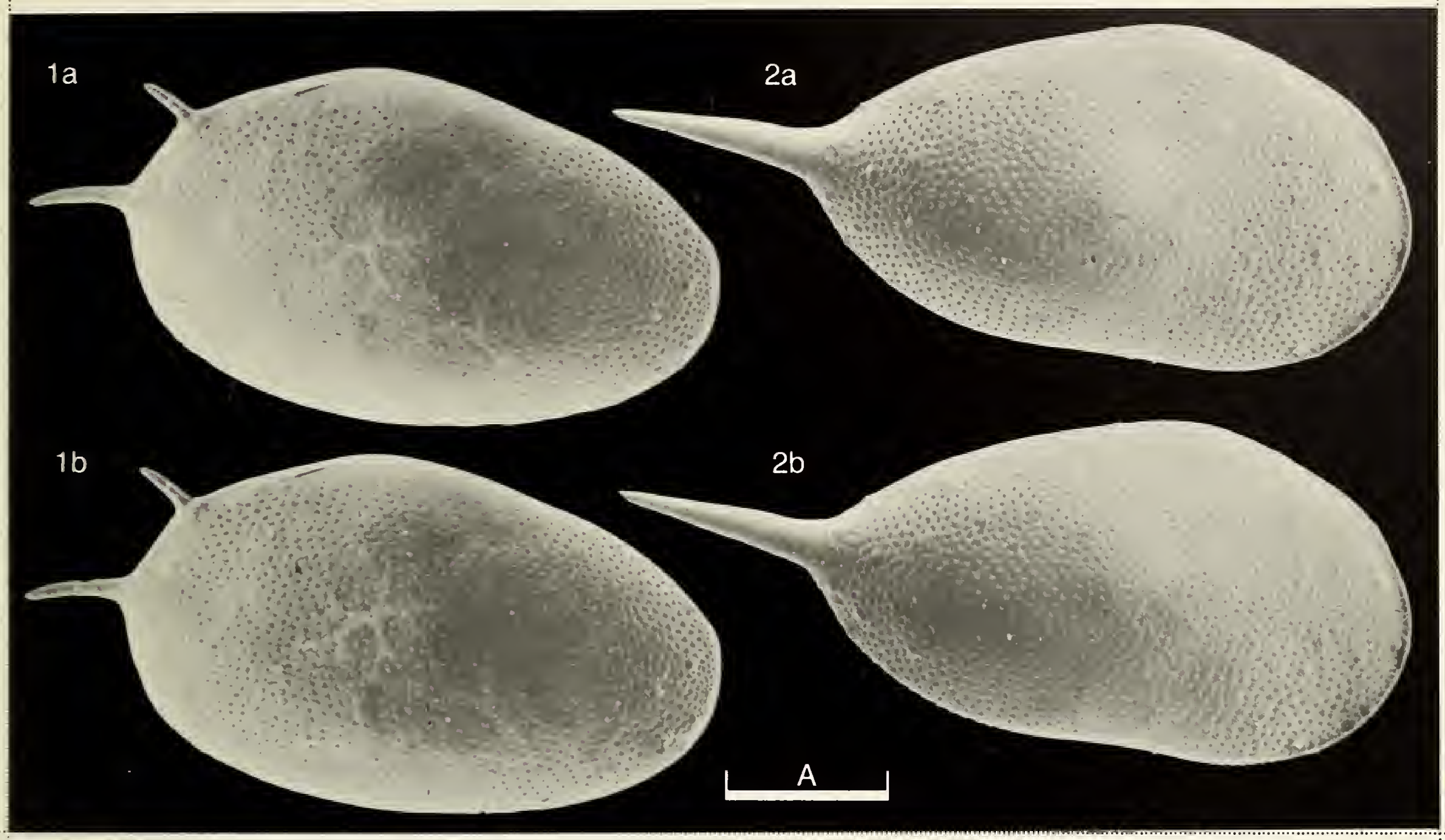
1a
2a
1b
2b
A

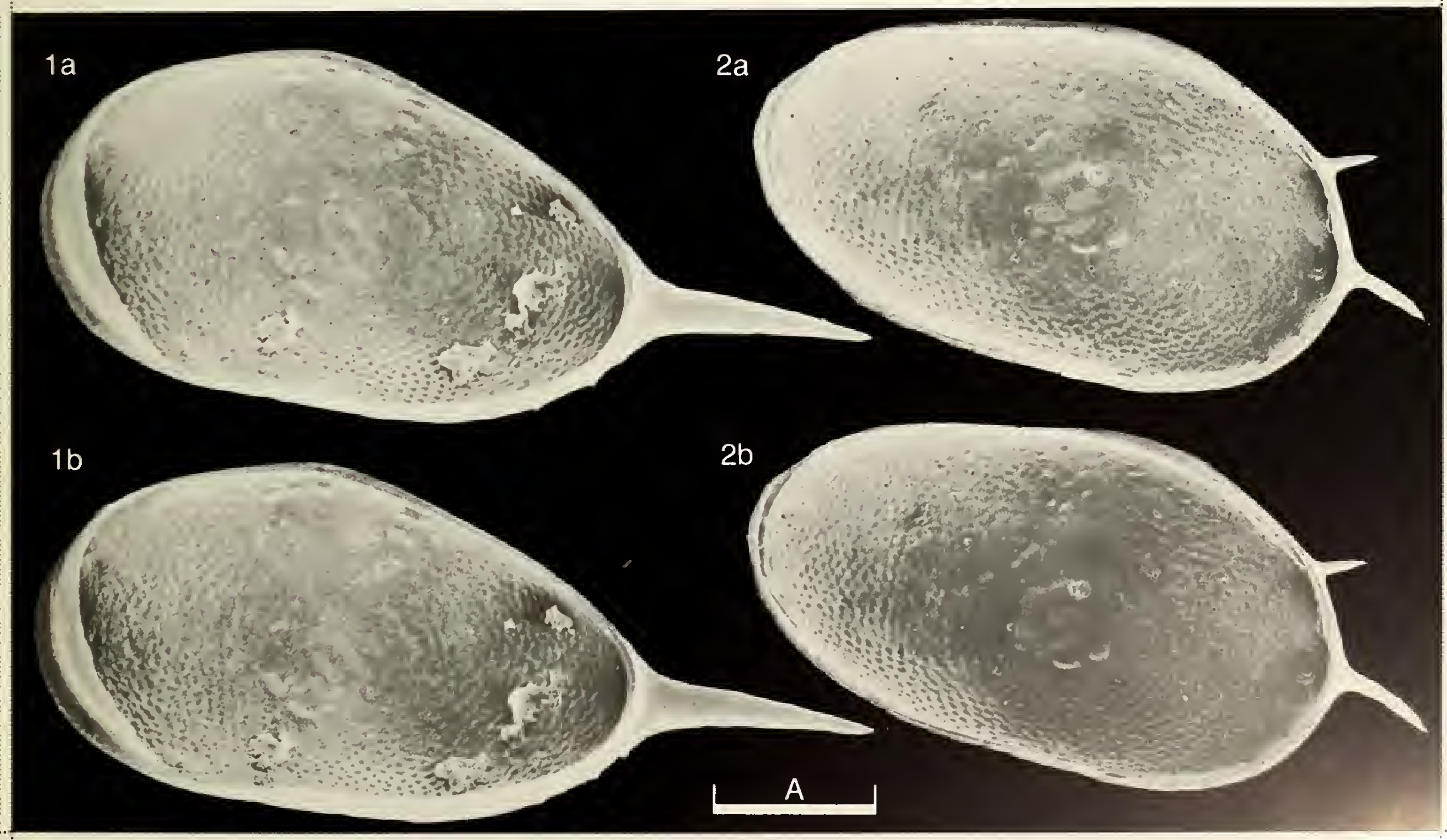
1a
2a
1b
2b
A

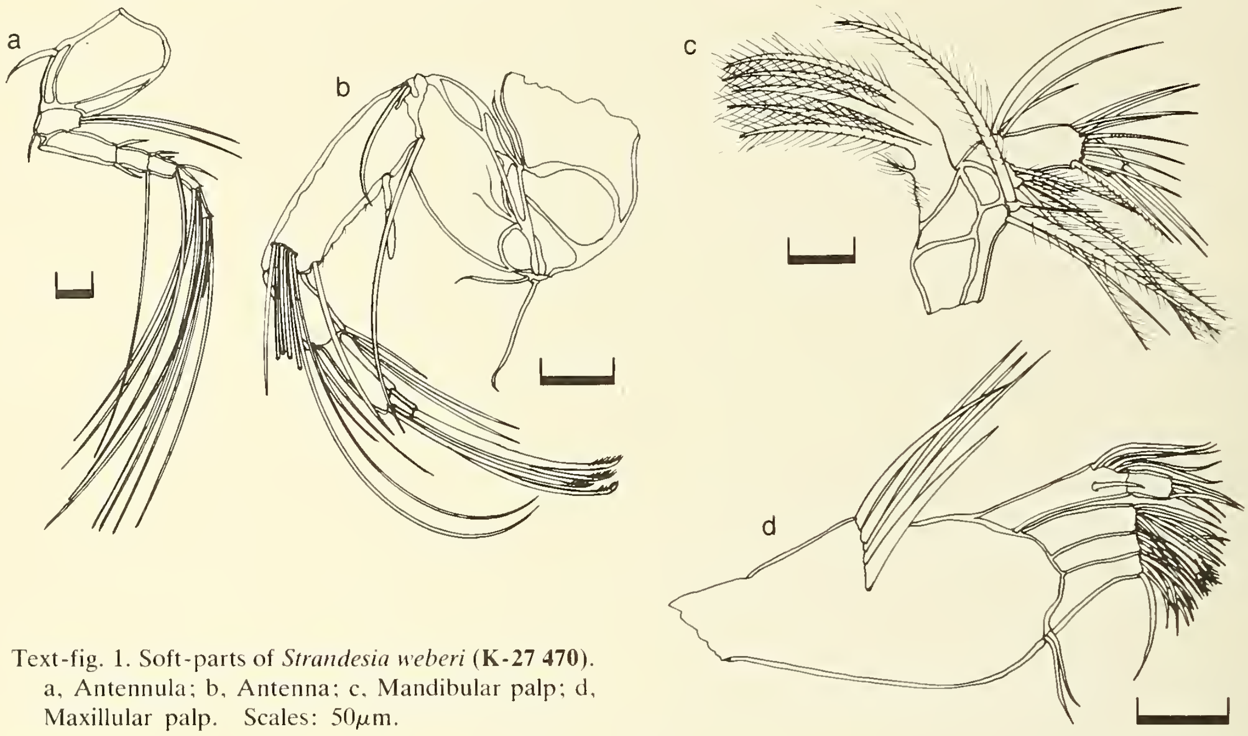

Text-fig. 1. Soft-parts of *Strandesia weberi* (**K-27 470**). a, Antennula; b, Antenna; c, Mandibular palp; d, Maxillular palp. Scales: 50μm.

Explanation of Plate 16, 133

Fig. 1, LV ext. dors. (**ZIM K-34 332**); fig. 2, RV ext. vent. (**ZIM K-34 332**). Scale A (300μm; $\times$73), figs. 1, 2.

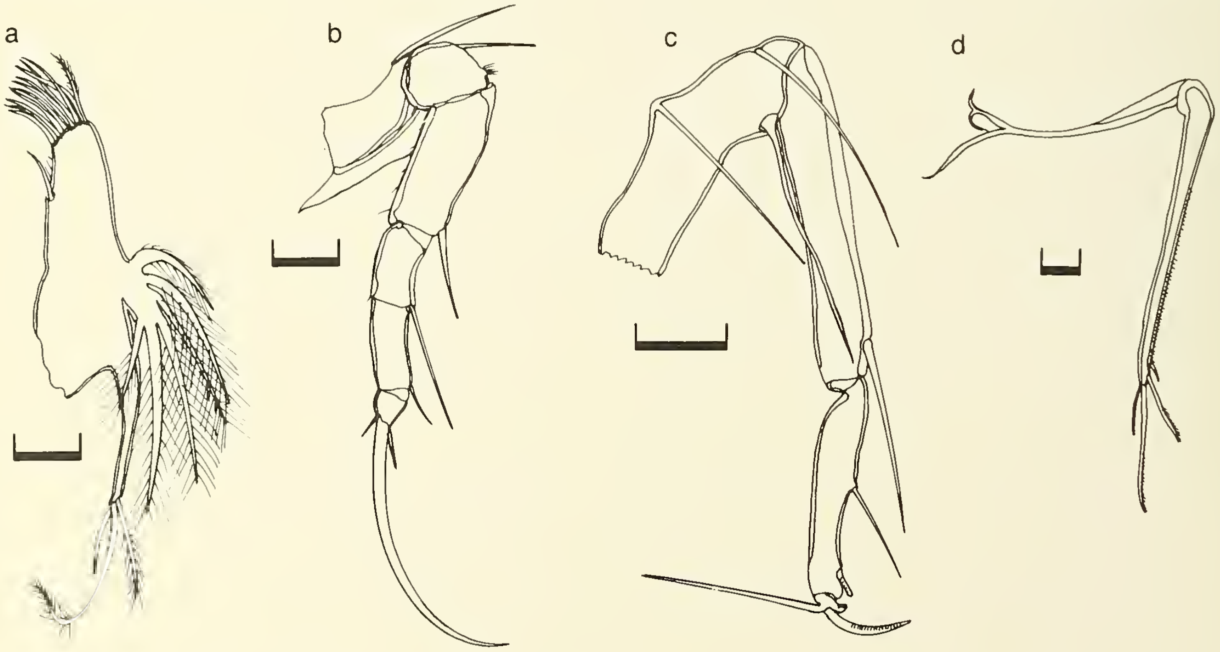

Text-fig. 2. Soft-parts of *Strandesia weberi* (**K-27 470**). a, Maxilla (P I); b, Thoracopod I (P II); c, Thoracopod II (P III); d, Furca. Scales: 50μm.

Explanation of Plate 16, 135

Fig. 1, LV (**ZIM K-34 332**) int. musc. sc.; fig. 2, RV (**ZIM K-34 332**), pore cone with broken bristle. Scale A (50μm; $\times$270), fig. 1; scale B (5μm; $\times$1,850), fig. 2.

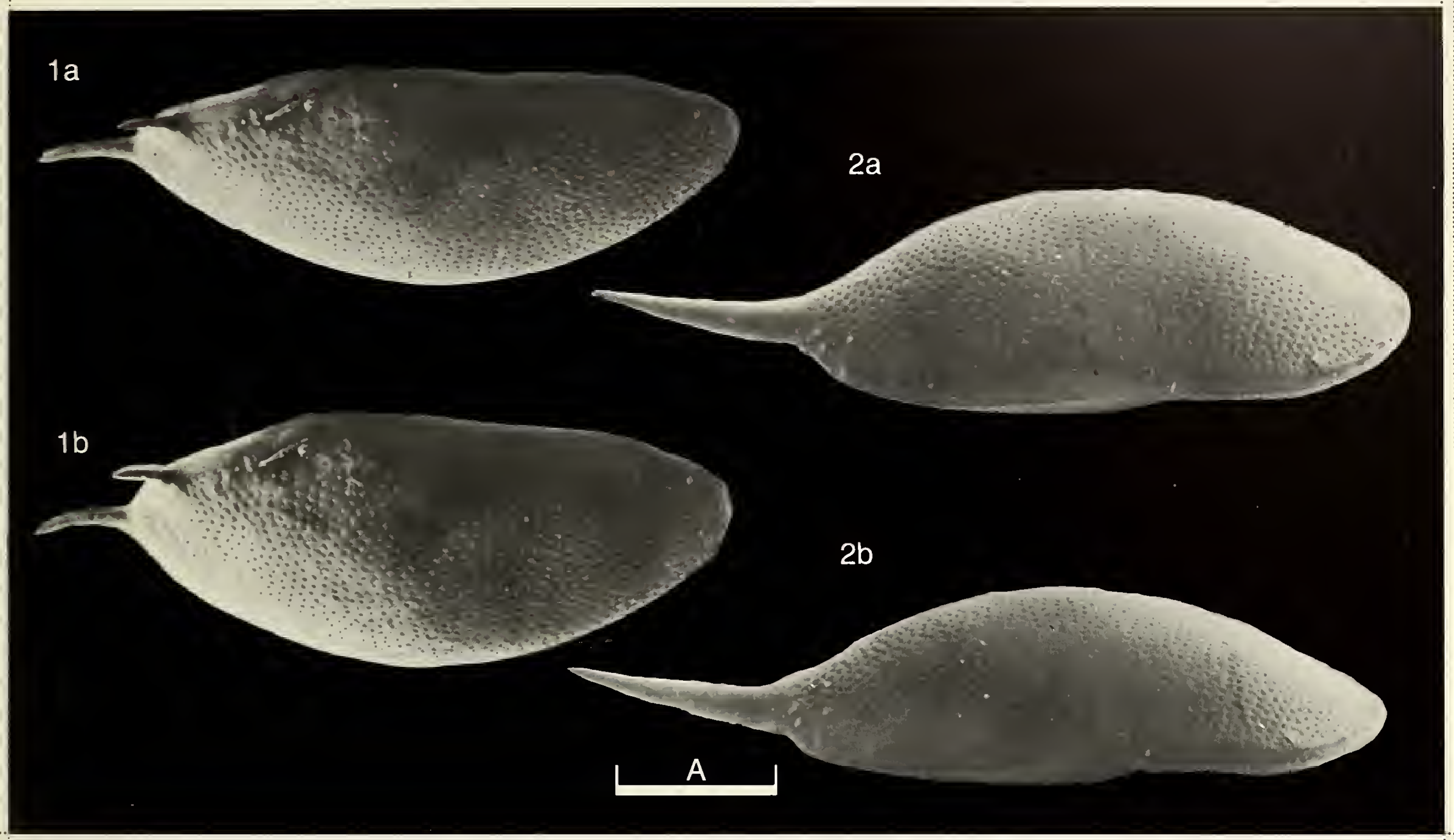
1a
2a
1b
2b
A

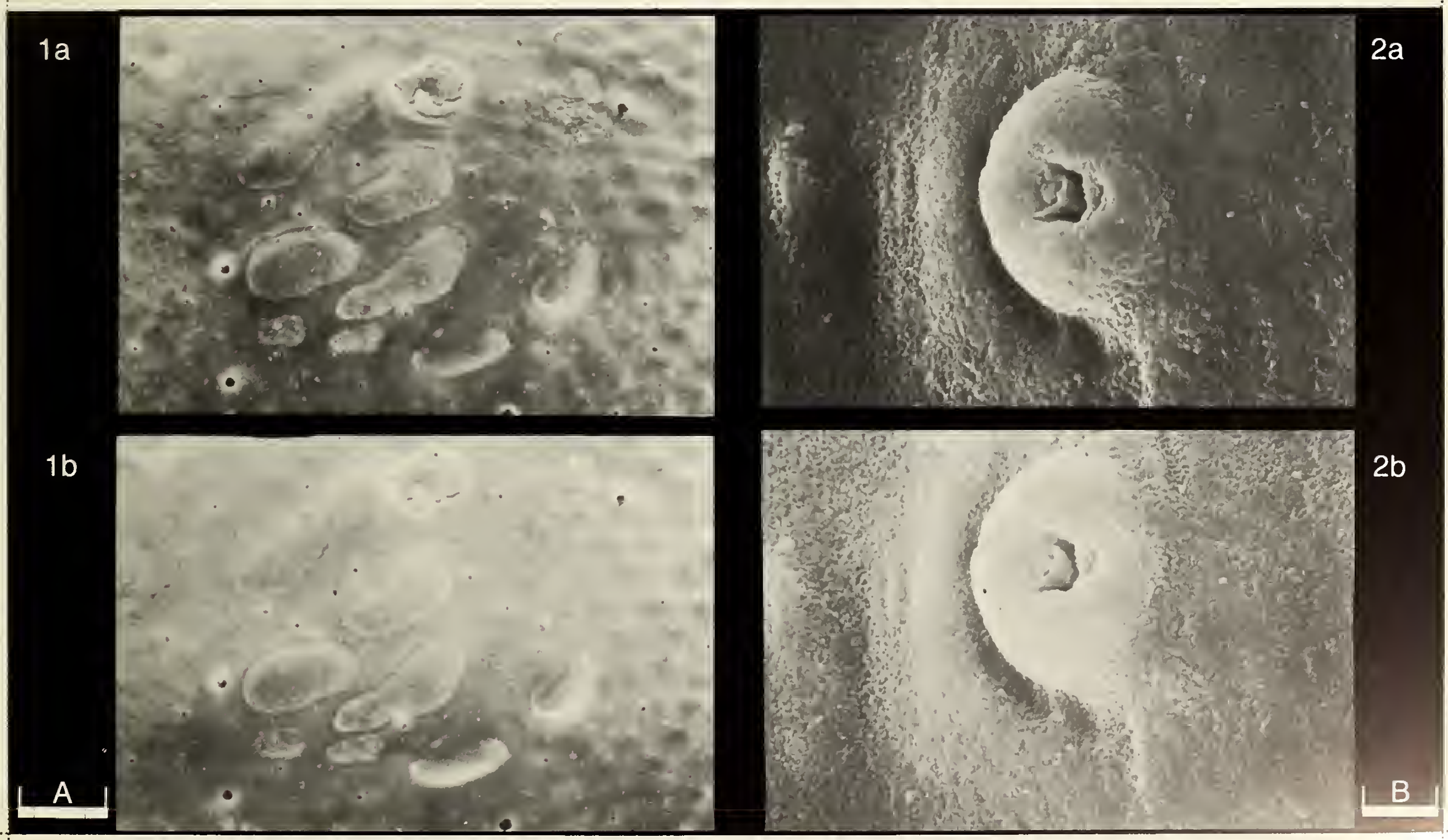
1a
2a
1b
2b
A
B

Stereo-Atlas of Ostracod Shells 16 (28) 136–139 (**1989**)
595.337.14 (119.1) (923 : 163.123.11) : 551.353

ON *ABYSSOBYTHERE GUTTATA* AYRESS & WHATLEY gen. et sp. nov.

by Michael A. Ayress & Robin C. Whatley
(Geochem Laboratories Ltd., Chester & University College of Wales, Aberystwyth)

Genus *ABYSSOBYTHERE* gen. nov.

Type-species (here designated): *Abyssobythere guttata* sp. nov.

Derivation of name: Alluding to the occurrence of this bythocytherid genus in the abyss.

Diagnosis: Carapace large; subovate to subrhomboidal. Anterior margin broadly rounded, posterior margin with well developed caudal process at mid-height. Dorsal margin of left valve straight or convex. Moderately thick-shelled. Surface smooth. Inner lamella broad, vestibulate. Radial pore canals numerous, narrow and straight.

Remarks: *Abyssobythere* is assigned to the Bythocytheridae because of its five adductor muscle scars and lophodont hinge. It differs from *Pseudocythere* Sars, 1866 in its thicker shell, more ventral caudal process and its numerous radial pore canals. Also, in *Pseudocythere* the right and left valve outlines are always equal. *Abyssobythere* differs from *Velibythere* Schornikov, 1982 in lacking an alar process; from *Rhombobythere* Schornikov, 1982 in lacking reticulation or costae; and from *Jonesia* Brady, 1866 in its ovate outline and blunt caudal process.

Four other species, as yet undescribed (from the Palaeogene of the SW Pacific, DSDP sites 207 and 209) are assigned to *Abyssobythere* (see K. Millson, *The Palaeobiology of Palaeogene Ostracoda from Deep Sea Drilling Project Cores in the SW Pacific*, unpubl. PhD. thesis, Univ. Wales, 1, 113–121; 2, pl. 4, figs. 24–29, pl. 5, figs. 1–9). A fifth species, as yet undescribed, has been recovered from the lower Miocene of the Loyalty Basin, SW Pacific (Harlow pers. comm. 1989).

Explanation of Plate 16, 137

Fig. 1, LV, ext. ant. (**OS13389**, 920 μm long); fig. 2, LV, ext. lat., (holotype, **OS13386**, 960 μm long); figs. 3–4, RV (**OS13387**, 950 μm long): fig. 3, ext. lat.; fig. 4 ext. ant. vent. obl.
Scale A (200 μm; ×60), fig. 1; scale B (500 μm; ×60); figs. 2–3; scale C (500 μm; ×60), fig. 4.

Abyssobythere guttata sp. nov.

Holotype: British Museum (Nat. Hist.) no. **OS13386**, LV.
[Paratypes British Museum (Nat. Hist.) nos. **OS13387–OS13389**].

Type locality: Timor Sea, DSDP Site 262, near axis of Timor Trough, lat. 10° 52.19′ S, long. 123° 50.78′ E. Water depth 2298 m. Brown foraminiferal ooze. Zone NN19, Pleistocene.

Derivation of name: Latin, alluding to the drop-like outline in lateral view.

Figured specimens: British Museum (Nat. Hist.) nos. **OS13386** (holotype, LV: Pl. **16**, 137, fig. 2), **OS13387** (RV: Pl. **16**, 137, figs. 3, 4), **OS13389** (LV: Pl. **16**, 137, fig. 1; Pl. **16**, 139, fig. 2), **OS13388** (RV: Pl. **16**, 139, figs. 1, 3). All from the type locality and horizon.

Diagnosis: Carapace subovate to subrhomboidal in lateral view. Dorsal margin in left valve convex. Right and left valve outlines virtually equal. Each radial pore canal extends into a box-like chamber distally and emerges at the base of an external peripheral groove.

Remarks: *A. guttata* is most similar to an undescribed species from the lower Miocene of the Loyalty Basin, SW Pacific, but in that species the dorsal margin of the left valve is straight.

Distribution:
Nannoplankton Zone NN19, Pleistocene of the Timor Trough (DSDP Site 262, Core 36, Section 6), Zone NN21, Pleistocene of northern flank of Naturaliste Plateau, eastern Indian Ocean (DSDP Site 258, Core 1, Section 1), Zone NN19–NN21, Pleistocene of southeast Wharton Basin, eastern Indian Ocean (DSDP Site 259, Core 1, Section 3).

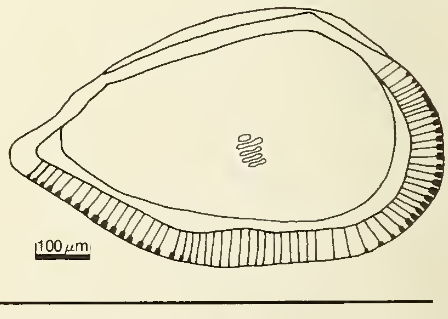

Text-fig. 1. Internal features observed through transmitted light. LV (**OS13389**, 920 μm long).

Explanation of Plate 16, 139

Figs. 1, 3, RV (**OS13388**, 920 μm long): fig. 1, int. lat.; fig. 3, adductor muscle scar detail. Fig. 2, LV, int. lat. (**OS13389**, 920 μm long).
Scale A (500 μm; ×70), figs. 1–2; scale B (100 μm; ×270), fig. 3.

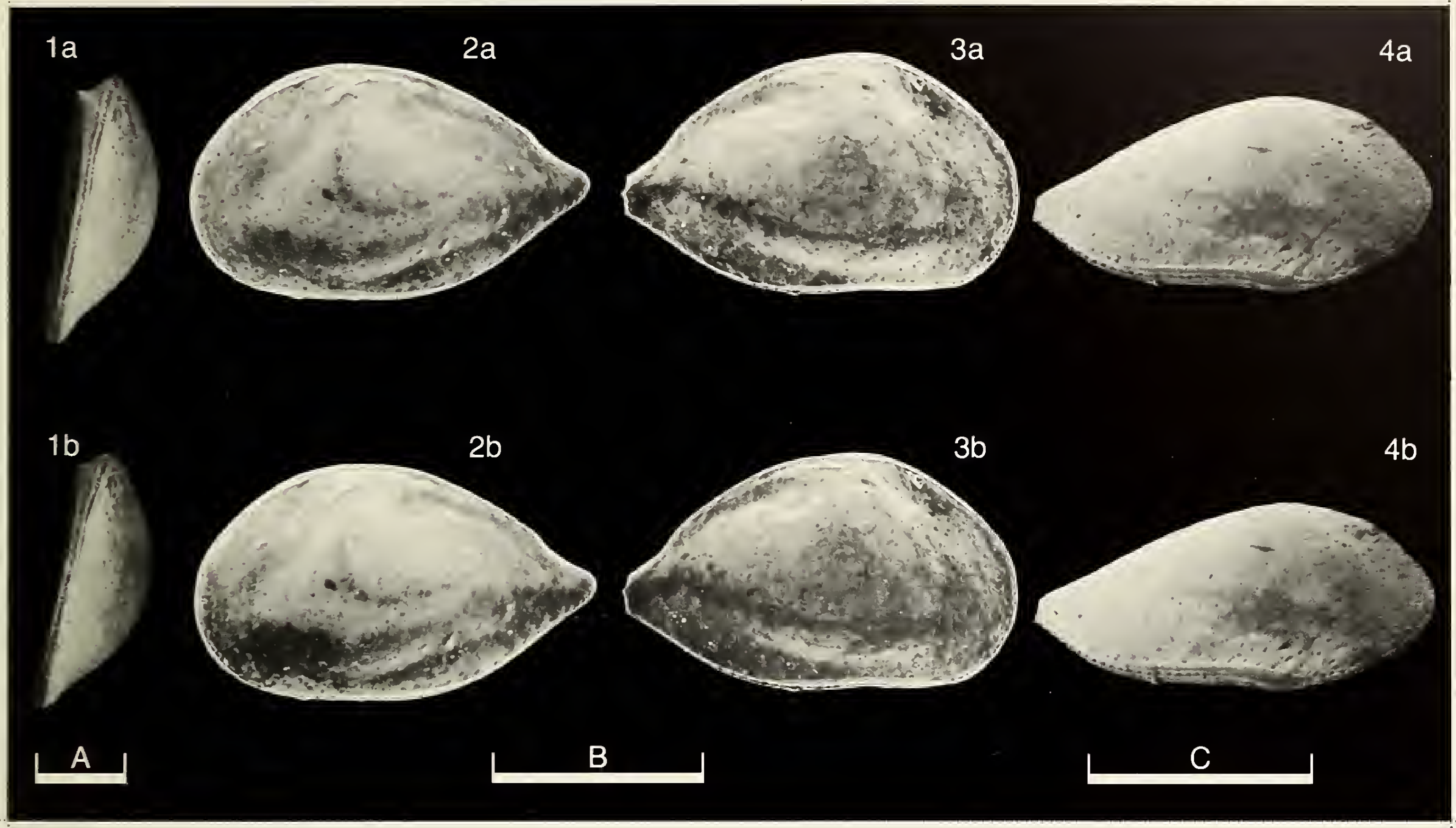
1a
2a
3a
4a
1b
2b
3b
4b
A
B
C

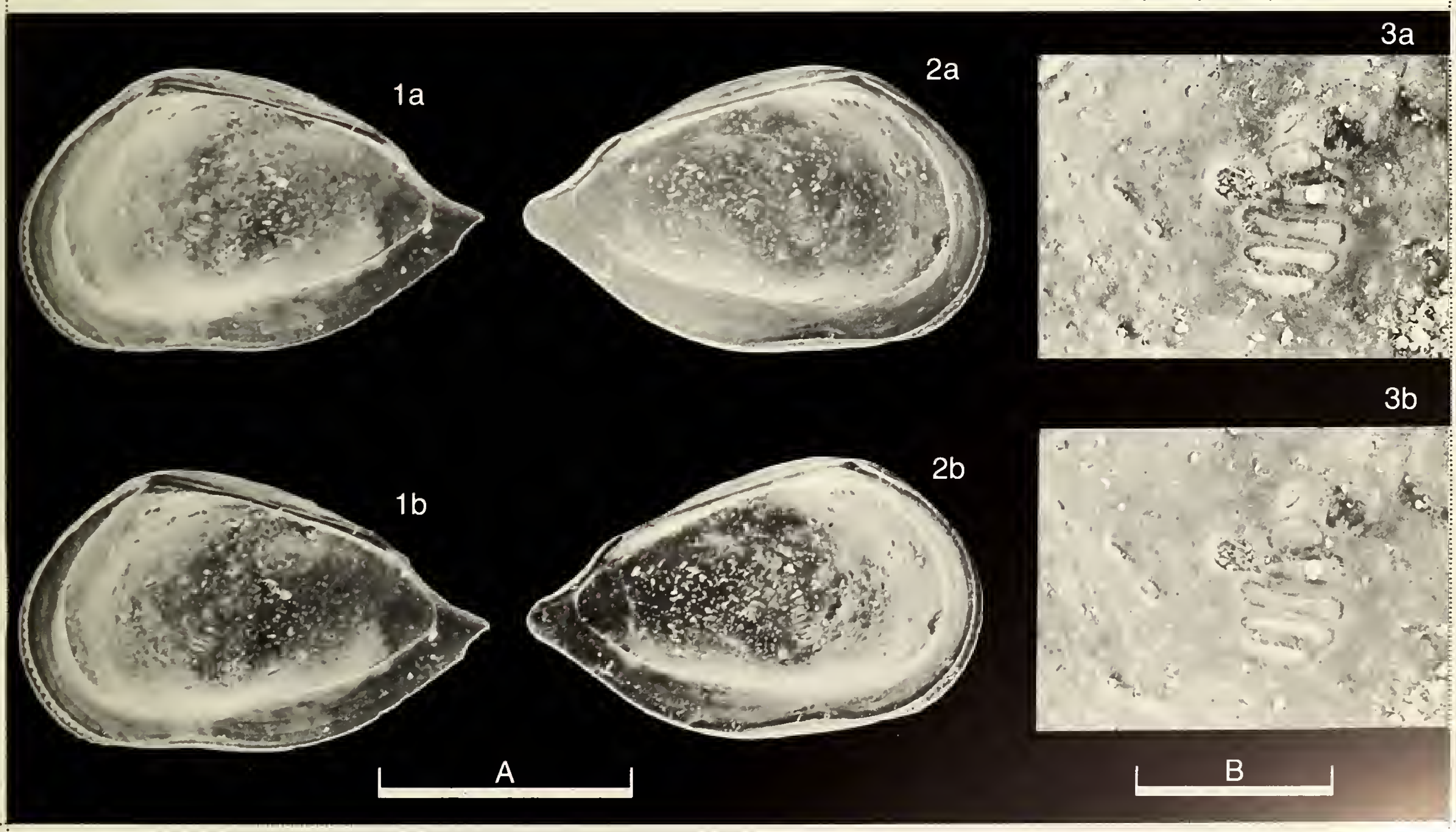
1a
2a
3a
1b
2b
3b
A
B

595.337.12 (119.9) (671.1 : 161.011.03) : 551.31/551.312

ON *BRYOCYPRIS GRANDIPES* RØEN

by Koen Martens

(Koninklijk Belgisch Instituut voor Natuurwetenschappen, Hydrobiologie, Brussels, Belgium)

Genus *BRYOCYPRIS* RØEN, 1956

Type-species (by original designation): *Bryocypris grandipes* RØEN, 1956

1956 *Bryocypris* gen. nov. U. Røen, *Bull. Inst. fr. Afr. noire*, **18**, sér. A (3), 916.

Diagnosis: Cypridopsine genus with elongated carapace, RV overlapping LV frontally, caudally and ventrally, RV with well developed frontal and caudal inner lists, LV with caudal, submarginal selvage and weak frontal inner list; 4 large adductor muscle scars present.

Antenna with typical cypridopsine sexual dimorphism in the apical armature: male antenna with claw G_3 reduced to a short seta, z_1 a stout claw and z_3 missing. Maxillular palp with distal segment rectangular and elongated. First thoracopod with penultimate segment divided. Second thoracopod with a pincer, i.e. fourth segment not individually developed. Hemipenis with inner spermiductus showing the typical cypridopsine coils in parts c and d. Males, as usually in this group, without a furca (see K. Martens & C. Meisch, *Hydrobiologia*, **127**, 9–15, 1985); females with a furca of the normal type.

Remarks: *Bryocypris* appears closely related to both *Sarscypridopsis* McKenzie, 1977 and *Plesiocypridopsis* Rome, 1965, yet differs from both genera by a number of morphological peculiarities, the most important ones being the general outline of the valves, the shape of the furcal ramus in the female and the external anatomy of the hemipenis.

Explanation of Plate 16, 141

Fig. 1, ♂ RV, int. lat. (paratype, **KM.512**, 534 μm long); fig. 2, ♂ car. vent. (paratype, **OC1477**, 534 μm long); fig. 3, ♂ LV, int. lat. (paratype, **KM.512**, 552 μm long); fig. 4, ♂ LV, ext. lat. (paratype, **OC1476**, 552 μm long).
Scale A (100 μm; ×110)

Bryocypris grandipes Røen, 1956

1956 *Bryocypris grandipes* sp. nov. U. Røen, *Bull. Inst. fr. Afr. noire*, **18**, sér. A (3), 916–920, figs. 7–19.

Type specimens: Zoologisk Museum (Copenhagen): unnumbered specimens labelled "holotype ♀, allotype ♂" (not designated in original publication); the ICZN is unclear with regard to the validity of such types, but since the designation was suggested by the original author, I propose to accept both holotype and allotype and consider all other specimens paratypes: ♂ with soft parts dissected in a sealed slide with glycerine, valves stored dry (**KM.512**); 200 ♂♂ and 648 ♀♀, the majority *in toto* in spirit (no number). Also 1 ♂ and 1 ♀ dissected and c. 10 *in toto* specimens in the KBIN, Brussels (nos. **OC1475–1481**).

Type locality: Mosses in caves just above the waterfall of Mpoumé. N bank of R. Nyong, Cameroon, Africa (approx. lat. 3°30′ N, long. 11°05′ E). The 'caves' actually consist of spaces between giant boulders and the thick mats of mosses lining the roofs and walls of the entrances are never submerged, but kept steadily moist by the fog-like splash from the fall (J. Birket-Smith, *Bull. Inst. fr. Afr. noire*, **18**, sér. 1(2), 567–582, 1956).

Figured specimens: Zoologisk Museum, Copenhagen: **KM.512** (paratype, ♂: Pl. **16**, 141, figs. 1, 3; Text-figs. 1 (B–D, G), 2 (A–D, F), 3 (A–C, E, F)). KBIN, Brussels, all paratypes: **OC1477** (♂; Pl. **16**, 141, fig. 2), **OC1476** (♂: Pl. **16**, 141, fig. 4; Pl. **16**, 143, fig. 5; Text-figs. 1 (F), 3 (D, G)), **OC1475** (♀: Pl. **16**, 143, figs. 1, 3); Text-figs. 1 (E), 2 (E), 3 (H, I)), **OC1478** (♀: Pl. **16**, 143, fig. 2), **OC1479** (♀: Pl. **16**, 143, fig. 4). **OC1480** (♀: Text-fig. 1 (A)).

Diagnosis: Valves elongated, with posterior margin more widely rounded than anterior one and with numerous marginal setae. Antennula without Rome-organ. Antenna with natatory setae short, hardly reaching beyond tip of their segment. Left prehensile palp with terminal segment elongated and distally dilated, proximally narrower, but not folded as in *Plesiocypridopsis*; right prehensile palp curved, shorter and narrower. First thoracopod with penultimate segment with only 1 apical seta and distal segment without lateral seta. Furca in female with a short, conical ramus, a small lateral seta and an extremely elongated and flagellum-like apical seta. Genital region in the female with a solid, elongated and curved genital hook. Hemipenis with lateral shield rounded, bearing a pronounced, subapical thumb-like processus. Inner spermiductus with a supplementary coil, with the bursa copulatryx large and simple and not surrounded by additional trabeculae.

Explanation of Plate 16, 143

All paratypes. Fig. 1, ♀ RV int. lat. (**OC1475**, 586 μm long); fig. 2, ♀ car. dors. (**OC1478**, 534 μm long); fig. 3, ♀ LV int. lat. (**OC1475**, 552 μm long); fig. 4, ♀ car. dors. (**OC1479**, 517 μm long); fig. 5, ♂ RV ext. lat. (**OC1476**, 552 μm long).
Scale A (100 μm; ×110).

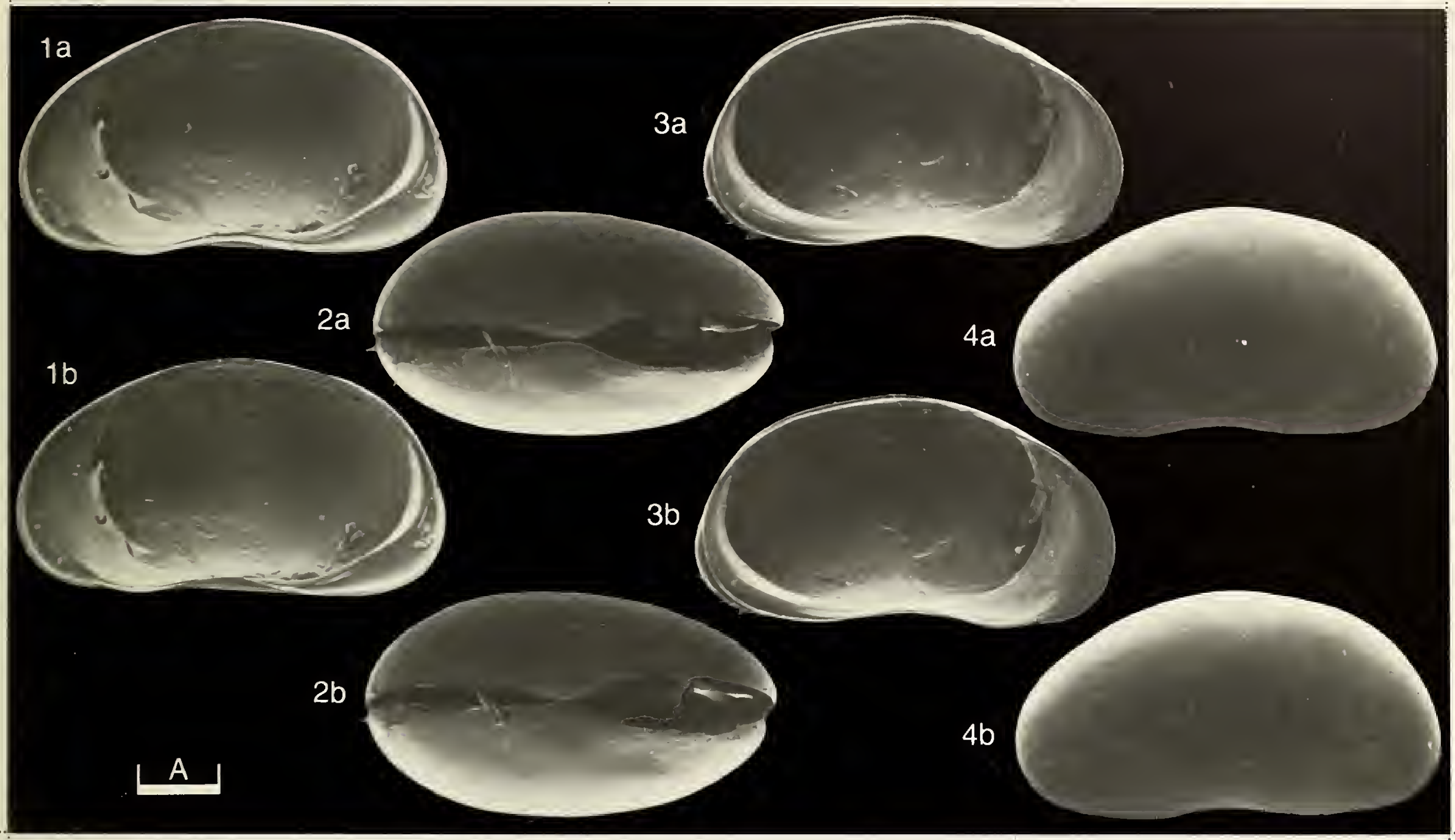
1a
3a
2a
4a
1b
3b
2b
4b
A

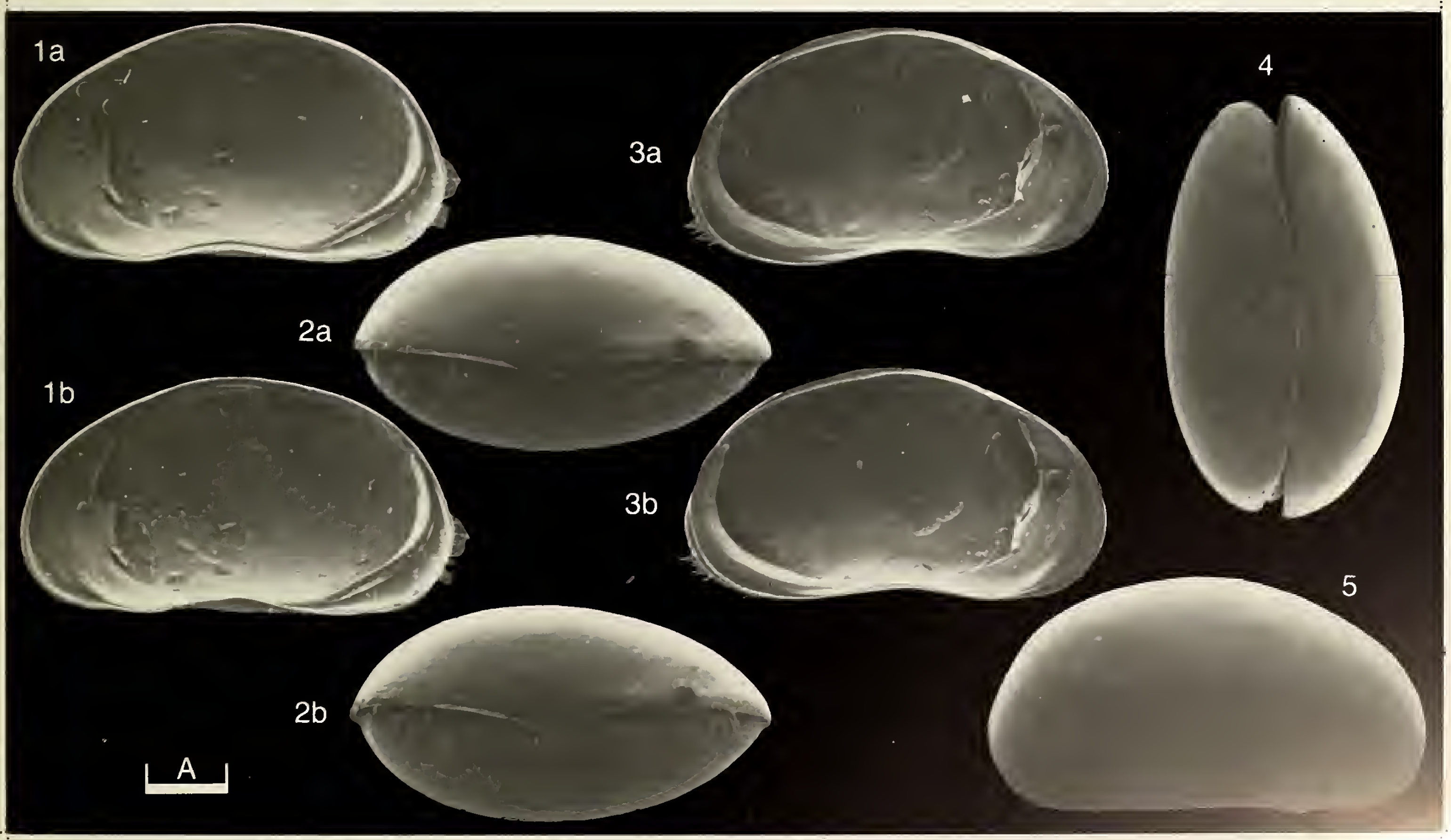
1a
3a
4
2a
1b
3b
5
2b
A

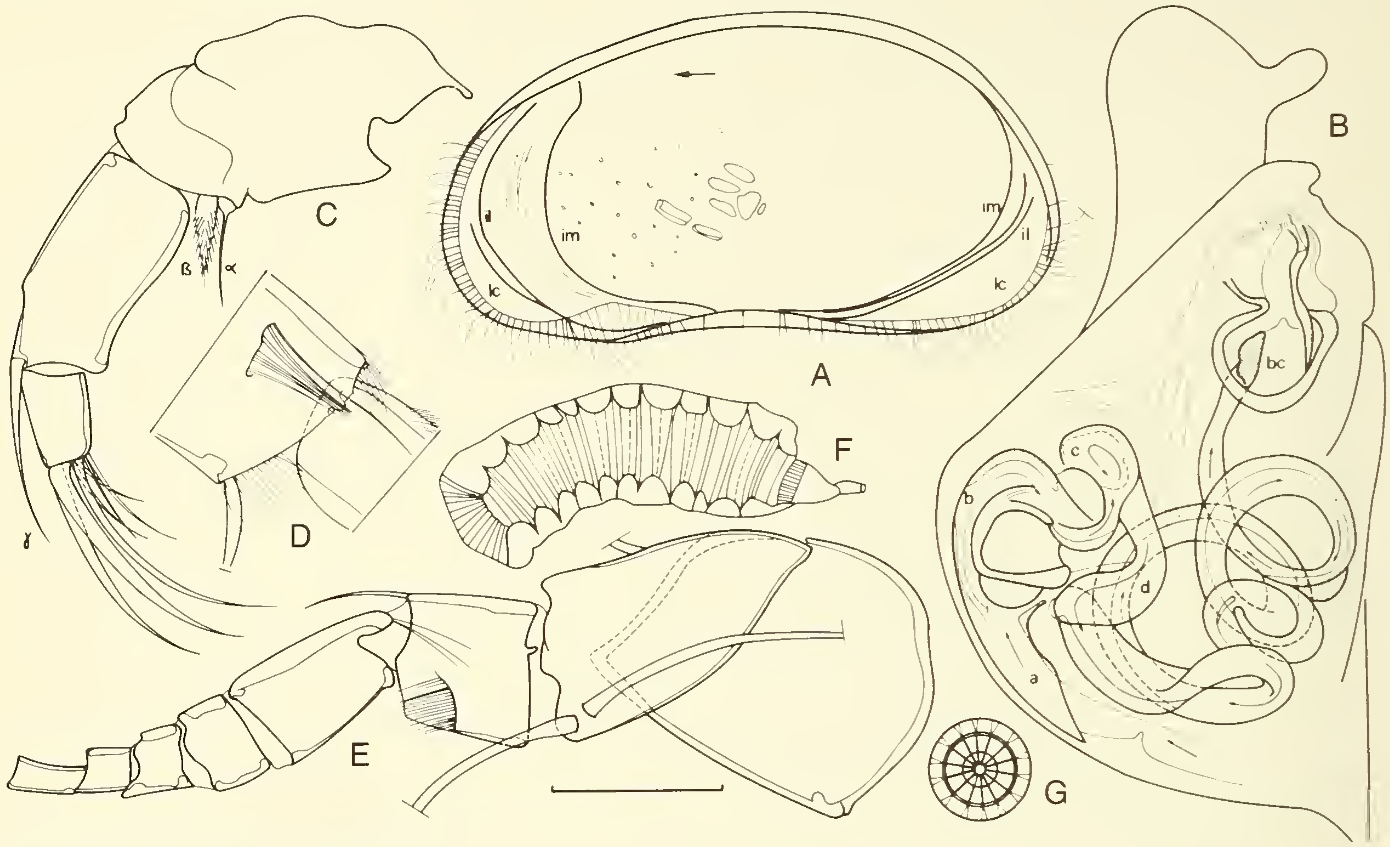

Text-fig. 1 (see **16**, 147 for explanation)

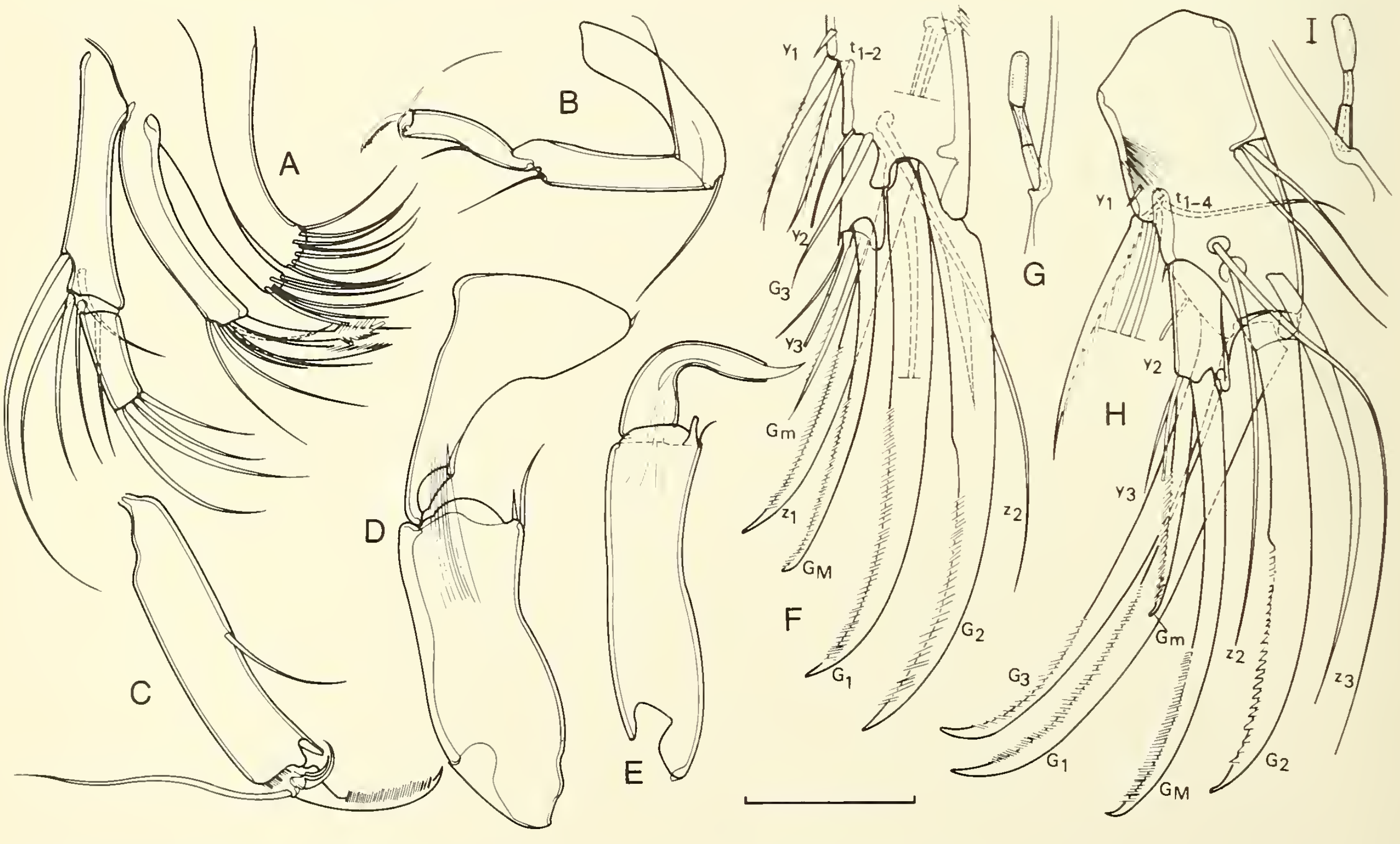

Text-fig. 3 (see **16**, 147 for explanation)

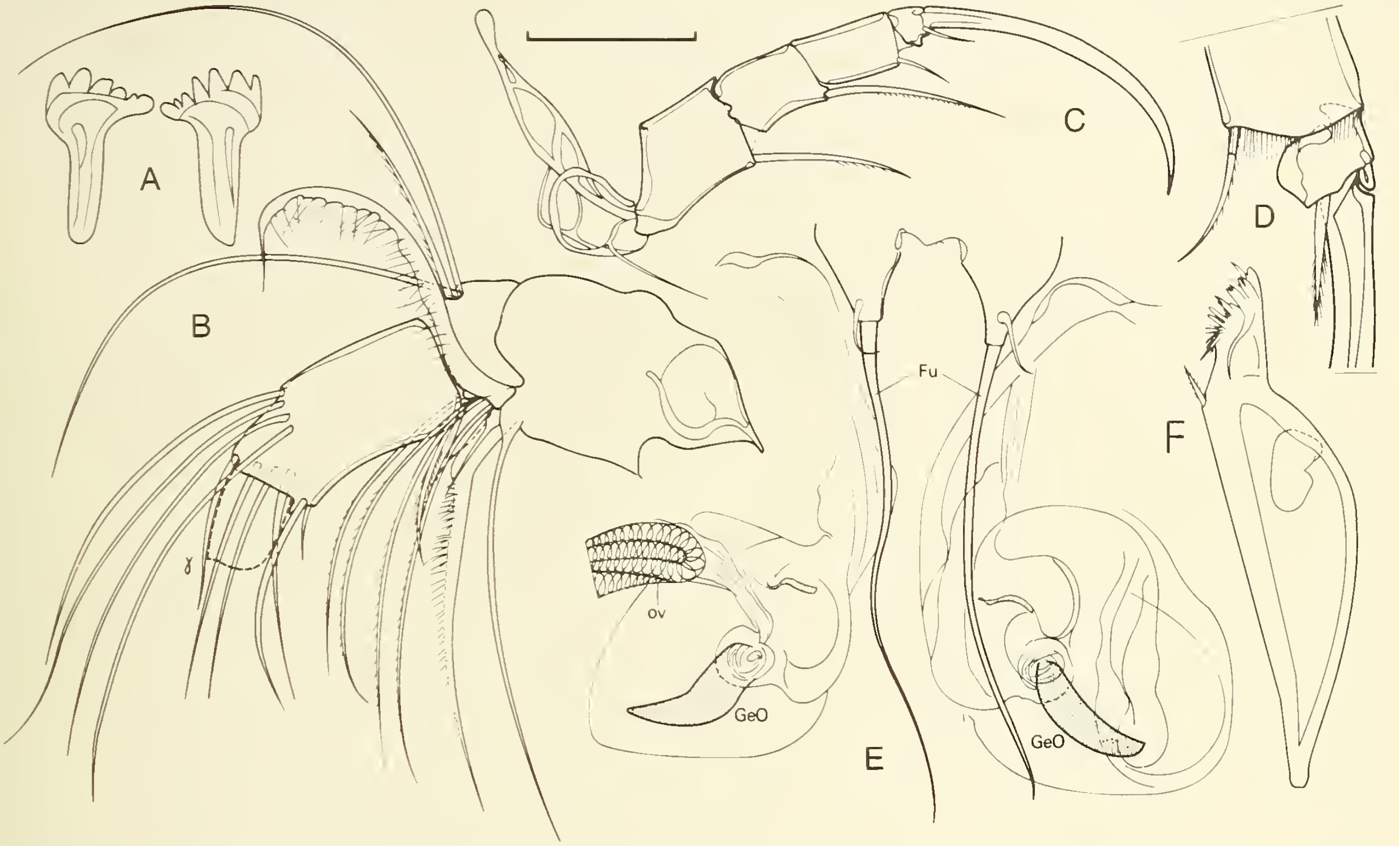

Text-fig. 2 (see **16**, 147 for explanation)

Remarks: *B. grandipes* is a typical cypridopsine species, the most important feature being the presence of a reduced furca in the female, but also because of the sexual dimorphism in the apical armature of the antenna (i.e. the reduction of z_3) and the structure of the inner spermiductus in the hemipenis. Together with *Potamocypris* Brady, 1870, *Bryocypris* is thus far the only genus where well developed genital hooks are known in the females. However, this region of the body has not yet been illustrated properly for most species and genera and the feature may prove to be present in a number of other genera. *Bryocypris* is only the second cypridopsine group which has adapted to the terrestrial environment, *Callistocypris* Schornikov, 1980 (*Zool. Zh.*, **59**, 1306–1319, 1980) being already described from purely terrestrial environments on the Solomon Islands. The latter genus (placed in a separate subfamily), however, displays far more morphological adaptations to such environments. For example, all segments, claws and setae in *Callistocypris* are short and stout and even the furca, although clearly cypridopsine, appears more solidly built and has a well developed, complex furcal attachment. *Bryocypris* has none of these features; its only adaptations to terrestrial conditions are the reduction of the natatory setae on the antenna (not unusual in Cypridopsinae), the disappearance of 2 setae on the first thoracopod and the presence of numerous marginal setae on the valves. This could indicate that its invasion in such habitats is a fairly recent phenomenon, and that it is unable to live in truly terrestrial situations (e.g. leaf litter in forests, like for example *Callistocypris* and *Terrestricandona* Danielopol & Betsch, 1980), but is rather restricted to semi-terrestrial environments (mosses in splash zones, etc.). It is of interest to note that species with a reduced furca can apparently still (re-)adapt to a crawling locomotion in difficult circumstances, although in one lineage (*Callistocypris*) this caused a secondary reinforcement of the furca.

Acknowledgements: Dr T. Wolff (Copenhagen) is acknowledged for his help in providing access to the type material. Mr J. Cillis and Mrs C. Behen offered technical assistance with the illustrations.

Text-fig. 1. A, ♀ paratype (**OC1480**, 574 μm long), B–D, G, ♂ paratype (**KM.512**), E, ♀ paratype (**OC1475**, F, ♂ paratype (**OC1476**). A, RV, int. lat.; B, hemipenis; C. mandibular palp, showing part of chaetotaxy; D, antenna, detail of natatory setae; E, antennula, chaetotaxy of endopodite not shown; F, Zenker's organ; G, idem, detail in frontal view. Scale: 156 μm for A; 81 μm for F, G; 33 μm for B–E.

Text-fig. 2. A–D, F, ♂ paratype (**KM.512**), E, ♀ paratype (**OC1475**). A, rake-like organs; B, mandibular palp (respiratory plate and chaetotaxy of fourth segment not shown); C, first thoracopod; D, idem, detail; E, furcae and genital region, showing genital hooks; F, mandibular coxa. Scale: 81 μm for C, F; 33 μm for A, B, D, E.

Text-fig. 3. A–C, E, F, ♂ paratype (**KM.512**), D, G, ♂ paratype (**OC1476**), H, I, ♀ paratype (**OC1475**). A, maxillula; B, second thoracopod; C, idem, detail; D, left prehensile palp; E, right prehensile palp; F, left antenna in medial view, detail of apical armature; G, antenna, detail of aesthetasc Y; H, right antenna in lateral view, detail of apical armature; I, antenna, detail of aesthetasc Y. Scale: 81 μm for B; 33 μm for A, C–I.

ON *LIMNOCYTHERE HIBERNICA* ATHERSUCH sp. nov.

by John Athersuch

(BP Research, Sunbury-on-Thames, England)

Limnocythere hibernica sp. nov.

Holotype: British Museum (Nat. Hist.) no. **OS13432**; ♀ car.
[Paratypes: British Museum (Nat. Hist.) nos. **OS13431**, **13433–13437**]

Type locality: The well 26/28–1 in the Porcupine Seabight, offshore SW Ireland (approx. lat. 52°02′ N, long. 12°33′ W); Middle Jurassic, probably Late Bathonian.

Derivation of name: Latin, *hibernia* = Ireland; alluding to the location of the type locality in Irish territorial waters.

Figured specimens: British Museum (Nat. Hist.) nos. **OS13432** (holotype. ♀ car.: Pl. **16**, 149, fig. 2), **OS13431** (♀ car.: Pl. **16**, 149, fig. 1), **OS13433** (♂ car.: Pl. **16**, 149, fig. 3), **OS13434** (♀ car.: Pl. **16**, 151, fig. 1), **OS13435** (♀ car.: Pl. **16**, 151, fig. 2), **OS13436** (♂ car.: Pl. **16**, 151, fig. 3), **OS13437** (LV: Text-fig. 1). All specimens from the type locality; **OS13432**, **13434** at 2370 m (cuttings); **OS13436** at 2435 m (cuttings); **OS13431**, **13433**, **13435**, **13437** at 2437.4 m (core).

Diagnosis: Each adult valve bears a group of variably coalesced protuberances and swollen ridges. Single subcentral and median dorsal tubercles are separated by two vertical sulci from single anterior and posterior ridges. The anterior ridge is positioned some way from and subparallel to the anterior margin; in some specimens it appears to be formed of two coalesced tubercles. The posterior ridge which runs parallel to the posterior margin has a pronounced C-shape, the dorsal branch being swollen terminally; the largest of the tubercles lies between the end of the ventral branch and the subcentral tubercle with which it tends to coalesce in some specimens. Surface ornament of subrounded reticulation; fossae largest and best developed in posterolateral areas, reducing to

Explanation of Plate 16, 149

Fig. 1, ♀ car., ext. lt. lat. (paratype, **OS13431**, 506 μm long); fig. 2, ♀ car., ext. lt. lat. (holotype, **OS13432**, 552 μm long); fig. 3, ♂ car., ext. lt. lat. (paratype, **OS13433**, 616 μm long). Scale A (250 μm; ×105), figs. 1–3.

foveolae towards margins.

Remarks: There is a considerable amount of variation in the development of the tubercles within a population of individuals of approximately the same size; this variation is not always the result of abrasion. In some individuals the anterior and posterior ridges are only weakly developed (Pl. **16**, 151, fig. 1). A posterodorsal concavity shows that the posterior ridge is, at least in part, hollow. There is also a small ocular sinus. The adductor muscle scar area is not clearly visible. More elongate specimens are presumed to be males.

This species is placed in the genus *Limnocythere* principally because of the remarkable similarity of its external morphology to many Recent and Neogene species of that genus (e.g. the living *L. porphyretica* De Deckker, 1981 (*Zoologica Scr.*, **10**, 41–42, figs. 3, 4).

The valve interior is known only from one damaged specimen (Text-fig. 1); it displays a lophodont hinge and at least 23 slightly sinuous, unbranched radial pore canals anteriorly. These are also features consistent with the genus *Limnocythere*.

Distribution: Known only from wells in the vicinity of the type locality in the Porcupine Seabight. By comparison with living species, *L. hibernica* is probably indicative of a non-marine lacustrine episode. At the type locality this species occurs in an interval with *Bisulcocypris* spp., *Darwinula* sp., conchostracans, gastropods and abundant terrestrial miospores and bisaccate pollen. Monotypic flood occurrences of this species have been observed in thin beds in core samples.

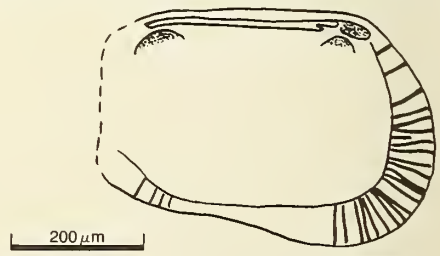

Text-fig. 1. Internal view of broken left valve; sex unknown (paratype, **OS13437**).

Explanation of Plate 16, 151

Fig. 1, ♀ car., ext. lt. lat. (paratype, **OS13434**, 506 μm long); fig. 2, ♀ car., ext. dors. (paratype, **OS13435**, 552 μm long); fig. 3, ♂ car., ext. dors. (paratype, **OS13436**, 607 μm long). Scale A (250 μm; ×105), figs. 1–3.

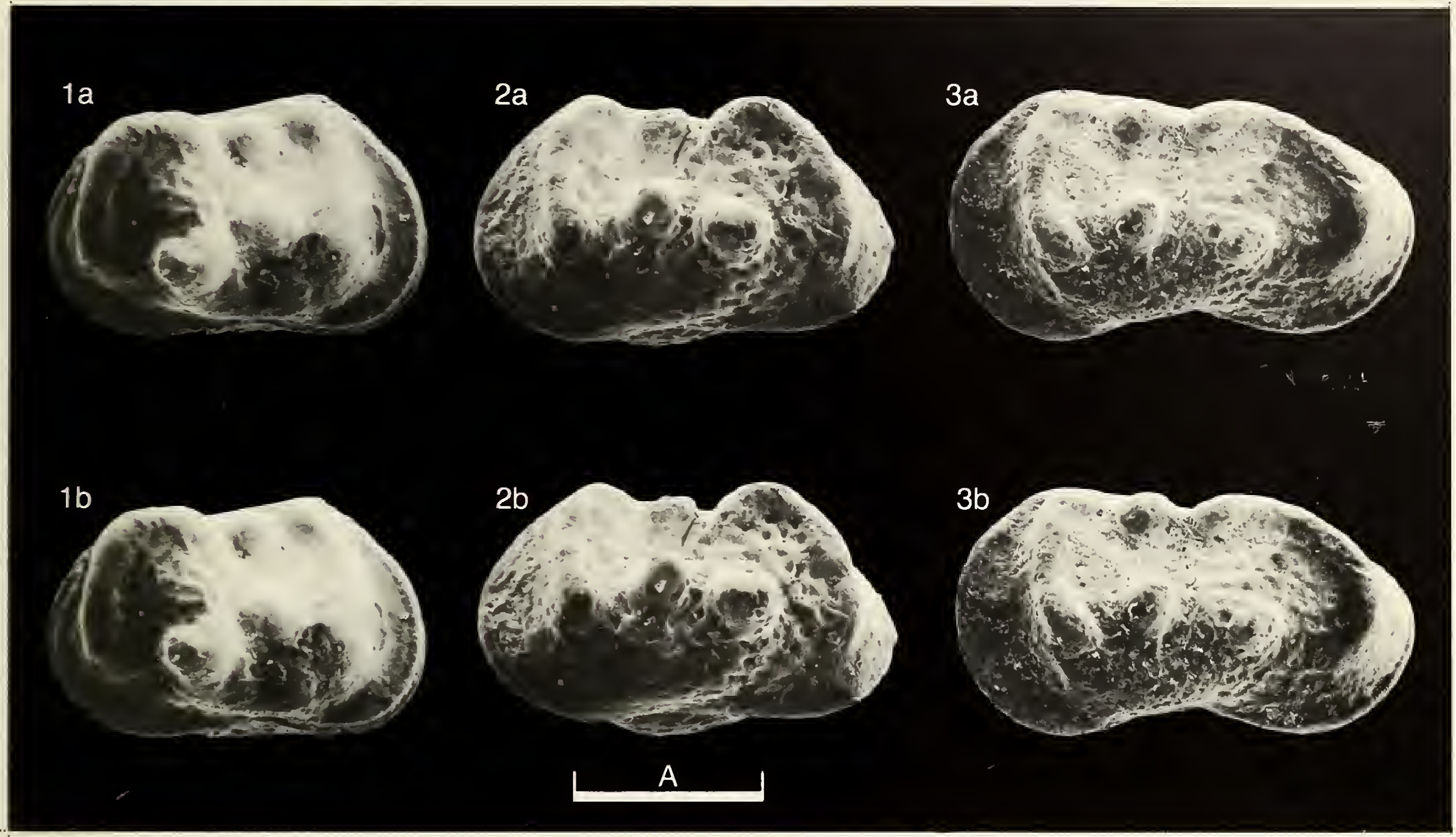
1a
2a
3a
1b
2b
3b
A

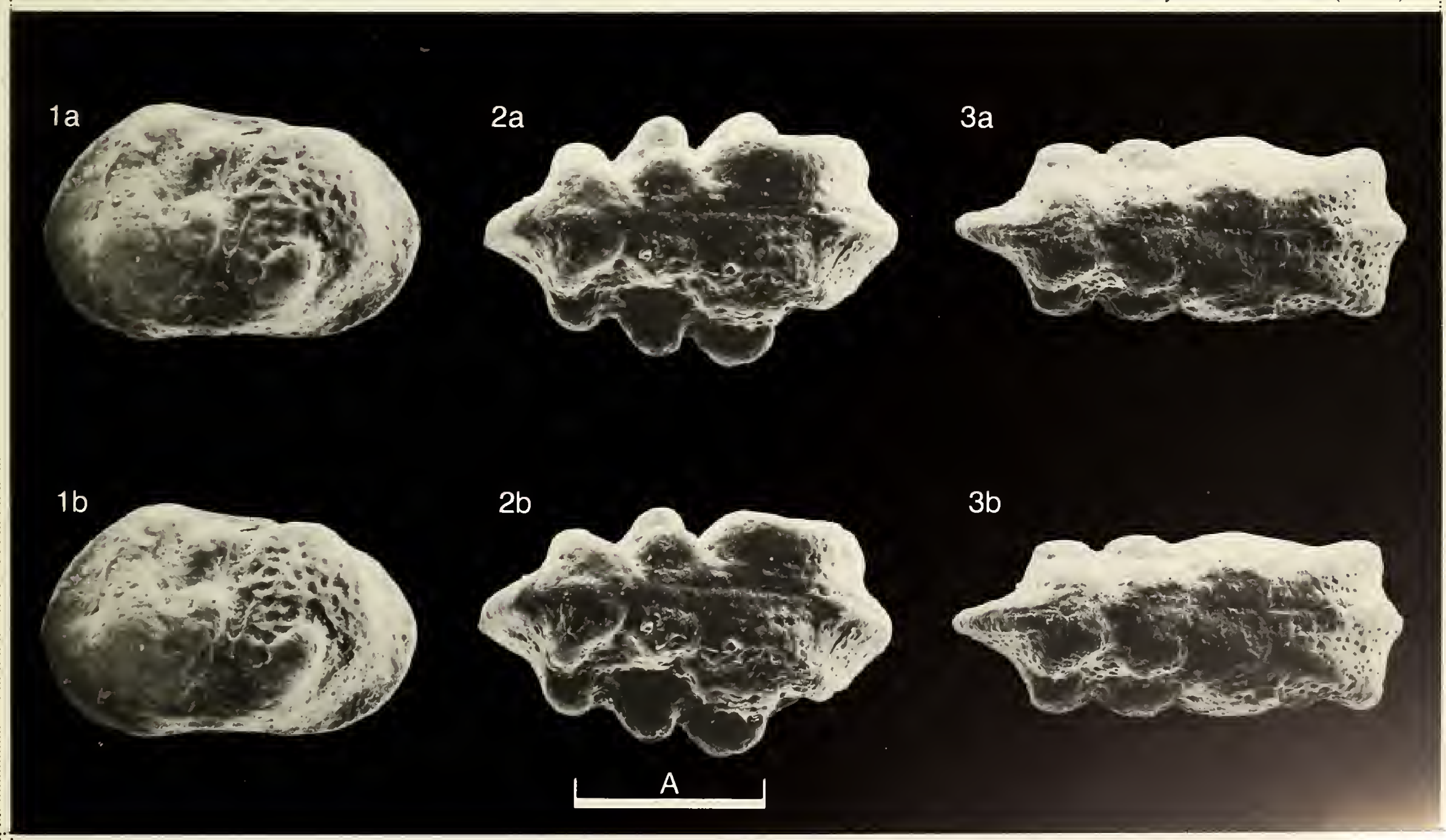
1a
2a
3a
1b
2b
3b
A

595.337.14 (119.9) (263 : 162.090.29) : 551.351

ON *ECHINOCYTHEREIS SPINIRETICULATA* KONTROVITZ

by Mervin Kontrovitz & Zhao Yuhong
*(Northeast Louisiana University, Monroe, USA &
Nanjing Institute of Geology & Palaeontology, Academia Sinica, Nanjing, China)*

Echinocythereis spinireticulata Kontrovitz, 1971

1971 *Echinocythereis spinireticulata* sp. nov. M. Kontrovitz, *Tulane Stud. Geol. Paleont.*, **8**, 166–168, pl. 1, figs. 1–3, text-fig. 1.
1975 *Echinocythereis spinireticulata* Kontrovitz; H. V. Howe & W. A. van den Bold, *Bull. Am. Paleont.*, **65**, 307, pl. 2, fig. 4.

Holotype: H. V. Howe Collection (HVH), Louisiana State University, Baton Rouge, USA, no. **HVH 8595**; ♀ left valve.
[Paratypes: nos. **HVH 8596–8599**]

Type locality: Gulf of Mexico, near the delta of the Mississippi River, approx. lat. 29° 00′ N, long. 90° 00′ W; Holocene, marine, sublittoral.

Figured specimens: Geosciences Department of Northeast Louisiana University (NLUGEO) nos. **NLUGEO 1021** (♀ RV: Pl. **16**, 153, fig. 1; Pl. **16**, 155, fig. 3), **NLUGEO 1022** (♀ LV: Pl. **16**, 153, fig. 3; Pl. **16**, 155, fig. 1), **NLUGEO 1023** (juv. RV: Pl. **16**, 153, fig. 2), **NLUGEO 1024** (juv. LV: Pl. **16**, 155, fig. 2).
From the Gulf of Mexico, near the delta of the Mississippi River; Recent, marine (kindly provided by Ms J. M. Slack (NLU)).

Explanation of Plate 16, 153

Fig. 1, ♀ RV, ext. lat. (**NLUGEO 1021**, 1110 μm long); fig. 2, juv. RV ext. lat. (**NLUGEO 1023**, 830 μm long); fig. 3, ♀ LV, ext. lat. (**NLUGEO 1022**, 1110 μm long).
Scale A (250 μm; ×70), figs. 1–3.

Diagnosis: Surface covered with minute, delicate spines, arranged in rows that form a reticulate pattern. Ornamentation centered around dorsomedial area of valve. Adults have a row of slender spines behind the denticulate anterior margin. Posterior margin without denticles. Heavy spine projecting from posterior ventrolateral convexity of adults. Vertical row of 4 adductor muscle scars: from dorsal to ventral, the first scar is oval, the second subreniform, the third and fourth elongate; second and fourth scars nearly touch in front of the third.

Remarks: This species differs from *Echinocythereis jacksonensis* (Howe & Pyeatt) (*in* Howe & Chambers, *Geol. Bull. La.*, **5**, 35–37, pl. 1, figs. 23–24; pl. 6, fig. 31, 1935) in being reticulate over the entire surface and having a higher posterior, therefore appearing to be shorter. The original description of *E. jacksonensis* included two forms, one larger than the other. The larger has anterior reticulations and only coarse spines from mid-length to the posterior.
Krutak (*J. Paleont.*, **35**, 783–784, pl. 91, fig. 9, 1961) figured examples of *E. jacksonensis* on which "tiny nodes are aligned, tending to form hexagonal, pentameral, or angular patterns". The specimens he reported also differ from this species in being smooth in the dorsal, posterior, and ventral areas. Muscle scars and length/height ratios are also significantly different.
E. clarkana (Ulrich & Bassler) (*in* Case *et al.*, *Systematic Paleontology of the Miocene Deposits of Maryland*, 98, pl. 35, figs. 1–10, Miocene Volume, Maryland Geological Survey, Baltimore, 1904) is distinguished from *E. spinireticulata* by its coarsely reticulate surface with heavy spines at the junctures of the ridges, denticulate posterior margin, and larger size.

Distribution: Common in shallow, sublittoral, marine waters of the Gulf of Mexico near the delta of the Mississippi River; also recovered from the Mississippi Mudlumps (Howe & van den Bold, 1975).

Explanation of Plate 16, 155

Fig. 1, ♀ LV, int. lat. (**NLUGEO 1022**, 1110 μm long); fig. 2, juv. LV int. lat. (**NLUGEO 1024**, 830 μm long); fig. 3, ♀ RV, int. lat. (**NLUGEO 1021**, 1110 μm long).
Scale A (250 μm; ×70), figs. 1–3.

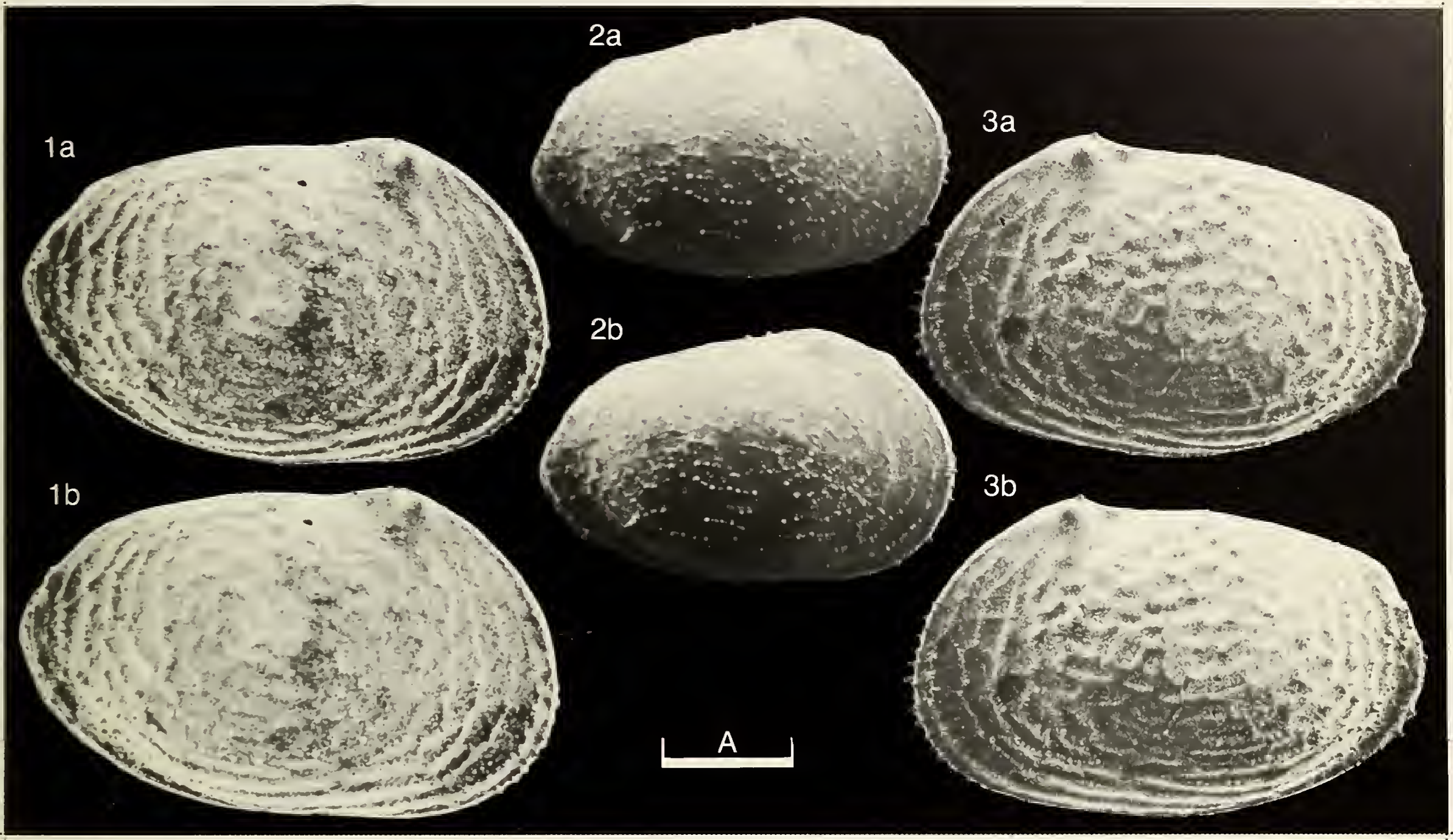
2a
1a
3a
2b
1b
3b
A

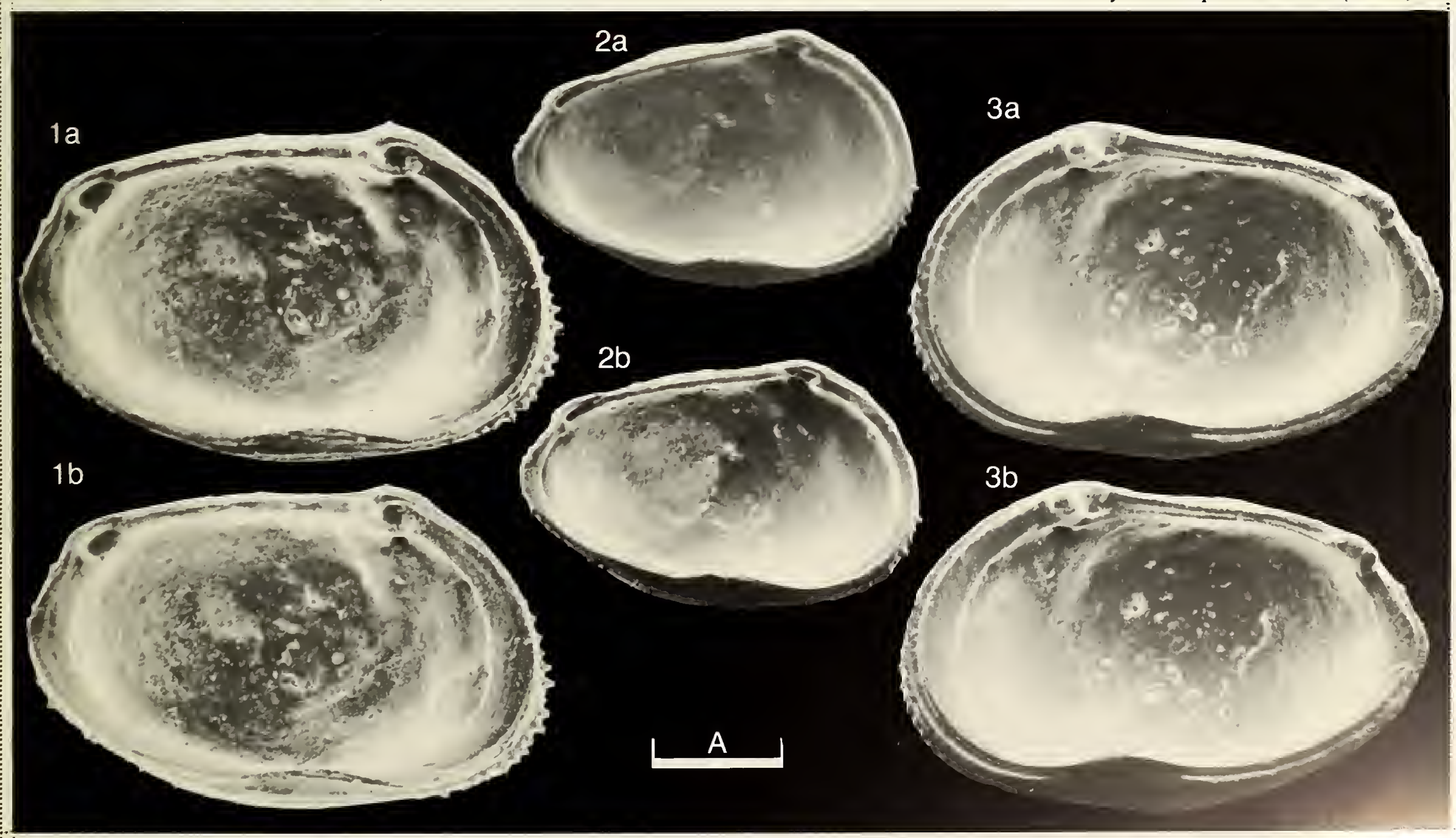
2a
1a
3a
2b
1b
3b
A

General Index

Index; Geological Horizon

See **1** (2) 5–22 (**1973**) for explanation of the Schedules in the Universal Decimal Classification

Index; Geographical Location

See **1** (2) 5–22 (**1973**) for explanation of the Schedules in the Universal Decimal Classification

Stereo-Atlas of Ostracod Shells: Vol. 16, Part 2

CONTENTS

ISSN 0952–7451